INFORMATION TO USERS

This manuscript has been reproduced from the microfilm master. UMI films the text directly from the original or copy submitted. Thus, some thesis and dissertation copies are in typewriter face, while others may be from any type of computer printer.

The quality of this reproduction is dependent upon the quality of the copy submitted. Broken or indistinct print, colored or poor quality illustrations and photographs, print bleedthrough, substandard margins, and improper alignment can adversely affect reproduction.

In the unlikely event that the author did not send UMI a complete manuscript and there are missing pages, these will be noted. Also, if unauthorized copyright material had to be removed, a note will indicate the deletion.

Oversize materials (e.g., maps, drawings, charts) are reproduced by sectioning the original, beginning at the upper left-hand corner and continuing from left to right in equal sections with small overlaps.

Photographs included in the original manuscript have been reproduced xerographically in this copy. Higher quality 6" x 9" black and white photographic prints are available for any photographs or illustrations appearing in this copy for an additional charge. Contact UMI directly to order.

ProQuest Information and Learning
300 North Zeeb Road, Ann Arbor, MI 48106-1346 USA
800-521-0600

UMI®

Analysis of Steady and Unsteady Flows past Fixed and Oscillating Airfoils

by

Mohammed Abdo

Department of Mechanical Engineering
McGill University
Montreal, Quebec, Canada.

March, 2000

A Thesis submitted to the Faculty of Graduate Studies and Research in partial fulfillment of the requirements for the degree of Master of Engineering.

© Mohammed Abdo, 2000

National Library of Canada

Bibliothèque nationale du Canada

Acquisitions and Bibliographic Services

Acquisitions et services bibliographiques

395 Wellington Street
Ottawa ON K1A 0N4
Canada

395, rue Wellington
Ottawa ON K1A 0N4
Canada

Your file Votre référence

Our file Notre référence

The author has granted a non-exclusive licence allowing the National Library of Canada to reproduce, loan, distribute or sell copies of this thesis in microform, paper or electronic formats.

L'auteur a accordé une licence non exclusive permettant à la Bibliothèque nationale du Canada de reproduire, prêter, distribuer ou vendre des copies de cette thèse sous la forme de microfiche/film, de reproduction sur papier ou sur format électronique.

The author retains ownership of the copyright in this thesis. Neither the thesis nor substantial extracts from it may be printed or otherwise reproduced without the author's permission.

L'auteur conserve la propriété du droit d'auteur qui protège cette thèse. Ni la thèse ni des extraits substantiels de celle-ci ne doivent être imprimés ou autrement reproduits sans son autorisation.

0-612-64209-7

Canada

Abstract

This thesis presents a method based on the velocity singularities for the analysis of oscillating airfoils. The method of velocity singularities has been originally developed by Mateescu for the analysis of the steady flows past airfoils. This method makes use of special singularities associated to the leading edge and ridges that directly represent the complex perturbation velocity.

Closed form solutions were derived for the pressure distributions and for the aerodynamic forces and moments acting on the oscillating airfoils with or without oscillating ailerons.

The solutions obtained with the velocity singularity method for steady flows past airfoils were found to be in very good agreement with the exact solutions obtained by conformal transformation in the case of thin Joukowski airfoils, as well as with the previous solutions for the case of flexible-membrane airfoils obtained by Mateescu & Newman, Nielsen and Thwaites.

For unsteady flows, this method has been validated for airfoils executing oscillatory motions in translation and pitching rotation and for airfoils with ailerons executing oscillatory rotations. The pressure distributions and the aerodynamic forces and moments obtained with the present method were found to be in excellent agreement with the previous solutions obtained by Theodorsen and Postel and Leppert.

The method has then been extended to the unsteady flows past airfoils executing flexural harmonic oscillations. Closed form solutions were also derived for the pressure distributions and the aerodynamic forces and moments acting on an airfoil with an aileron executing flexural oscillations. No comparisons were presented for the cases of flexural oscillations since there are no previous results known.

The present approach displayed an excellent accuracy and efficiency in all problems studied.

Résumé

Cette thèse présente une méthode d'analyse basée sur les singularités de vitesse pour les profils aérodynamiques ayant des mouvements oscillatoirs. La méthode des singularités de vitesse a été développée originalement par Mateescu pour l'analyse d'écoulements stationnaires autour des profils aérodynamiques. Cette méthode utilise des singularités spéciales asociées au bord d'attaque et aux arêtes qui représentent directement la vitesse complexe de perturbation .

Des solutions explicites ont été établies pour la distribution de pression et pour les forces et les moments aérodynamiques agissant sur les profils aérodynamiques en mouvements oscillatoirs, avec ou sans aileron en mouvement oscillatoire.

Les solutions obtenues avec la méthode des singularités de vitesse pour les écoulements stationnaires autour des profils aérodynamiques sont en excellent accord avec la solution exacte obtenue par transformation conformale pour le cas des profils aérodynamiques de Joukowski, ainsi que avec les solutions antérieures obtenues par Mateescu & Newman, Nielsen and Thwaites pour les profils aérodynamiques flexibles.

Pour les ecoulements instationnaires, cette méthode a été validée pour les profils aérodynamiques exécutant des mouvements oscillatoires en translation et en rotation, ainsi que pour des profils munies d'un aileron oscillant. Les distributions de pression et les forces et moments aérodynamiques obtenus par la présente méthode ont été trouvées en excellent accord avec les solutions obtenues dans ces cas par Theodorsen et par Postel et Leppert.

La méthode a été puis utilisée pour étudier les écoulements instationnaires autour des profils aérodynamiques exécutant des oscillations harmoniques en flexion. Des formules explicites ont été aussi établies pour la distribution de pression et pour les forces et moments aérodynamiques agissant sur un profil aérodynamique muni d'un aileron exécutant des oscillations flexurales. Aucune comparaison n'est pas présentée pour le cas des oscillations en flexion parce qu'il n'y a pas des résultats précédent connus.

La présente méthode a démontré une excellente précision et efficacité dans tous les problémes étudiés.

Acknowledgements

I would like to thank my thesis supervisor, Professor Dan Mateescu, for his guidance, knowledge, and dedication throughout the course of this work.
I am grateful to my parents for their support and encouragement.
I would like also to thank all my friends at McGill University.

Contents

Page

Page

List of figures

Page

Page

List of tables

Chapter 1

Introduction

The analysis of unsteady flows past oscillating airfoils and wings is very important for the aeronautical applications. The problem of predicting the aerodynamic characteristics of such airfoils is among the first ones that have been studied in the development of the aeronautical sciences. This analysis has proved to be of considerable practical importance. Studies of unsteady airfoil flows require predicting the unsteady aerodynamic loads acting on thin lifting surfaces. Potentially beneficial effects of unsteadiness has also been given some attention, such as controlled periodic vortex generation, improve the performance of turbo-machinery, helicopter rotors, and wind turbines by controlling the unsteady forces in some optimum way. Most of these studies concern either periodic motion of an airfoil in a uniform stream or periodic fluctuations in the approaching flow. There is a need to develop efficient methods of analysis that can be used in conjunction with the structural research to study the dynamics and stability of the airfoil and wing structure subjected to the unsteady aerodynamic forces.

The analysis of thin airfoil theory has been a subject under research and development for many years. Since it is in general difficult to develop an exact solution for the ideal flow past an airfoil of arbitrary shape, approximate methods have been developed to solve this problem. Among the pioneering works are the ones of Glauert [6,14] and Birnbaum. Glauert's method approximates the airfoil by its camber line and by modeling this camber line as a vortex sheet. An integral equation resulted for the distribution of the vortex sheet by linearizing the boundary conditions and transferring these boundary conditions from the surface of the airfoil to the chordline. Glauert solved the integral equation by means of Fourier series. This approach is the basis of thin airfoil theories.

The fact that the boundary conditions are in general non-linear makes the problem of finding an exact solution for the motion of an ideal flow very complicated. Few solutions are available for a limited number of geometries only. For instance, Joukowski [21,14] airfoils, which can be directly obtained from the conformal transformation of a circle. However, these airfoils are of limited use in practice because of their pre-determined shapes, but they are essential in assessing the accuracy of the approximate methods.

The method of velocity singularities has been first introduced for supersonic flow past wings and wing-fuselage systems, Mateescu [11]. Mateescu [12,13] has also introduced a new method for the solution of the steady flow past thin airfoils in subsonic flows. The method of velocity singularities developed by Mateescu, makes use of special singularities at the airfoil leading edge and ridges along the airfoil. This method, does not directly use the velocity potential but instead operates directly on the velocity field by considering the singular behavior of the flow at geometrically important elements of the airfoil. In addition, this solution satisfies the Kutta condition at the trailing edge. This method is characterized by a simple and direct approach, leading to closed-form solutions in all cases when the airfoil contour is specified. Although the initial method was developed as a linear theory, a non-linear development is also possible [12]. This method has been extended to analyze the problems of flexible airfoils and jet-flapped airfoils, in which the shape of the jet sheet or the flexible membrane depends on the pressure difference across them, see Mateescu & Newman [13], Nielsen [22] and Thwaites [27].

Studies of unsteady-airfoil flows have been motivated mostly by efforts to prevent or reduce such undesirable effects as flutter and vibrations. Among the best known and most enlightening analysis of this class of problems are those by Theodorsen [26,15] and Von Kármán & Sears [28], who considered a thin flat plate and a trailing flat wake of vortices in incompressible fluid. Theodorsen developed the velocity potentials due to the unsteady flow around the airfoil. The aerodynamic forces and moments on an oscillating airfoil are then determined on this basis.

Küssner and Schwarz [5,9,25] obtained a solution of the lift and moment for an airfoil oscillating with arbitrary mode, which depends on a Fourier series expansion.

A more specific solution for the unsteady lift and moment for an airfoil was introduced by Biot [5]. The solution is limited to the special cases of an airfoil executing vertical-translation and rotational oscillations.

Many important features of the unsteady airfoil behavior were described by McCroskey [18,19]. A number of scientists such as Dietz, Schwarz, Kemp, and Basu [2,4,8,25] covered various aspects of the unsteady flow past airfoils. In these investigations, the primary objective was to obtain the lift forces and moments; therefore, computations were not made to show typical pressure distributions. Theodorsen [26] derived the forces and moments for the harmonically oscillating airfoil without actually calculating the pressure distributions. Postel and Leppert [24] have calculated pressures acting on a thin airfoil with harmonic plunging and pitching oscillations of small amplitude in incompressible flow. These previous solutions are restricted to the special cases of oscillatory translation and rotation of an airfoil. However, the previous formulas of the aerodynamic forces are complicated and are obtained for special cases of the airfoils oscillating as rigid bodies without considering the flexural oscillations.

In the present thesis, a new analytical method of solution for the analysis of the unsteady flow past airfoils and ailerons, based on velocity singularities, is developed. Closed form formulas of the aerodynamic forces along with the pressures acting on a thin airfoil oscillating with various harmonic motions are determined. The formulas obtained are of a simple and efficient form and the mathematical treatment provides an effective approach for the general case of oscillations, including the flexural oscillations.

The first objective of the present work is to obtain the solutions of the unsteady flow past oscillating airfoils, which could efficiently avoid the mathematical difficulties encountered in the classical theories. The second objective of the present study is to develop a comprehensive approach for the analysis of the unsteady flow past oscillating airfoils.

Chapter 2 is devoted to the problem formulation of the steady and unsteady flows past fixed or oscillating airfoils. The previous theory developed by Theodorsen [26] is also presented.

In Chapter 3, the method of velocity singularities for steady flows past airfoils is discussed. This method of solution is applied for various problems of specific airfoils. The method of velocity singularities is first validated by comparison with the exact solutions obtained by conformal transformation [13,14], and then with the results obtained by Nielsen [22] and Thwaites [27] for flexible-membrane airfoils.

In Chapter 4, a new method for the analysis of the unsteady flow past oscillating airfoils using velocity singularities is presented. The method is extended to the analysis of the unsteady flow past airfoils with oscillating ailerons. The aerodynamic forces and the pressure distribution on the oscillating airfoils and ailerons are then determined.

The solutions of the flow past airfoils executing more general oscillations such as, flexural oscillations are also determined.

Chapter 5 presents numerical results for various cases of oscillating airfoils obtained with the method of solution developed in Chapter 4. First, the present solutions are compared for validation with the results obtained by Theodorsen [26] and Postel & Leppert [24] for the case of oscillations in translation and pitching rotation. Then, the present solutions obtained for airfoils with ailerons executing flexural oscillations are presented.

The last chapter is devoted to the conclusions and recommendations for future further studies.

Chapter 2

Problem formulation and review of Theodorsen theory

2.1 Problem formulation

Consider the flow around an airfoil having an angle of attack α with respect to the free stream velocity U_∞ as shown in Figure 2.1.

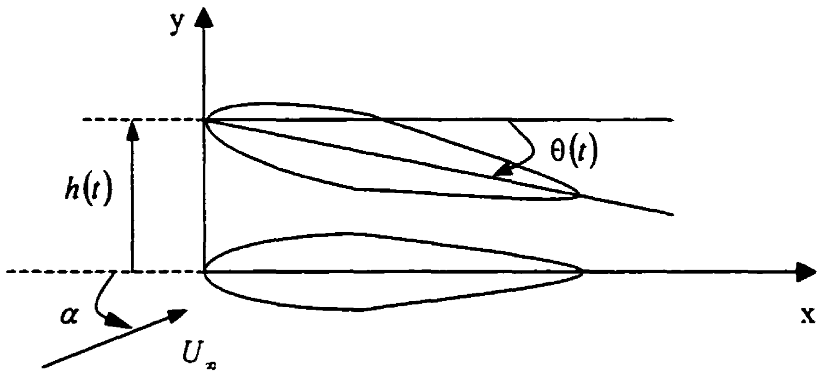

Fig 2.1 Geometry of an airfoil at an incidence α in uniform flow of velocity U_∞.

The airfoil could be stationary or can execute various types of oscillations. The most common types of oscillations are the linear translation and the pitching rotation defined, respectively, as,

$$h(t) = h_0 \cos(\omega t + \varphi_h), \tag{2-1}$$

$$\theta(t) = \theta_0 \cos(\omega t + \varphi_\theta), \tag{2-2}$$

where, ω and t are the frequency of oscillations and the time, respectively. In linear translation oscillations, h_0 and φ_h are the amplitude and the phase angle. Similarly, θ_0 and φ_θ are the amplitude and the phase angle of the pitching rotation oscillations.

The above equations can also be expressed in complex form as,

$$h(t) = \mathrm{Re}\left\{\hat{h}\, e^{i\omega t}\right\}, \tag{2-3}$$

$$\theta(t) = \mathrm{Re}\left\{\hat{\theta}\, e^{i\omega t}\right\}, \tag{2-4}$$

where the complex amplitudes $\hat{h}$ and $\hat{\theta}$ are defined by,

$$\hat{h} = h_0\, e^{i\varphi_h}, \tag{2-5}$$

$$\hat{\theta} = \theta_0\, e^{i\varphi_\theta}, \tag{2-6}$$

For simplification, in the following, the real part symbol, $\mathrm{Re}\{\ \}$, will be omitted and thus equations (2-3), (2-4) are expressed in the form,

$$h(t) = \hat{h}\, e^{i\omega t}, \tag{2-7}$$

$$\theta(t) = \hat{\theta}\, e^{i\omega t}. \tag{2-8}$$

However, this will imply that the real part will have to be taken from the final complex solution (in fact, this is a common practice for this type of harmonic oscillation problems).

The velocity potential equation for unsteady potential flows defined by the fluid velocity and velocity components is,

$$\nabla\cdot\mathbf{V} - \frac{\mathbf{V}}{2a^2}\cdot\nabla\left(V^2\right) = \frac{1}{a^2}\left[\frac{\partial^2\phi}{\partial t^2} + \frac{\partial}{\partial t}\left(V^2\right)\right], \tag{2-9}$$

where, ϕ represents the velocity potential and $\overline{\mathbf{V}}$ is the fluid velocity, are defined as,

$$\overline{\mathbf{V}} = \nabla\phi\ , \tag{2-10}$$

$$\overline{\mathbf{V}} = \left(U_\infty\cdot\cos\alpha + u\right)\cdot\mathbf{i} + \left(U_\infty\cdot\sin\alpha + v\right)\cdot\mathbf{j}\ . \tag{2-11}$$

The Bernoulli-Lagrange equation for barotropic incompressible fluids (for which the density is a function of pressure only) is,

$$\frac{\partial\phi}{\partial t} + \frac{1}{2}V^2 + \frac{p}{\rho} = C(t)\ . \tag{2-12}$$

The pressure coefficient equation in second order approximation is,

$$C_p = -\left(\frac{V^2}{U_\infty^2} - 1\right) - \frac{2}{U_\infty^2}\cdot\frac{\partial\phi}{\partial t} + \frac{1}{4}M_\infty^2\left[\frac{V^2}{U_\infty^2} - 1 + \frac{2}{U_\infty^2}\frac{\partial\phi}{\partial t}\right]^2, \tag{2-13}$$

It is important to note that in the case of incompressible unsteady potential flows, the velocity potential equation and the pressure coefficient equation are,

$$\nabla \cdot \overline{\mathbf{V}} = 0 , \tag{2-14}$$

$$C_p = \frac{p - p_\infty}{\frac{1}{2}\rho U_\infty^2} , \tag{2-15}$$

$$C_p = -\left(\frac{V^2}{U_\infty^2} - 1 \right) - \frac{2}{U_\infty^2} \frac{\partial \phi}{\partial t} . \tag{2-16}$$

In Cartesian coordinates, the perturbation velocity components (u, v) and the perturbation velocity potential (φ) equations are,

$$u = \frac{\partial \varphi}{\partial x} \quad , \quad v = \frac{\partial \varphi}{\partial y} \quad . \tag{2-17}$$

$$\frac{\partial^2 \varphi}{\partial x^2} + \frac{\partial^2 \varphi}{\partial y^2} = 0 . \tag{2-18}$$

Boundary conditions

The boundary condition on an airfoil executing vertical translation and pitching rotation oscillations is determined in the assumption of small amplitude oscillations. Consider a body executing a small oscillations, the equation of the body surface is expressed generally as,

$$f(x, y, z, t) = 0 , \tag{2-19}$$

The boundary condition on the body surface is given by,

$$\frac{\partial f}{\partial t} + \left(\overline{\mathbf{U}}_\infty + \overline{\mathbf{q}} \right) \cdot \nabla f = 0 . \tag{2-20}$$

where, $\mathbf{U}_\infty$ is the uniform stream velocity and $\overline{\mathbf{q}}$ is the disturbance velocity.

Consider a flat plate airfoil in oscillation as shown in Figure 2.2.

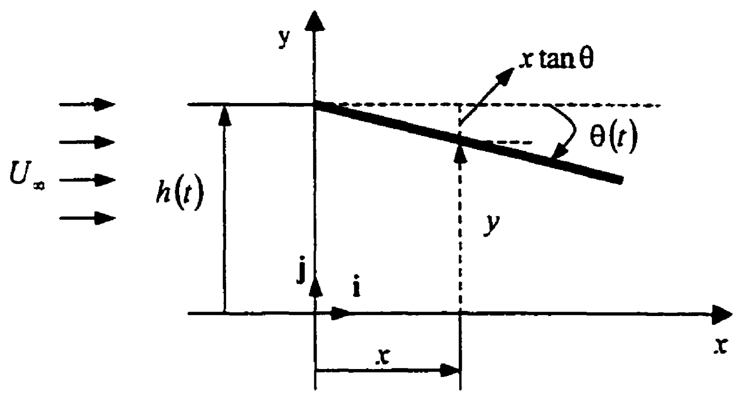

Fig 2.2 Geometry of a flat plate airfoil executing translation and pitching rotation oscillations.

The equation of the body surface of flat plate airfoil is.

$$y = h(t) - x\tan\theta. \tag{2-21}$$

In the assumption of small amplitude oscillations ($\tan\theta \approx \theta$), the equation of the body surface $f(x, y, t)$, is expressed as,

$$f(x, y, t) = y + x\cdot\theta(t) - h(t) = 0. \tag{2-22}$$

The boundary condition on the oscillating plate is derived from,

$$\frac{\partial f}{\partial t} + (\overline{\mathbf{U}}_\infty + \overline{\mathbf{q}})\cdot\nabla f = 0, \tag{2-23}$$

where, U_∞ is the uniform stream velocity and $\overline{q}$ is the disturbance velocity. The equations of which, are expressed as,

$$\overline{\mathbf{U}}_\infty = \mathbf{i}U_\infty, \tag{2-24}$$

$$\overline{\mathbf{q}} = \mathbf{i}u + \mathbf{j}w, \tag{2-25}$$

in which, ∇f is derived from,

$$\nabla f = \mathbf{i}\frac{\partial f}{\partial x} + \mathbf{j}\frac{\partial f}{\partial y}, \tag{2-26}$$

The values of $\dfrac{\partial f}{\partial t}$ and ∇f in equation (2-23) are expressed as.

$$\frac{\partial f}{\partial t} = x\frac{d\theta}{dt} - \frac{dh}{dt} \,, \tag{2-27}$$

$$\nabla f = \mathbf{i}\,\theta(t) + \mathbf{j}\,1, \tag{2-28}$$

The vertical translation and pitching rotation oscillations are given by,

$$h(t) = \hat{h}\,e^{i\omega t}, \tag{2-29}$$

$$\theta(t) = \hat{\theta}\,e^{i\omega t}, \tag{2-30}$$

The value of the time derivative $\dfrac{\partial f}{\partial t}$ is expressed as,

$$\frac{\partial f}{\partial t} = i\omega\left[\hat{\theta}\,x - \hat{h}\,\right]e^{i\omega t}, \tag{2-31}$$

Hence, the boundary condition on the oscillating plate is,

$$w(x,y,t)\Big|_{plate} = \left[-U_\infty\,\hat{\theta} + i\omega\left(\hat{h} - \hat{\theta}\,x\right)\right]e^{i\omega t}. \tag{2-32}$$

which can be expressed as.

$$w(x,y,t)\Big|_{plate} = \left[\,\hat{w}(x,y)\,\right]_{plate}\;e^{i\omega t}, \tag{2-33}$$

where the reduced vertical disturbance velocity $\hat{w}(x,y)$ is expressed as,

$$\hat{w}(x,y)\Big|_{plate} = -U_\infty\;\hat{\theta} + i\omega\left(\,\hat{h} - \hat{\theta}\,x\,\right). \tag{2-34}$$

2.2 Previous studies for unsteady flows past oscillating airfoils: Theodorsen's theory

The unsteady flow past an airfoil oscillating around a mean position defined by the mean incidence α, can be decomposed into the steady flow past the fixed airfoil at the mean incidence α and the unsteady motion past an oscillating flat plate in the assumption of small perturbations, Figure 2.3.

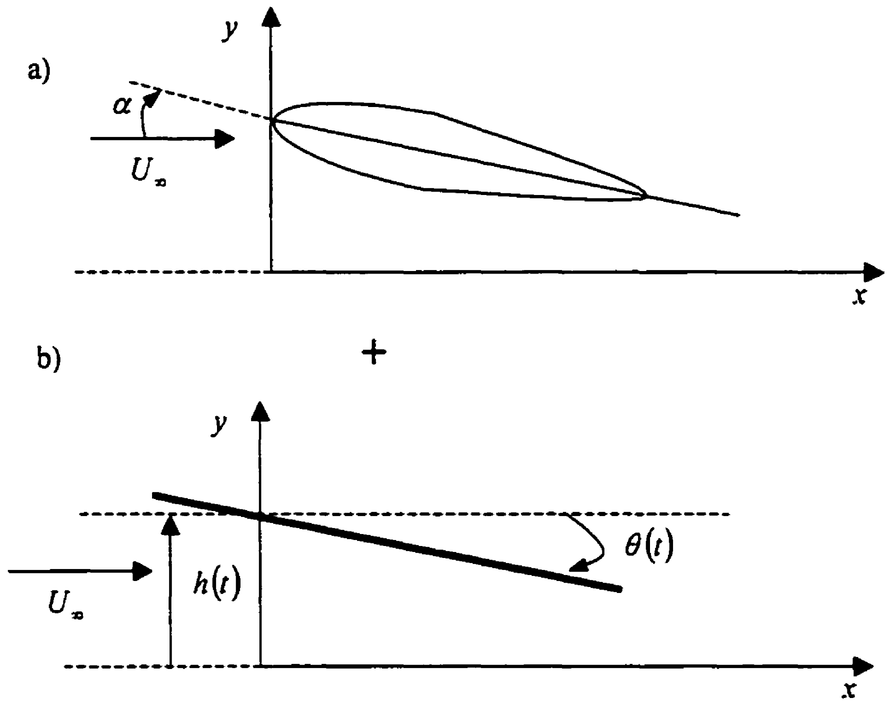

Fig 2.3 Decomposition of the unsteady flow around an oscillating airfoil into: (a) The steady flow past a fixed airfoil, and (b) The unsteady motion past an oscillating flat plate.

For the unsteady flow past an oscillating plate, Theodorsen [15,26] has developed a method to determine the aerodynamic forces on an oscillating airfoil. The theory was based on the potential flow and the Kutta condition. In this method, the perturbation velocity potential, φ, around the oscillating airfoil is decomposed into two parts:(i) the perturbation potential φ_1, corresponding to the motion without circulation around the airfoil, and, (ii) the potential φ_2, corresponding to the motion with circulation due to the shedding vortices.

The equation of the perturbation potential for the unsteady incompressible flow is given by,

$$\nabla^2\varphi = \frac{\partial^2\varphi}{\partial x^2} + \frac{\partial^2\varphi}{\partial y^2} = 0, \tag{2-35}$$

The pressure coefficient equation is given by,

$$C_p(x,y,t) = -\frac{2}{U_\infty^2}\left(\frac{\partial\varphi}{\partial t} + U_\infty\frac{\partial\varphi}{\partial x}\right), \tag{2-36}$$

Introducing the reduced potential $\hat{\varphi}(x,y)$ and the reduced pressure coefficient $\hat{C}_p(x,y)$ in the form,

$$\varphi(x,y,t) = \hat{\varphi}(x,y)e^{i\omega t}, \tag{2-37}$$

$$C_p(x,y,t) = \hat{C}_p(x,y)e^{i\omega t}, \tag{2-38}$$

the above equations become,

$$\nabla^2\hat{\varphi} = \frac{\partial^2\hat{\varphi}}{\partial x^2} + \frac{\partial^2\hat{\varphi}}{\partial y^2} = 0, \tag{2-39}$$

$$\hat{C}_p(x,y) = -\frac{2}{U_\infty^2}\left(i\omega\hat{\varphi}(x,y) + U_\infty\frac{\partial\hat{\varphi}}{\partial x}\right), \tag{2-40}$$

The general form of the boundary condition on the oscillating airfoil is given by,

$$w(x,0,t)\big|_{airfoil} = W(x,t), \tag{2-41}$$

where,

$$W(x,t) = \hat{W}(x)e^{i\omega t}. \tag{2-42}$$

For the considered case of plunging and pitching oscillations, the boundary conditions are given by equation (2-34).

$$\hat{w}(x,y)\big|_{plate} = -U_\infty\ \hat{\theta} + i\omega\left(\hat{h} - \hat{\theta}x\right). \tag{2-43}$$

In this manner, the unsteady aerodynamics problem has been reduced to the study of the reduced motion defined by the reduced potential.

2.2.1 Motion without circulation

Consider the flow without circulation around a flat plate, the effect of the vertical velocity jump is replaced by a source $(+\Delta Q)$ and sink $(-\Delta Q)$ system situated on the upper and lower sides of the plate as shown in Figure 2.4. The relation between the velocity jump and the strength of the source (ΔQ) is given by.

$$\Delta Q = 2bW(x_1,t)dx_1, \tag{2-44}$$

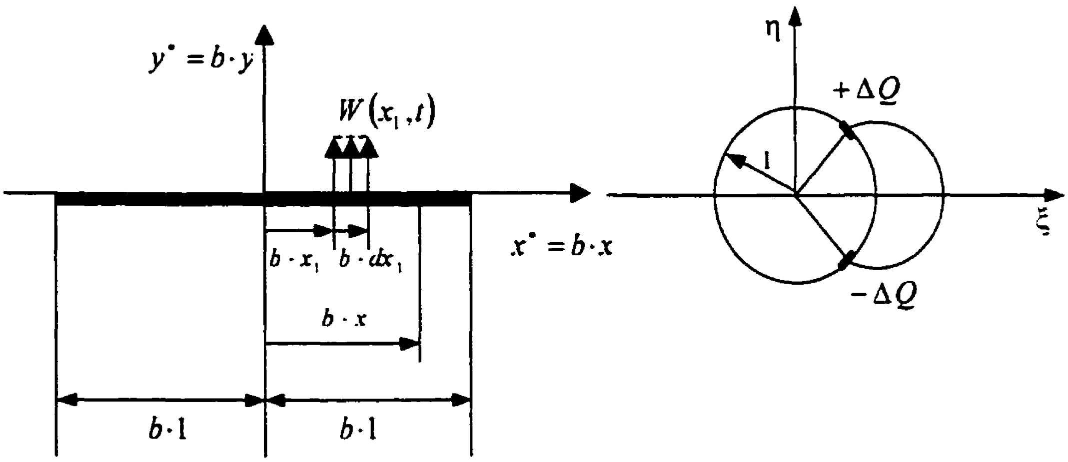

Fig 2.4 Effect of a jump in the vertical velocity on a flat plate in the motion without circulation.

Joukowski's conformal transformation is used to transform the flat plate in the plane $z = x + iy$ into a circle in the plane $\zeta = \xi + i\eta$. The transformation is defined by,

$$z = \frac{1}{2}\left(\zeta + \frac{1}{\zeta}\right), \tag{2-45}$$

The complex potential of the source and sink is given by,

$$F_1(\zeta) = \frac{\Delta Q}{2\pi} \ln \frac{\zeta - \zeta_1}{\zeta - \bar{\zeta}_1}, \tag{2-46}$$

where,

$$\zeta - \zeta_1 = \rho_1 e^{i\theta_1} \rightarrow \left\{ \begin{aligned} \rho_1 &= \sqrt{(x - x_1)^2 + \left(\sqrt{1 - x^2} - \sqrt{1 - x_1^2}\right)^2} \\ \theta_1 &= \tan^{-1} \frac{\sqrt{1 - x^2} - \sqrt{1 - x_1^2}}{x - x_1} \end{aligned} \right\}, \tag{2-47}$$

$$\zeta - \bar{\zeta}_1 = \rho_2 e^{i\theta_2} \rightarrow \left\{ \begin{aligned} \rho_2 &= \sqrt{(x-x_1)^2 + \left(\sqrt{1-x^2} + \sqrt{1-x_1^2}\right)^2} \\ \theta_2 &= \tan^{-1} \frac{\sqrt{1-x^2} + \sqrt{1-x_1^2}}{x - x_1} \end{aligned} \right\}. \tag{2-48}$$

The velocity perturbation potential for the flow without circulation is denoted by,

$$d\varphi_1(x,x_1,t) = W(x_1,t)\ \frac{b \cdot d x_1}{2\pi}\ L(x,x_1), \tag{2-49}$$

where,

$$L(x,x_1) = \ln \frac{(x-x_1)^2 + \left(\sqrt{1-x^2} - \sqrt{1-x_1^2}\right)^2}{(x-x_1)^2 + \left(\sqrt{1-x^2} + \sqrt{1-x_1^2}\right)^2}, \tag{2-50}$$

The axial perturbation velocity is given by,

$$d u_1(x,x_1,t) = \frac{\partial}{b \cdot \partial x}\left[d\varphi_1(x,x_1,t)\right] = W(x_1,t)\,\frac{d x_1}{\pi}\,\frac{\sqrt{1-x_1^2}}{(x-x_1)\sqrt{1-x^2}}. \tag{2-51}$$

The corresponding pressure coefficient is expressed by,

$$C_{p1} = -\frac{2}{U_\infty^2}\left(\frac{\partial(d\varphi_1)}{\partial t} + U_\infty \frac{\partial(d\varphi_1)}{\partial x}\right). \tag{2-52}$$

The pressure difference across the plate is given by,

$$\frac{d}{d x_1}\left[\Delta p_1(x,x_1,t)\right] = \frac{2\rho}{\pi} U_\infty W(x_1,t) \frac{\sqrt{1-x_1^2}}{(x-x_1)\sqrt{1-x^2}} + \frac{\rho}{\pi} b \frac{\partial W(x_1,t)}{\partial t} . L(x,x_1). \tag{2-53}$$

2.2.2 Motion with circulation around a flat plate

The motion with circulation around a flat plate is studied by considering an elementary shedding vortex $\Delta\Gamma$ situated downstream at $z = x_0$. Joukowski's conformal transformation is used to transform the flat plate into a circle and hence, a vortex of opposite sense has to be introduced inside the circle at the symmetrical point in order to render the circle, the streamline property, as shown in Figure 2.5.

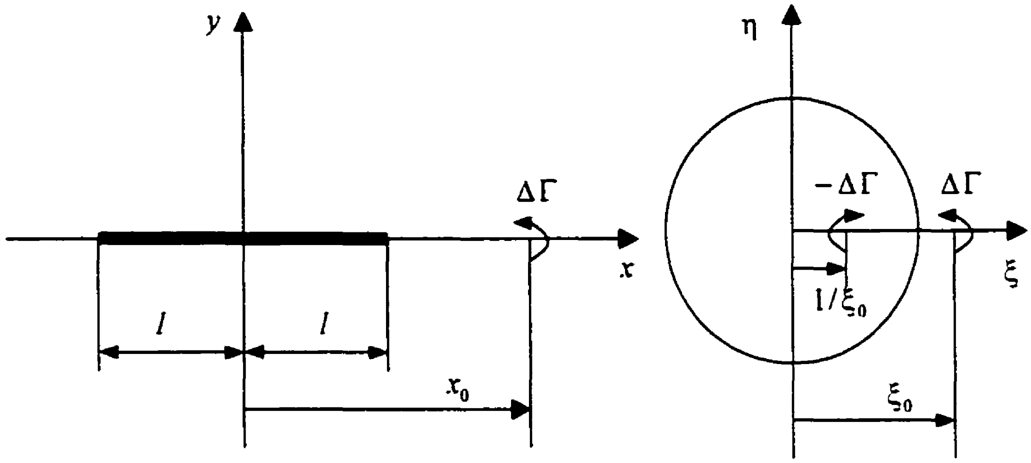

Fig 2.5 Motion with circulation around a flat plate due to a vortex placed downstream.

The complex potential is given by,

$$F_2(\zeta) = -\frac{i\Delta\Gamma}{2\pi}\ln\frac{\zeta-\xi_0}{\zeta-1/\xi_0}, \tag{2-54}$$

where $\zeta = z+\sqrt{z^2-1}$.

The perturbation velocity potential is,

$$d\varphi_2 = \frac{\Delta\Gamma}{2\pi}\tan^{-1}\frac{\sqrt{x_0^2-1}\ \sqrt{1-x^2}}{1-x_0\ x}, \tag{2-55}$$

The axial perturbation velocity is,

$$du_2 = \frac{\partial\varphi_2}{\partial x} = -\frac{\Delta\Gamma}{2\pi}\frac{\sqrt{x_0^2-1}}{(x-x_0)\ \sqrt{1-x^2}}, \tag{2-56}$$

In the unsteady case, at any instant of time t, a free vortex $\frac{d\Gamma}{dt}dt$ is shedding at the trailing edge of the profile. Since this free vortex is moving downstream with the velocity U_∞ of the uniform stream, the intensity of the free vortex distribution γ_f, along the axis of the plate, is expressed as,

$$\gamma_f(1,t) = -\frac{1}{U_\infty}\frac{d\Gamma}{dt} = \gamma_0^* e^{i\omega t}, \tag{2-57}$$

A free vortex located at the instant t at the distance $b\,x_0$, was shedding at the trailing edge at a previous instant of time, and hence,

$$\gamma_f(x_0,t) = \gamma_f\left(1, t - b\frac{x_0 - 1}{U_\infty}\right), \tag{2-58}$$

The reduced frequency k and the harmonic oscillations are given by,

$$k = \frac{\omega b}{U_\infty}, \tag{2-59}$$

$$\gamma_f(x_0,t) = \gamma_0^* e^{ik} e^{-ikx_0} e^{i\omega t}, \tag{2-60}$$

where, γ_0^* is a constant that will be determined by imposing the Kutta condition at the trailing edge of the profile. The free vortex distribution is related to the perturbation potential by,

$$\Delta\Gamma = \gamma_f(x_0,t)\; b\,dx_0 \ . \tag{2-61}$$

Since the free vortex is moving towards downstream with the velocity of the free stream, the pressure coefficient corresponding to the purely circulatory motion produced by the perturbation velocity potential after considering the effect of all the free vortices situated in the wake of the oscillating airfoil, is given by,

$$d\Delta p_2 = \rho U_\infty \gamma_0^* e^{ik} e^{i\omega t} \frac{2}{\pi}\frac{1}{\sqrt{1-x^2}} \int_1^\infty e^{-ikx_0} \frac{x_0 + x}{\sqrt{x_0^2 - 1}} dx_0 \ . \tag{2-62}$$

2.2.3 Complete motion

By adding the potential corresponding to the motion without circulation around the flat plate, due to the normal velocity jump $W(x_1, t)$, and the potential corresponding to the pure circulatory motion, produced by the shedding free vortices in the wake of the airfoil, one obtains the total perturbation velocity potential for the complete motion around the oscillating plate or airfoil.

Replacing the unknown constant $\gamma_0^{\bullet}$ by the equation,

$$\gamma_0^{\bullet} = \gamma_0 \frac{W(x_1, t)\ dx_1}{e^{ik}\ e^{i\omega t}}, \tag{2-63}$$

and imposing the Kutta condition at the trailing edge of the profile, one obtains the unknown constant γ_0. The axial disturbance velocity is given by,

$$d\,u(x, x_1, t) = W(x_1, t)\frac{dx_1}{\pi}\left[\frac{\sqrt{1-x_1^2}}{x-x_1} + \frac{1}{2}\gamma_0 \int_1^{\infty} e^{-ikx_0} \frac{\sqrt{x_0^2-1}}{x_0 - x} dx_0\right]\frac{1}{\sqrt{1-x^2}}, \tag{2-64}$$

By imposing the Kutta condition at the trailing edge $(x = 1)$, one obtains,

$$\left[d\,u(x, x_1, t)\right]_{x=1} = \text{finite}, \tag{2-65}$$

$$\gamma_0 = \frac{4}{\pi} \frac{1}{H_1^{(2)}(k) + i H_0^2(k)} \sqrt{\frac{1+x_1}{1-x_1}}, \tag{2-66}$$

where $H_0^{(2)}(k)$, $H_1^{(2)}(k)$ represent the Hankel functions of second kind of orders zero and one [7,20,29]. See Appendices A and B for details. The pressure difference across the plate combines a quasi-steady term, inertia force term and the effect of the free vortices in the wake of the airfoil. The equation of the pressure equation is given by,

$$\begin{aligned}\Delta p(x,t) = &\frac{2}{\pi}\rho U_\infty \sqrt{\frac{1-x}{1+x}} \int_{-1}^{1} W(x_1, t) \sqrt{\frac{1+x_1}{1-x_1}} \frac{dx_1}{x-x_1} \\ &+ \frac{1}{\pi}\rho b \int_{-1}^{1} \frac{\partial W(x_1, t)}{\partial t} \cdot L(x, x_1) \cdot dx_1 \qquad , \\ &+ \frac{2}{\pi}\rho U_\infty \left[1 - C(k)\right] \cdot \sqrt{\frac{1-x}{1+x}} \int_{-1}^{1} W(x_1, t) \sqrt{\frac{1+x_1}{1-x_1}} dx_1\end{aligned} \tag{2-67}$$

where Theodorsen's function $C(k)$, is defined as,

$$C(k)=\frac{H_1^{(2)}(k)}{H_1^{(2)}(k)+iH_0^{(2)}(k)}=F(k)+iG(k), \tag{2-68}$$

where $H_0^{(2)}(k)$, $H_1^{(2)}(k)$ represent the Hankel functions of second kind of orders zero and one [7,20,29]. See Appendices A and B for details.

The function $L(x,x_1)$ is given by,

$$L(x,x_1)=\ln\frac{(x-x_1)^2+\left(\sqrt{1-x^2}-\sqrt{1-x_1^2}\right)^2}{(x-x_1)^2+\left(\sqrt{1-x^2}+\sqrt{1-x_1^2}\right)^2}. \tag{2-69}$$

Theodorsen's results are presented for the following oscillatory motions of the airfoil (Figure 2.6),

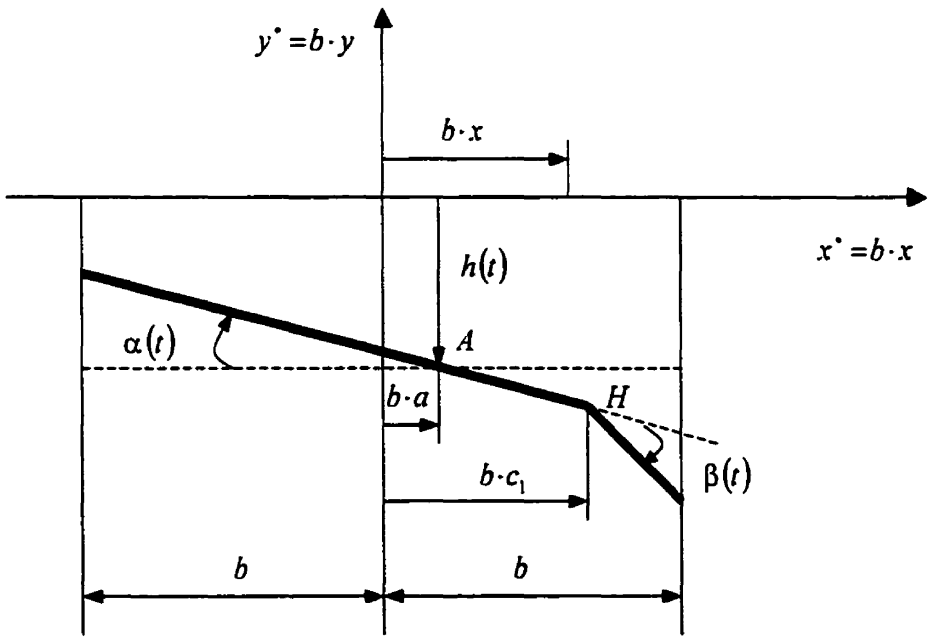

Fig 2.6 Flat plate geometry as presented in Theodorsen's solution.

The oscillations of the airfoil are denoted as,

$$h(t)=\hat{h}\cdot e^{i\omega t}, \tag{2-70}$$

$$\alpha(t)=\hat{\alpha}.e^{i\omega t}, \tag{2-71}$$

$$\beta(t)=\hat{\beta}\cdot e^{i\omega t}, \tag{2-72}$$

The boundary conditions on the airfoil-aileron combination are defined as,

$$W(x,t) = -\alpha U_\infty - \dot{h} - b(x-a)\dot{\alpha} \qquad \text{for } x \in (-1, c_1), \tag{2-73}$$

$$W(x,t) = -\alpha U_\infty - \dot{h} - b(x-a)\dot{\alpha} - b(x-c_1)\dot{\beta} - \beta U_\infty \qquad \text{for } x \in (c_1, 1). \tag{2-74}$$

The lift force is given by,

$$L = \pi \rho b^3 \omega^2 \left\{ P_\omega \frac{h}{b} + \left[P_\varphi - \left(\frac{1}{2} + a \right) P_\omega \right] \alpha + P_\beta \, \beta \right\}, \tag{2-75}$$

The pitching moment equation is,

$$M_A = \pi\rho b^4 \omega^2 \{ \left[M_\omega - \left(\frac{1}{2} + a \right) P_\omega \right] \frac{h}{b} + \left[M_\varphi - \left(\frac{1}{2} + a \right) (P_\varphi + M_\omega) + \left(\frac{1}{2} + a \right)^2 P_\omega \right] \alpha + + \left[M_\beta - \left(\frac{1}{2} + a \right) P_\beta \right] \beta \} \tag{2-76}$$

The hinge moment equation is given by,

$$M_H = \pi \rho b^4 \omega^2 \left\{ T_\omega \frac{h}{b} + \left[T_\varphi - \left(\frac{1}{2} + a \right) T_\omega \right] \alpha + T_\beta \, \beta \right\}. \tag{2-77}$$

A list of the terms that appear in the above formulas is given in Appendix B.

Chapter 3

Method of velocity singularities for steady flows

3.1 Method of velocity singularities for steady flows past airfoils

Prototype Problem

Consider a very thin airfoil extending on the real axis in the complex plane $z = x + \mathbf{i}\,y$ from $z = 0$ to $z = c$ with a sudden change of slope, due to a single ridge, at $z = s$ Figure 3.1. A typical configuration of a flapped, otherwise uncambered airfoil Figure 3.1a is first considered. This gives the basic singularities at the leading edge $L(x=0)$ and the ridge $R(x=s)$, where the airfoil slope suddenly changes by an angle β.

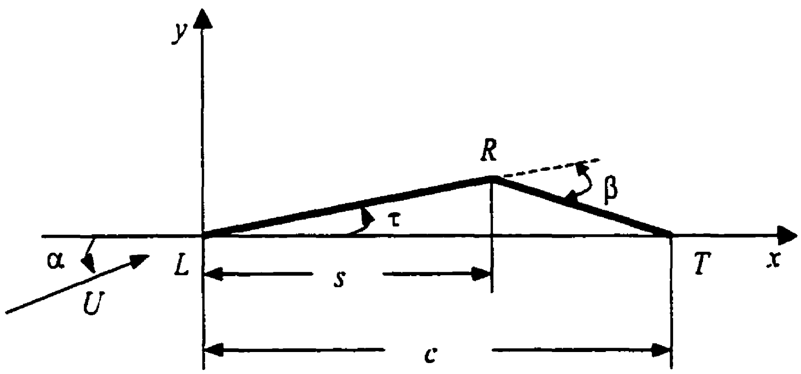

a)

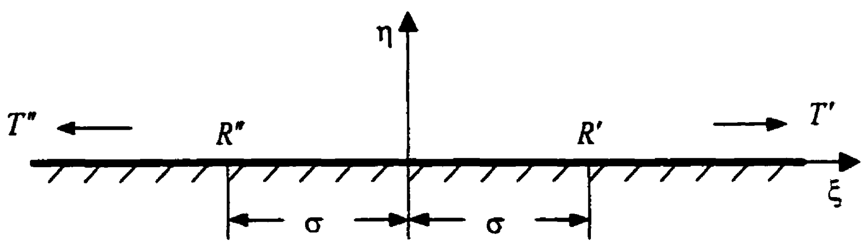

b)

Fig 3.1 Geometry of a thin flapped airfoil: a) in the physical complex plane; b) in the complex plane defined by the conformal transformation.

The boundary conditions are,

$$v=\begin{cases}U(\tau-\alpha)=v_0, & \text{for } 0<x<s\\ U(\tau-\alpha-\beta)=v_0+\Delta v. & \text{for } s<x<c\end{cases} \tag{3-1}$$

where α is the angle of attack, τ is the leading-edge slope with respect to the cord, $v_0=U(\tau-\alpha)$ represents the normal-to-chord perturbation velocity v at the leading edge and $\Delta v=-\beta U$ denotes the change in v at the ridge. In the complex plane $z=x+\mathbf{i}\,y$, the conjugate complex perturbation velocity is defined as,

$$w(z)=u-\mathbf{i}(v-v_0). \tag{3-2}$$

The boundary conditions (3-1) applied on the airfoil chord are, thereby, simplified to,

$$\mathrm{IMAG}[\mathrm{w}(\mathrm{z})]_{z=x}=\begin{cases}0 & \text{for } 0<x<s\\ -\Delta v & \text{for } s<x<c\end{cases}, \tag{3-3}$$

and, due to the antisymmetric nature of the perturbation flow past the airfoil in the complex plane,

$$\mathrm{REAL}[w(z)]_{z=x}=0 \qquad \text{for } \mathrm{x}<0,\ \mathrm{x}>\mathrm{c}. \tag{3-4}$$

The local behavior of the perturbation velocities at the leading and trailing edges are, respectively,

$$\begin{aligned} &w(z)\Big|_{z\to 0}\to\frac{A_0}{\sqrt{z}} \qquad (\text{where } A_0 \text{ is independent of z})\\ &\mathrm{REAL}[w(z)]_{z\to c}=0 \end{aligned}. \tag{3-5}$$

where the first condition represents the leading-edge singularity for a flat plate at $z=0$, and the second is the Kutta condition at the trailing edge $(z=c)$.

The complex velocity $w(z)$ should also contain a logarithmic singularity in order to provide the jump Δv at the ridge $(z=s)$:

$$w(z)\Big|_{z\to s}=\frac{\Delta v}{\pi}\ln(z-s). \tag{3-6}$$

Indeed, considering $z - s = r_1 e^{i\theta}$ in the vicinity of the ridge $R(z = s)$ Figure 3.2, one can successively write,

$$\mathrm{Imag}\{w(z)\}_{z=x_B} - \mathrm{Imag}\{w(z)\}_{z=x_A} = \mathrm{Imag}\left\{\frac{\Delta v}{\pi}\ln\left(r_1 e^{i\theta}\right)\right\}_{z=x_A}^{z=x_B} = \frac{\Delta v}{\pi}[\theta]_{\theta_A=\pi}^{\theta_B=0} = -\Delta v. \tag{3-7}$$

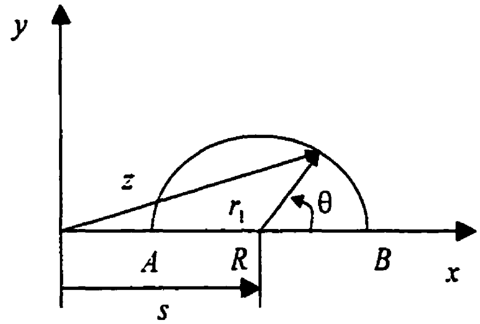

Fig 3.2 The jump of the imaginary component of the complex velocity $w(z)$.

The expression of $w(z)$ can be easily determined in an auxiliary plane $\zeta = \xi + i\eta$ Figure 3.1b, defined by the conformal transformation of the Schwarz-Christoffel type.

$$\zeta^2 = \frac{z}{(c - z)}. \tag{3-8}$$

which transforms the airfoil (the x axis between 0 and c) into the whole of the real axis in the ζ plane, and the rest of the x axis into the imaginary axis. The velocity components do not change under conformal transformation in contrast to the usual complex potential theory, the boundary conditions become,

$$\mathrm{IMAG}[w]_{\eta=0} = \begin{cases} 0 & \text{for } -\sigma < \xi < \sigma \\ -\Delta v & \text{for } \xi < -\sigma,\ \zeta > \sigma \end{cases}, \tag{3-9}$$

$$\left[\text{where } \sigma = \sqrt{s/(c-s)}\right]$$

$$\mathrm{REAL}[w]_{\xi=0} = 0. \tag{3-10}$$

The leading-edge singularity becomes a doublet singularity $1/\zeta$ at the origin, and the ridge singularity becomes in this plane $\pm(\Delta v/\pi)\ln(\zeta \mp \sigma)$, and, thus,

$$w = A\frac{1}{\zeta} + \frac{\Delta v}{\pi}\left[\ln\frac{\zeta - \sigma}{\zeta + \sigma} - i\pi\right], \tag{3-11}$$

where the constant A has to be determined.

In the physical complex plane z, the solution becomes,

$$w(z) = A\sqrt{\frac{c-z}{z}} - \frac{2}{\pi}\Delta v \cosh^{-1}\sqrt{\frac{(c-z)s}{c(s-z)}}. \tag{3-12}$$

and the constant A comes from the requirement that $u = v = 0$ at $z \to -\infty$, resulting in,

$$A = -v_0 - \frac{2}{\pi}\Delta v \cos^{-1}\sqrt{\frac{s}{c}} = U\left[\alpha - \tau + \frac{2}{\pi}\beta \cos^{-1}\sqrt{\frac{s}{c}}\right], \tag{3-13}$$

On the upper surface of the airfoil $(y = 0, z = x)$, the chordwise perturbation velocity $u = \text{REAL } w(z)$ may, therefore, be expressed as,

$$u(x) = A\sqrt{\frac{c-x}{x}} - \frac{2}{\pi}\Delta v G(c,s,x), \tag{3-14}$$

where the singular ridge contribution $G(c,s,x)$ is defined as,

$$G(c,s,x) = \begin{cases} \cosh^{-1}\sqrt{\dfrac{(c-x)s}{c(s-x)}} & \text{for } 0 < x < s \\ \sinh^{-1}\sqrt{\dfrac{(c-x)s}{c(x-s)}} & \text{for } s < x < c \\ 0 & \text{for } x < 0 \text{ and } x > c \end{cases}. \tag{3-15}$$

The pressure difference across the airfoil in dimensionless form $\Delta C_p = 4u/U$, where $\pm u$ are the chordwise perturbation velocity components on the upper and lower surfaces of the airfoil, can now be expressed as,

$$\Delta C_p(x) = -\frac{4}{U}\left[\left(v_0 + \frac{2}{\pi}\Delta v \cos^{-1}\sqrt{\frac{s}{c}}\right)\sqrt{\frac{c-x}{x}} + \frac{2}{\pi}\Delta v G(c,s,x)\right], \qquad (3\text{-}16)$$

where $v_0 = (\tau - \alpha)U$ and $\Delta v = -\beta U$.

The lift coefficient and the pitching moment coefficient about the leading edge are obtained by integration of the pressure coefficient over the airfoil:

$$C_L = 2\pi(\alpha - \tau) + 4\beta\left[\cos^{-1}\sqrt{\frac{s}{c}} + \sqrt{\frac{s}{c}\left(1 - \frac{s}{c}\right)}\right]. \qquad (3\text{-}17)$$

$$C_m = \frac{1}{4}C_L + 2\beta\left(\frac{s}{c}\right)^{3/2}\left(1 - \frac{s}{c}\right)^{1/2}. \qquad (3\text{-}18)$$

A comparison between the present closed-form solution and Glauert's [6,13,14] thin airfoil theory based on a modified Fourier expansion with N terms is given in Figure 3.3. One can notice that the results obtained with Galuert's theory using an increasing number of terms, in the Fourier expansion oscillate about the present closed-form solution or tend asymptotically, but very slowly, toward the present solution.

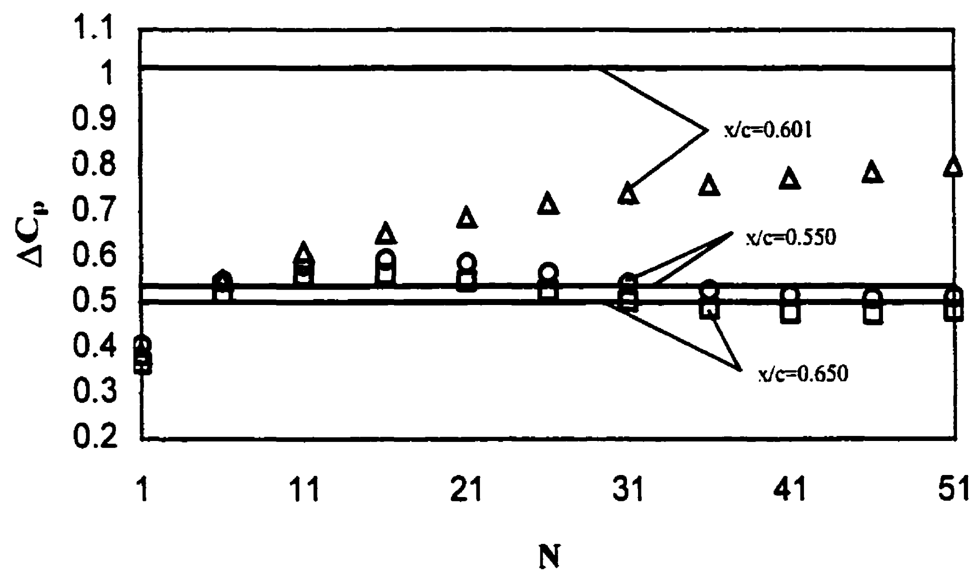

Fig 3.3 Comparison between the present solution (–) and Glauert's solution (o,Δ,□) with various number of terms N for a flapped airfoil ($\alpha = 0, \beta = 0.1$ rad, $s/c = 0.6$) at three chordwise locations.

3.2 Flow solutions for continuously cambered rigid airfoils

Consider a thin continuously cambered airfoil defined by the camber slope,

$$h'(X) = \alpha + v_b(X)/U\,, \tag{3-19}$$

where v_b is the normal-to-chord perturbation velocity v at the solid boundary, and $X = x/c$ is a nondimensional coordinate. Using the two typical singular contributions for the leading edge and ridge, the solution for any camberline shape can be obtained by superimposing infinitesimally flapped airfoils equation (3-16) in the form.

$$\begin{aligned}\Delta C_P(X) = -\frac{4}{U}\Bigg\{ &\left[v_b(0) + \frac{2}{\pi}\int_0^1 v_b'(S)\cos^{-1}\sqrt{S}\,\mathrm{d}S \right]\sqrt{\frac{1-X}{X}} \\ &+ \frac{2}{\pi}\int_0^1 v_b'(S)G(1,S,X)\,\mathrm{d}S \Bigg\}\end{aligned} \tag{3-20}$$

where $X = x/c$ and $S = s/c$.

Considering a polynomial representation for the camberline slope (which was also adopted in the design of the NACA 5 digit airfoil series),

$$h'(X) = \frac{1}{U}v_b(X) + \alpha = \sum_{k=0}^{n} h_k X^k\,, \tag{3-21}$$

the pressure difference across the airfoil is obtained in nondimensional form as,

$$\Delta C_P(X) = 4\left[\alpha - \sum_{k=0}^{n} h_k \sum_{j=0}^{k} g_{k-j} X^j \right]\sqrt{\frac{1-X}{X}}\,. \tag{3-22}$$

where,

$$g_q = \frac{1\cdot 3\cdot 5\cdots(2q-1)}{2\cdot 4\cdot 6\cdots(2q)} = \frac{(2q)!}{2^{2q}(q!)^2}, \qquad g_0 = 1\,. \tag{3-23}$$

The lift and pitching moment coefficients are,

$$C_L = 2\pi\left[\alpha - 2\sum_{k=0}^{n} h_k\, g_{k+1} \right], \tag{3-24}$$

$$C_m = \frac{\pi}{2}\left[\alpha - 4\sum_{k=0}^{n} h_k g_{k+1}\frac{k+1}{k+2} \right]. \tag{3-25}$$

Parabolic thin airfoil

Consider a parabolic thin airfoil (Figure 3.4) defined by,

$$h(x) = 4\varepsilon x\left(1 - \frac{x}{c}\right), \tag{3-26}$$

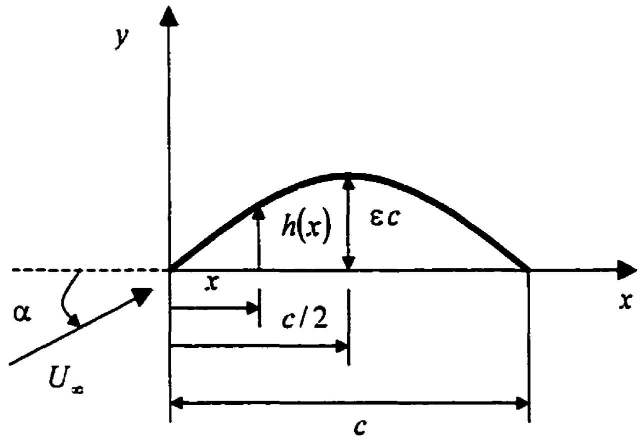

Fig 3.4 Geometry of a parabolic thin airfoil.

The derivative of the airfoil contour is expressed as,

$$h'(x) = 4\varepsilon\left(1 - 2\frac{x}{c}\right), \tag{3-27}$$

From equation (3-21),

$$h_0 = 4\varepsilon \quad , \quad h_1 = -8\varepsilon \quad \text{and} \quad h_k = 0 \quad \text{for} \quad k \geq 2. \tag{3-28}$$

The expression of the pressure difference coefficient is given by,

$$\Delta C_p(x) = 4\left(\alpha + 8\varepsilon\frac{x}{c}\right)\sqrt{\frac{c-x}{x}}, \tag{3-29}$$

The lift and pitching moment coefficients are expressed, respectively, as,

$$C_L = 2\pi(\alpha + 2\varepsilon). \tag{3-30}$$

$$C_m = \frac{\pi}{2}(\alpha + 4\varepsilon). \tag{3-31}$$

The general expression of the geometry of a circular arc airfoil is given by,

$$h(x) = -(a - \varepsilon c) + \sqrt{(a - \varepsilon c)^2 + x(c - x)}, \tag{3-32}$$

where,

$$a - \varepsilon c = \frac{c}{8\varepsilon}\left(1 - 4\varepsilon^2\right). \tag{3-33}$$

The derivative of the airfoil is expanded in Taylor series and is expressed by,

$$h'(x) = \left(1 - 2\frac{x}{c}\right)\frac{4\varepsilon}{\left(1 - 4\varepsilon^2\right)}\left[1 - \frac{1}{2}\gamma + \frac{3}{8}\gamma^2\right], \tag{3-34}$$

where,

$$\gamma = \frac{x(c - x)}{c^2}B_0 \quad \text{and} \quad B_0 = \frac{64\varepsilon^2}{\left(1 - 4\varepsilon^2\right)^2}, \tag{3-35}$$

From equation (3-21), the 9 terms are expressed by,

$$h_0 = A_1\,, h_1 = -A_1\left(2 + \frac{B_0}{2}\right), h_2 = A_1\left(\frac{3}{2}B_0 + \frac{3}{8}B_0^2\right), h_3 = -A_1\left(B_0 + \frac{3}{2}B_0^2 + \frac{5}{16}B_0^3\right), \tag{3-36}$$

$$h_4 = \left(\frac{15}{8}B_0^2 + \frac{25}{16}B_0^3 + \frac{35}{128}B_0^4\right)A_1\,, h_5 = -A_1\left(\frac{3}{4}B_0^2 + \frac{45}{16}B_0^3 + \frac{105}{64}B_0^4\right), \tag{3-37}$$

$$h_6 = A_1\left(\frac{35}{16}B_0^3 + \frac{245}{64}B_0^4\right), h_7 = -A_1\left(\frac{5}{8}B_0^3 + \frac{140}{32}B_0^4\right), \tag{3-38}$$

$$h_8 = A_1\left(\frac{315}{128}B_0^4\right), h_9 = -A_1\left(\frac{35}{64}B_0^4\right), \quad h_k = 0, k \geq 10, \tag{3-39}$$

where,

$$A_1 = \frac{4\varepsilon}{\left(1 - 4\varepsilon^2\right)}. \tag{3-40}$$

A numerical comparison made for a circular arc airfoil (with 2 and 9 terms) with a camber ratio $\varepsilon = 0.01$ and $\varepsilon = 0.02$ (at the angles of incidence $\alpha = 2^o$ and $\alpha = 5^o$) indicated that the present solution was in a very good agreement with the exact conformal transformation solution, as shown in Figures 3.5a, 3.5b.

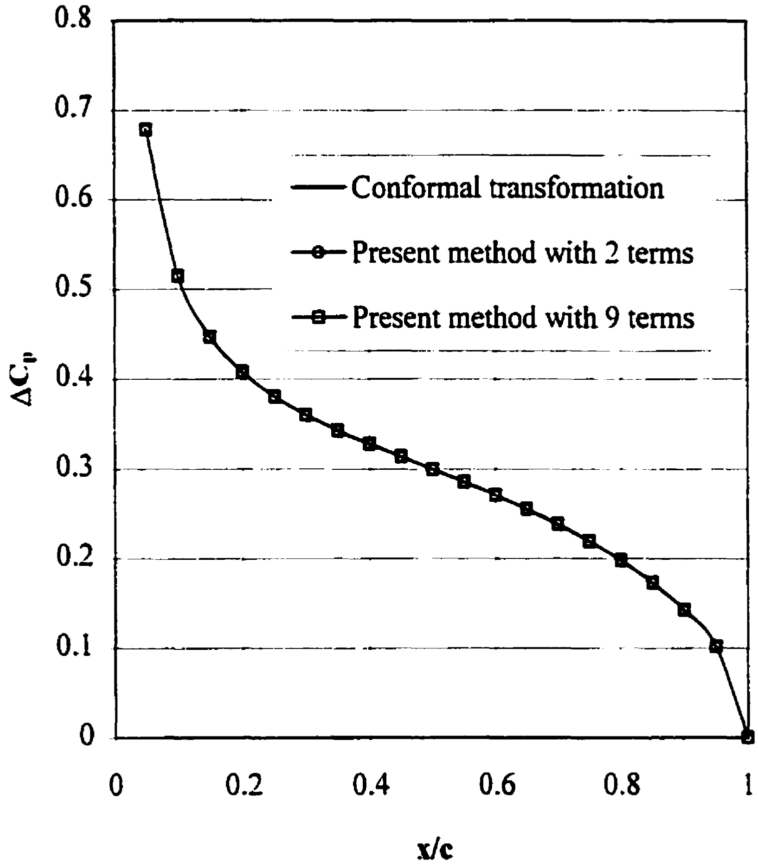

Fig 3.5a Comparison between the present solution and the exact solution for a circular arc airfoil at $\alpha = 5^o$ and $\varepsilon = 0.02$.

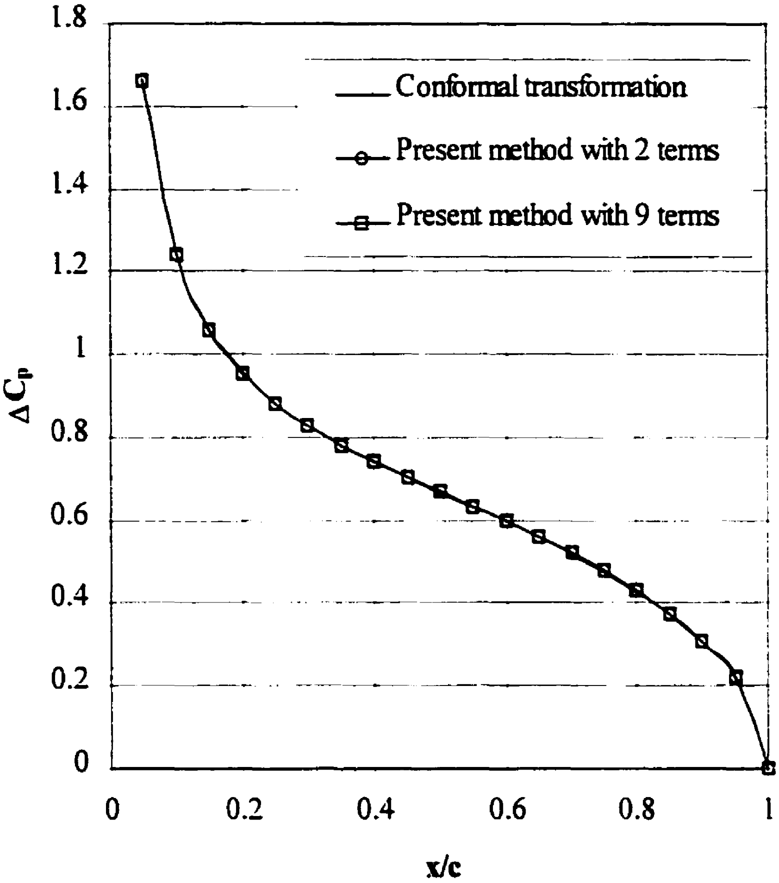

Fig 3.5b Comparison between the present solution and the exact solution for a circular arc airfoil at $\alpha = 2^{\circ}$ and $\varepsilon = 0.01$.

3.3 Flow solutions for flexible-membrane airfoils

When the airfoil is a flexible, impervious, and nonstretchable membrane (or a two-dimensional sail, as shown in Figure 3.6), its shape is unknown but it has to satisfy the normal equilibrium equation between the tension and the local pressure difference across the membrane:

$$\Delta p = \frac{T}{R} \approx -T\,h''(x), \tag{3-41}$$

The latter approximation for the radius of curvature R is for small slopes. The tension T, per unit span, can be considered constant since the skin friction is zero in theory and very small in practice.

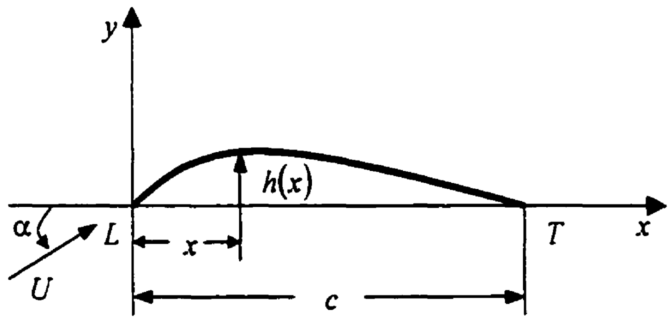

Fig 3.6 Geometry of a flexible membrane airfoil.

Introducing the nondimensional coefficient $\Delta C_p = 2\Delta p/(\rho U^2)$ and the coefficient $C_T = 2T/(\rho U^2 c)$, where c is the chord length, equation (3-41) becomes,

$$\Delta C_p = -c\,C_T\,h''(x), \tag{3-42}$$

where the nondimensional pressure difference is $\Delta C_p = 4u/U$.

The aerodynamic boundary condition on the airfoil is expressed in terms of the normal perturbation velocity component v in the form,

$$v = v_b(x) \approx [-\alpha + h'(x)]U, \tag{3-43}$$

Nielsen [13,22] treated this problem by using Glauert's [6,13,14] approach based on a modified Fourier expansion for the circulation $\gamma = 2U\,\Delta C_p$ in the form,

$$\Delta C_p = \frac{\gamma}{2U} = A_0 \tan\frac{\theta}{2} + \sum_{k=1}^{N} A_k \sin k\theta \ . \tag{3-44}$$

where the constants A_0 and A_k are related to the cosine Fourier expansion of the airfoil slope, $h'(x)$, in terms of the variable $\theta = \cos^{-1}(2x/c - 1)$ in the form,

$$\alpha - h'(x) = A_0 + \sum_{k=1}^{N} A_k \cos k\theta \,, \tag{3-45}$$

On this basis, equation (3-42) was rewritten as,

$$\frac{1}{2} C_T \sum_{k=1}^{N} k\, A_k \sin k\theta = A_0 (1 - \cos\theta) + \sin\theta \sum_{k=1}^{N} A_k \sin k\theta \,. \tag{3-46}$$

which had to be used to determine the coefficients A_0 and A_k that define the membrane shape. However, at the leading edge, $\theta = \pi$, equation (3-46) leads to $A_0 = 0$, which corresponds to the ideal incidence for which the Kutta condition is also satisfied at the leading edge. At any other incidence, the constant A_0 should not be zero, and then equation (3-46) is not satisfied at the leading edge. Nielsen [13,22] avoided this particular difficulty by expanding each term of equation (3-46), including 1 and $\cos\theta$, as sine Fourier series, and equating the coefficients of $\sin k\theta$. The present method does not contain the above ambiguity. By differentiating equation (3-43), the membrane equilibrium equation (3-42) may be recast only in terms of u and v as,

$$h''(x) = v_b'(x)/U = -\frac{4}{cC_T}\frac{u(x)}{U}. \tag{3-47}$$

For any shape of the camberline, equation (3-20) shows that u contains the factor $\sqrt{(1-X)/X} = \sqrt{(c-x)/x}$, which satisfies the Kutta condition at $X = 1$ and has the $X^{-1/2} = \sqrt{c/x}$ singularity at the leading edge. Hence, according to equation (3-47), $h''(x)$ and $v_b'(x)$ both have to contain the same singularity factor $\sqrt{(1-X)/X}$ as u.

The following expansion for $v_b(x)$ satisfies all of these requirements:

$$\frac{1}{U}v_b'(X) = h''(X) = a\left(\frac{1}{2} - 2X\right)\sqrt{\frac{1-X}{X}} + \sum_{k=1}^{n} k b_k X^{k-1}\ , \tag{3-48}$$

$$\frac{1}{U}v_b(X) = h'(X) - \alpha = aX^{1/2}(1-X)^{3/2} + \sum_{k=0}^{n} b_k X^k\ , \tag{3-49}$$

where, to satisfy the Kutta condition at the trailing edge $(X = 1)$ in equation (3-47),

$$\sum_{k=1}^{n} k b_k = 0\ . \tag{3-50}$$

The lead term of equation (3-48) contains $[(1/2) - 2X]$ and, although not essential, leads to a more compact expression for $v_b(x)$. The antisymmetrical chordwise velocity component u on the flexible membrane corresponding to the above expansion of $v_b(x)$ is obtained from equation (3-20) in the form,

$$\frac{1}{4}\Delta C_p = \frac{1}{U}u(X) = -\left\{\frac{a}{\pi}\left[\frac{1}{2} - X + X(1-X)\ln\frac{1-X}{X}\right] + \sum_{k=0}^{n} b_k \sum_{j=0}^{k} g_{k-j} X^j\right\}\sqrt{\frac{1-X}{X}}\ . \tag{3-51}$$

where g_{k-j} is defined by equation (3-23).

The camber shape of the flexible membrane can be obtained by integrating equation (3-49), in the form,

$$h(X) = c\left[\alpha X + aJ_0 + \sum_{k=0}^{n} \frac{b_k}{k+1} X^{k+1}\right], \tag{3-52}$$

where,

$$J_0 = \frac{1}{8}\cos^{-1}\sqrt{1-X} - \sqrt{(1-X)X}\left(\frac{1}{8} - \frac{7}{12}X + \frac{1}{3}X^2\right). \tag{3-53}$$

There are $(n+2)$ coefficients defining the membrane camber defined by the above equations, a and b_k $(k = 0,1,2,\dots,n)$, which have to be determined using the condition (3-50) and the membrane equilibrium equation (3-47). At the leading edge $(X = 0)$, equation (3-47), which involves u and v_b', reduces to,

$$a\frac{1}{2}\left(\frac{1}{\pi} - \frac{1}{4}C_T\right) + \sum_{k=0}^{n} b_k g_k = 0\ , \tag{3-54}$$

Other $(n-1)$ equations can be obtained satisfying equation (3-47) at other convenient locations $X_i\ (i = 1,2,.........,n-1)$ along the chord,

$$u(X_i) = -\frac{1}{4}C_T v'(X_i), \qquad i = 1,2,..........,(n-1). \tag{3-55}$$

The final equation is obtained from (3-52) by requiring that the chord lies along the x-axis, i.e., $h(1) = h(0)$,

$$\frac{\pi}{16}a + \sum_{k=0}^{n}\frac{1}{k+1}b_k = -\alpha. \tag{3-56}$$

Eliminating the coefficient a, using equation (3-56), the system of equations reduces to the form,

$$[D_{ik}]\left[\frac{b_k}{\alpha}\right] = [e_i]. \tag{3-57}$$

This can be solved for the coefficients (b_k/α), which are independent of α, provided that the matrix $[D_{ik}]$ is not singular, as, for example, when $C_T = 1.727$, which corresponds to the case of a flexible membrane at an ideal incidence, $\alpha = 0$.

At this ideal incidence, $a = 0$ and, hence, the pressure distribution, as well as the membrane curvature, do not contain the leading edge singularity $x^{-1/2}$.

The excess length, defined as $\varepsilon = l/c - 1$, is given by the relation,

$$\begin{aligned}\varepsilon &= \int_0^1 \sqrt{1 + \left[\frac{1}{U_\infty}v_b(x) + \alpha\right]^2}\, dX - 1 \\ &\cong \frac{\alpha^2}{2}\int_0^1 \left[1 + \frac{v_b(X)}{\alpha U}\right]^2 dX\end{aligned} \tag{3-58}$$

and the lift coefficient of the flexible membrane airfoil is expressed, using equation (3-47), as,

$$\frac{C_L}{\alpha} = -C_T\sum_{k=1}^{n}\left(\frac{b_k}{\alpha}\right). \tag{3-59}$$

A numerical comparison (Table 3.1) of the results obtained for the overall parameters $\alpha / C_L, \alpha / \sqrt{\varepsilon}$, and C_T between the present method and Nielsen [13,22] and Thwaites [13,27] methods, indicated that the results are generally in fair agreement, although there are detailed differences. The present method is in good agreement for $C_T > 8$ with Thwaites method. The comparison with Nielsen's method shows good agreement for $C_T < 8$. The results are presented in Table 3.1.

Table 3.1 Comparison between the present solution for flexible-membrane airfoils and the previous results of Nielsen and Thwaites.

C_T		$\alpha / \sqrt{\varepsilon}$	α / C_L
	Present method	0.322	28.250
2	Nielsen	0.322	28.148
	Thwaites	0.340	24.989
	Present method	2.434	8.952
4	Nielsen	2.411	8.821
	Thwaites	2.480	8.848
	Present method	6.424	7.255
8	Nielsen	6.329	7.120
	Thwaites	6.400	7.277
	Present method	8.400	7.021
10	Nielsen	8.266	6.884
	Thwaites	8.371	7.120
	Present method	13.33	6.744
15	Nielsen	13.10	6.605
	Thwaites	13.29	6.762
	Present method	96.88	6.345
100	Nielsen	------	------
	Thwaites	96.86	6.349
	Present method	391.69	6.298
400	Nielsen	--------	------
	Thwaites	391.83	6.299

3.4 Flow solutions for jet-flapped airfoils

Consider a thin cambered airfoil of chord length c, provided with a thin jet flap inclined at an angle β, with respect to the chord, at the trailing edge Figure 3.7.

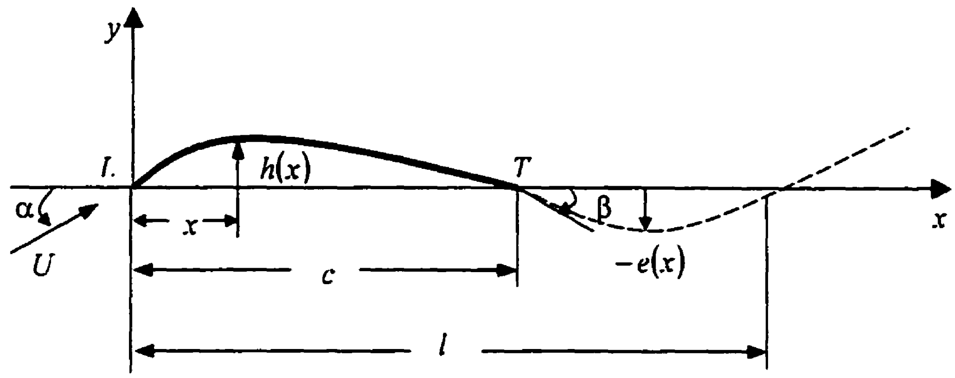

Fig 3.7 Geometry of a jet-flapped airfoil.

The jet is assumed to be a thin sheet and have a small slope, and to have a constant momentum J per unit length of slot. The sheet curvature $1/R \approx e''(x)$, where $y_J = e(x)$ is the jet-flap shape, is related to the pressure difference across the jet sheet by the momentum equation normal to the jet:

$$\Delta p = J/R \approx J e''(x), \tag{3-60}$$

Using the dimensionless jet momentum coefficient $C_J = 2J/(\rho U^2 c)$, this equation can also be expressed in terms of u and v as,

$$(4/C_J)u(x) = cv'(x). \tag{3-61}$$

The aerodynamic boundary condition (3-43) has to be satisfied on the airfoil, where $h(x)$ is specified, and furthermore, the same condition has to be satisfied on the jet sheet itself:

$$v = v_J(x) = [-\alpha + e'(x)]U. \tag{3-62}$$

where the jet flap shape, $y_J = e(x)$, has to be determined.

At the trailing edge $(x=c)$, the jet slope with respect to the chord is specified as β, which leads to the additional condition,

$$e'(c) = -\tan\beta \approx -\beta, \tag{3-63}$$

or

$$v(c) = -U\sin(\alpha+\beta)/\cos\beta \approx -(\alpha+\beta)U. \tag{3-64}$$

Due to the pressure difference across it, the jet sheet is deflected upwards and, eventually, at large distance l behind the airfoil, becomes flat and parallel to the free ream direction. This can be expressed by,

$$e'(l) = e''(l) = 0, \tag{3-65}$$

or

$$v(l) = v'(l) = 0, \qquad [\text{also } u(l) = 0]. \tag{3-66}$$

where l tends, theoretically, to infinity. However, the jet curvature practically tends to zero at a finite distance $(l-c)$, measured from the trailing edge, which depends on the jet coefficient C_J, the jet angle β, and the incidence α, and, in general, has the same order of magnitude as the chord length c.

In this situation, the jet-flapped airfoil can be considered as a fictitious rigid airfoil of an overall chord length l, with the Kutta condition $u(l)=0$ satisfied at $x=l$.

Considering the nondimensional coordinates $X = x/c$ and $L = l/c$, the following expansion of the normal-to-chord velocity component on the jet sheet, $v_J(X)$, satisfies the preceding considerations:

$$\frac{1}{U}v_J'(X) = e''(X) = -\sum_{k=2}^{n} e_k \frac{k+1}{X^{k+2}} + a\frac{2}{\pi}\sinh^{-1}\sqrt{\frac{L-X}{L(X-1)}}, \tag{3-67}$$

and, by integration,

$$\frac{1}{U}v_J(X) + \alpha = e'(X) = \sum_{k=2}^{n} e_k \frac{1}{X^{k+1}} + aF(X). \tag{3-68}$$

where $L = l/c$, and

$$F(X) = (X-1)\frac{2}{\pi}\sinh^{-1}\sqrt{\frac{L-X}{L(X-1)}} - \sqrt{L-1}\,\frac{2}{\pi}\cos^{-1}\sqrt{\frac{X}{L}}. \tag{3-69}$$

The last term of equation (3-67) accounts for trailing-edge singularity appearing in u when the jet is not tangent to the camberline, i.e., when $h'(1) \neq \tan\beta \approx -\beta$.

The boundary condition regarding the jet slope β at the trailing edge can be expressed in the form,

$$\sum_{k=2}^{n} e_k = -\tan\beta - a\,F(1), \tag{3-70}$$

At the other end of the jet sheet $(X = L)$, the boundary conditions can be expressed as,

$$e'(L) = \sum_{k=2}^{n} e_k / L^{k+1} = 0, \tag{3-71}$$

$$e''(L) = -\sum_{k=2}^{n} (k+1) e_k / L^{k+2} = 0. \tag{3-72}$$

However, the terms (3-71) & (3-72) may be omitted in order to avoid having to many terms in expansion (3-68) since the jet slope at $X = L$ is at least in order of magnitude smaller than the slope at the trailing edge β (since L is chosen to be larger than 2).

The velocity $v_b(S)$ should correspond to two different variations of the camberline slope on the airfoil itself, $v_b(S)$, and on the jet sheet, $v_J(S)$, i.e.,

$$\frac{1}{U} v_b(S) + \alpha = \begin{cases} \sum_{k=0}^{n} h_k S^k, & \text{for } 0 < S < 1 \\ \sum_{k=2}^{n} e_k \frac{1}{S^{k+1}} + a\,F(S), & \text{for } 1 < S < L \end{cases}. \tag{3-73}$$

where S represents the new nondimensional coordinates with respect to $c\,(S = s/c)$. For convenience, a polynomial expansion is considered on the jet sheet,

$$F(S) = \sum_{k=2}^{n} b_k / S^{k+1}. \tag{3-74}$$

The chordwise perturbation velocity u on the airfoil and the jet is obtained as,

$$\begin{aligned} \frac{1}{U} u(X) = & \left\{ \alpha - \sum_{k=0}^{n} h_k \sum_{j=0}^{k} I_j X^{k-j} - \sum_{k=2}^{n} (e_k + a b_k) \sum_{j=1}^{k} \frac{J_j}{X^{k+1-j}} \right\} \sqrt{\frac{L-X}{X}} \\ & + \left\{ \sum_{k=0}^{n} h_k X^k - \sum_{k=2}^{n} \frac{e_k + a b_k}{X^{k+1}} \right\} \frac{2}{\pi} G(L,1,X) \end{aligned}, \tag{3-75}$$

where $G(L,1,X)$ has the expression (3-15).

The expressions of I_j and J_j are defined by,

$$I_j = -\frac{1}{j}\frac{1}{\pi}\sqrt{L-1} + \frac{2j-1}{2j} L I_{j-1}, \qquad I_0 = 1 - \frac{2}{\pi}\cos^{-1}\sqrt{\frac{1}{L}} \tag{3-76}$$

$$J_{j+1} = \frac{2j}{2j+1}\frac{1}{L}\left[\frac{1}{j}\frac{1}{\pi}\sqrt{L-1} + J_j\right], \qquad J_1 = \frac{1}{L}\frac{2}{\pi}\sqrt{L-1} \tag{3-77}$$

The constant a is given as,

$$a = \frac{4}{C_l}\left[\tan\beta + h'(1)\right] \approx \frac{4}{C_l}\left[\beta + h'(1)\right]. \tag{3-78}$$

The $(n-1)$ unknown coefficients e_k $(k = 2,3,\ldots\ldots..n)$, can be determined by satisfying equation (3-61) at $(n-1)$ convenient locations X_i, situated between $X = 1$ and $X = L$, i.e.,

$$u(X_i) = 1/4\, C_l\, v'(X_i), \qquad (1,2,\ldots\ldots\ldots\ldots..,n-1) \tag{3-79}$$

The lift coefficient is obtained by integrating the pressure difference, in the form,

$$C_L = 4\alpha L\cos^{-1}\sqrt{\frac{L-1}{L}} - 4\Big[\sum_{k=0}^{n} h_k\left(2I_{k+1}\cos^{-1}\sqrt{\frac{L-1}{L}} + \frac{1}{k+1}\sqrt{L-1}\sum_{j=0}^{k} I_j\right) + \sum_{k=2}^{n}(e_k + ab_k)\left[2J_k\cos^{-1}\sqrt{\frac{L-1}{L}} + \frac{1}{k}\sqrt{L-1}\sum_{j=0}^{k-1} J_{j+1}\right]\Big] \tag{3-80}$$

Chapter 4

Method of velocity singularities for unsteady flows

4.1 Method of velocity singularities for unsteady flows past airfoils

Consider the general flat plate airfoil given in Figure 4.1,

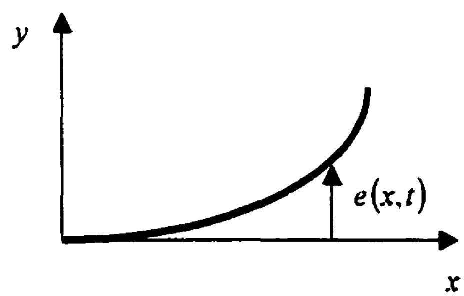

Fig 4.1 Flat plate airfoil with a boundary condition $e(x,t)$.

The vertical displacement of the airfoil surface is defined by,

$$y = e(x,t), \tag{4-1}$$

where $e(x,t)$ is given by

$$e(x,t) = \hat{e}(x)e^{i\omega t}. \tag{4-2}$$

The equation of the body surface $f(x,y,t)$ is hence

$$f(x,y,t) = y - e(x,t) = 0, \tag{4-3}$$

The boundary condition on the surface of the airfoil is defined by

$$\frac{\partial f}{\partial t} + [(U_\infty + u)\mathbf{i} + \mathbf{j}v] \cdot \nabla f = 0, \tag{4-4}$$

where u and v are the perturbation velocities in the x and y directions, respectively.

By performing the derivatives and inserting them into the boundary equation, one obtains the perturbation velocity v in terms of $e(x,t)$,

$$v=\frac{\partial e}{\partial t}+(U_\infty+u)\frac{\partial e}{\partial x}, \tag{4-5}$$

$$v=\left[i\omega\hat{e}(x)+(U_\infty+u)\frac{\partial \hat{e}}{\partial x}\right]e^{i\omega t}. \tag{4-6}$$

The boundary condition on the airfoil can be expressed as

$$v=V(x), \tag{4-7}$$

where,

$$V(x)=\left[i\omega\hat{e}(x)+(U_\infty+u)\frac{\partial \hat{e}}{\partial x}\right]e^{i\omega t}, \tag{4-8}$$

The velocity $V(x)$ can be also expressed by

$$V(x)=\hat{V}(x)e^{i\omega t}. \tag{4-9}$$

where,

$$\hat{V}(x)=\left[i\omega\hat{e}(x)+(U_\infty+u)\frac{\partial \hat{e}}{\partial x}\right], \tag{4-10}$$

In the small perturbation assumption $\frac{u}{U_\infty}$ is smaller than the unity and hence can be neglected in the above equations. The general form of the velocity boundary condition is given by

$$\hat{V}(x)=\sum_{k=0}^{n}b_k\,x^k\ . \tag{4-11}$$

where the coefficients b_k can be determined for each specific case from the boundary conditions on the oscillating airfoil. The complex perturbation velocity is given by

$$W(z)=u(x,y)-j\,v(x,y), \tag{4-12}$$

and can be expressed in the form,

$$W(z)=\hat{W}(z)e^{i\omega t}, \tag{4-13}$$

where,

$$\hat{W}(z)=\hat{u}(x,y)-j\,v(x,y), \tag{4-14}$$

Note that,

$$j = \sqrt{-1}\,. \tag{4-15}$$

The boundary conditions on the oscillating airfoil can now be expressed in the complex form, (where $\mathrm{IMAG}_j[\ ]$ represents the imaginary part of the corresponding expression),

$$\mathrm{IMAG}_j\left[\hat{W}(z)\right]_{z=x} = \hat{V}(x). \quad \text{for} \quad 0 < x < c \tag{4-16}$$

To derive the boundary conditions on the wake of the airfoil, consider a flat plate airfoil with a chord c, placed on the x-axis as shown in Figure 4.2,

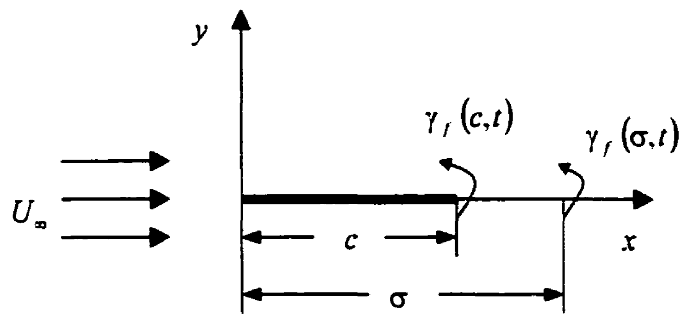

Fig 4.2 Geometry of a flat plate airfoil indicating the free vortex distribution.

The circulation $\Gamma(c,t)$ around the airfoil is expressed as a function of the reduced circulation $\hat{\Gamma}(c)$,

$$\Gamma(c,t) = \hat{\Gamma}(c)\, e^{j\omega t}. \tag{4-17}$$

where ω is the frequency and t is the time.

At any instant of time t a free vortex $\frac{d\Gamma}{dt}dt$ is shedding at the trailing edge of the profile as shown in Figure 4.3.

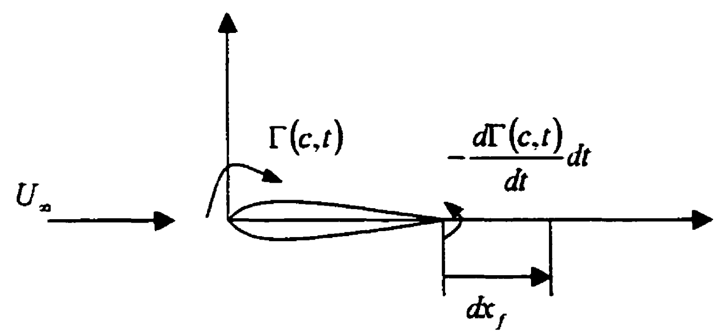

Fig 4.3 Free vortices shedding at the trailing edge of the airfoil.

The shedding (trailing edge) free vortex is moving downstream with the uniform stream velocity U_∞. This means that during the time interval *dt*, the shedding free vortex will move along the distance $d\,x_f$ given by,

$$d\,x_f = U_\infty .dt, \tag{4-18}$$

Hence, the corresponding distribution of the intensity of the shedding free vortices, in the proximity of the trailing edge is given by,

$$\gamma_f(c,t) = \frac{-\dfrac{d\Gamma(c,t)}{dt}dt}{d\,x_f}, \tag{4-19}$$

The intensity of the free vortex distribution $\gamma_f(c,t)$ at the trailing edge of the airfoil is expressed as,

$$\gamma_f(c,t) = -\frac{1}{U_\infty}\frac{d\Gamma(c,t)}{dt}. \tag{4-20}$$

where U_∞ is the free stream velocity.

The intensity of the free vortex distribution $\gamma_f(c,t)$ can be expressed in terms of the reduced intensity of the free vortex $\hat{\gamma}_f(c)$, as,

$$\gamma_f(c,t) = \hat{\gamma}_f(c)e^{i\omega t}, \tag{4-21}$$

After taking the derivative of equation (4-17), the intensity of the free vortex distribution at the trailing edge of the airfoil is given by,

$$\gamma_f(c,t) = -\frac{1}{U_\infty}\hat{\Gamma}(c)i\omega e^{i\omega t}, \tag{4-22}$$

The reduced intensity of free vortex distribution is given by,

$$\hat{\gamma}_f(c) = -\frac{i\omega}{U_\infty}\hat{\Gamma}(c). \tag{4-23}$$

The intensity of free vortex distribution, at a distance σ behind the trailing edge of the airfoil, is calculated considering the fact that a free vortex at a distance behind the trailing edge moves with the free stream velocity U_∞ and was initiated at a previous time interval Δt (time lag) from the trailing edge of the airfoil.

The time lag is expressed as,

$$\Delta t = \frac{\sigma - c}{U_\infty}. \tag{4-24}$$

The intensity of the free vortex distribution at a distance σ behind the trailing edge of the airfoil $\gamma_f(\sigma,t)$ is derived as,

$$\gamma_f(\sigma,t) = \gamma_f\left(c, t - \frac{\sigma - c}{U_\infty}\right) = -\frac{1}{U_\infty}\frac{d\Gamma(c, t - \Delta t)}{dt} = -\frac{i\omega}{U_\infty}\hat{\Gamma}(c)e^{i\omega(t-\Delta t)}. \tag{4-25}$$

The reduced frequency λ, is expressed as,

$$\lambda = \frac{\omega c}{U_\infty}. \tag{4-26}$$

The reduced free vortex distribution at σ is given by,

$$\hat{\gamma}_f(\sigma) = -i\frac{\lambda}{c}\hat{\Gamma}(c)e^{-i\lambda\left(\frac{\sigma}{c}-1\right)}, \tag{4-27}$$

The reduced free vortex distribution at σ, is related to the reduced velocity $\hat{U}(\sigma)$ by the relation,

$$\hat{\gamma}_f(\sigma) = 2\hat{U}(\sigma). \tag{4-28}$$

and hence,

$$\hat{U}(\sigma) = \frac{1}{2}\hat{\gamma}_f(\sigma) = -i\frac{1}{2}\frac{\lambda}{c}\hat{\Gamma}(c)e^{-i\lambda\left(\frac{\sigma}{c}-1\right)}. \tag{4-29}$$

The boundary condition on the wake of the airfoil is hence,

$$\mathrm{REAL}_j\left[\hat{W}(z)\right]_{z=x} = \hat{U}(x). \qquad \text{for } x > c \tag{4-29a}$$

where, $\mathrm{REAL}_j[\ ]$ represents the real part of the corresponding expression.

4.2 Prototype problem

Consider a flat plate airfoil with the jumps of velocities due to the bound vortices on the airfoil are represented by a constant b_0 and a variable $\delta\hat{V}$. The jump of velocity due to the free vortices behind the trailing edge of the airfoil is represented as $\delta\hat{U}$ as shown in Figure 4.4,

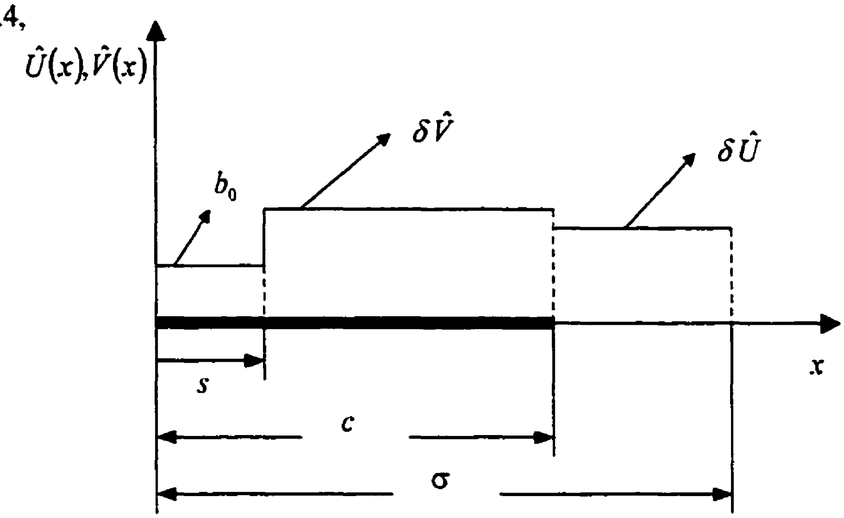

Fig 4.4 Representation of the velocity jumps in the boundary conditions of the prototype problem of an oscillating airfoil.

Complex singularity functions

Special singularities are used to determine the complex perturbation velocity $\hat{W}(z)$ (rather than the complex potential) in the airfoil plane (see Figure 4.4). The velocity singularities are expressed by,

At the leading edge, $z = 0$

$$\sqrt{\frac{c-z}{z}}, \tag{4-30}$$

At the velocity jump on the airfoil, $s \le z \le c$

$$H_1(z,s) = \cosh^{-1}\sqrt{\frac{(c-z)s}{c(s-z)}}, \tag{4-31}$$

At the velocity jump due to the free vortices outside the airfoil, $c < z \le \sigma$

$$A_1(z,\sigma) = \cos^{-1}\sqrt{\frac{(c-z)\sigma}{c(\sigma-z)}}. \tag{4-32}$$

The general behavior and the derivations of the above special complex singularities are given in Appendix C.

The elementary complex velocity $\delta\hat{W}_e(z)$ is expressed in terms of the velocity jumps, due to the bound and free vortices, and singularities related to the complex variable $z = x + iy$. The expression of the complex velocity $\delta\hat{W}_e(z)$ is given by

$$\delta\hat{W}_e(z) = \delta A\sqrt{\frac{c-z}{z}} - \frac{2}{\pi}b_0\,(j\frac{\pi}{2}) - \frac{2}{\pi}\delta\hat{V}\cosh^{-1}\sqrt{\frac{(c-z)s}{c(s-z)}} + \frac{2}{\pi}\delta\hat{U}\cos^{-1}\sqrt{\frac{(c-z)\sigma}{c(\sigma-z)}}, \tag{4-33}$$

The velocity $\hat{U}(\sigma)$ is given by

$$\hat{U}(\sigma) = -\frac{i}{2}\frac{\lambda}{c}\hat{\Gamma}(c)e^{-i\frac{\lambda}{c}(\sigma-c)}, \tag{4-34}$$

The velocity jump $\delta\hat{U}$ due to an elementary free vortex behind the trailing edge is defined by

$$\delta\hat{U} = \frac{d\hat{U}}{d\sigma}\delta\sigma, \tag{4-35}$$

where $\hat{U}(\sigma)$ is defined by equation (4-29).

From equations (4-34) and (4-35),

$$\frac{d\hat{U}}{d\sigma} = -\frac{1}{2}\frac{\lambda^2}{c^2}\hat{\Gamma}(c)e^{-i\frac{\lambda}{c}(\sigma-c)}. \tag{4-36}$$

Taking the effects of all the free vortices from the trailing edge c to infinity ∞, the complex velocity $\delta\hat{W}(z)$ is expressed by,

$$\begin{aligned}\delta\hat{W}(z) = \delta A\sqrt{\frac{c-z}{z}} - \frac{2}{\pi}b_0\,(j\frac{\pi}{2}) - \frac{2}{\pi}\delta\hat{V}\cosh^{-1}\sqrt{\frac{(c-z)s}{c(s-z)}} + \\ + \frac{2}{\pi}\lim_{\sigma_\infty\to\infty}\int_c^{\sigma_\infty}\left[\frac{d\hat{U}}{d\sigma}d\sigma\right]\cos^{-1}\sqrt{\frac{(c-z)\sigma}{c(\sigma-z)}}\end{aligned}, \tag{4-37}$$

By taking into account equation (4-36), equation (4-37) can be recast as,

$$\delta\hat{W}(z)=\delta A\sqrt{\frac{c-z}{z}}-jb_0-\frac{2}{\pi}\delta\hat{V}\cosh^{-1}\sqrt{\frac{(c-z)s}{c(s-z)}}+\frac{2}{\pi}\left[-\frac{1}{2}\frac{\lambda^2}{c^2}\hat{\Gamma}(c)\right]F(z), \tag{4-38}$$

where,

$$F(z)=\lim_{\sigma_\infty\to\infty}\{\int_c^{\sigma_\infty}e^{-i\frac{\lambda}{c}(\sigma-c)}\cos^{-1}\sqrt{\frac{(c-z)\sigma}{c(\sigma-z)}}d\sigma\}. \tag{4-39}$$

The complex function $F(z)$ is derived in Appendix A and is given by,

$$F(z)=\left(-\frac{c}{i\lambda}\right)E_\infty\cos^{-1}\sqrt{\frac{c-z}{c}}-\left(-\frac{c}{i\lambda}\right)\lim_{\sigma_\infty\to\infty}\{\int_c^{\sigma_\infty}e^{-i\frac{\lambda}{c}(\sigma-c)}\frac{\sqrt{(c-z)z}}{2(\sigma-z)\sqrt{(\sigma-c)\sigma}}d\sigma\}, \tag{4-40}$$

where,

$$E_\infty=\lim_{\sigma\to\infty}\left[e^{-i\frac{\lambda}{c}(\sigma-c)}\right]. \tag{4-41}$$

To determine the constant δA, we note that at $z\to\infty$, the perturbation velocity vanishes,

$$\delta\hat{W}(\infty)=0, \tag{4-42}$$

The complex velocity at infinity is given by,

$$\delta\hat{W}(\infty)=\delta A(-j)-jb_0-\frac{2}{\pi}\delta\hat{V}\left[j\cos^{-1}\sqrt{\frac{s}{c}}\right]+\frac{2}{\pi}\left[-\frac{1}{2}\frac{\lambda^2}{c^2}\hat{\Gamma}(c)\right]F(\infty)=0. \tag{4-43}$$

where,

$$\begin{aligned}F(\infty)=\lim_{z\to\infty}\{&\left(-\frac{c}{i\lambda}\right)E_\infty\left[\frac{\pi}{2}+j\lim_{z\to\infty}\sinh^{-1}\sqrt{\frac{z-c}{c}}\right]-\\&-\left(-\frac{c}{i\lambda}\right)\lim_{\sigma_\infty\to\infty}(\int_c^{\sigma_\infty}e^{-i\frac{\lambda}{c}(\sigma-c)}\frac{(-j)\sqrt{(z-c)z}}{(-2)(z-\sigma)\sqrt{(\sigma-c)\sigma}}d\sigma\ )\}\end{aligned} \tag{4-44}$$

The real and imaginary parts of the complex velocity at infinity are equal to zero.

Imposing the condition,

$$\mathrm{REAL}_j\left[\delta\hat{W}(\infty)\right]=0, \tag{4-45}$$

one obtains for the indeterminate value of the constant E_∞,

$$E_\infty=\lim_{\sigma\to\infty}\left[e^{-i\frac{\lambda}{c}(\sigma-c)}\right]=0. \tag{4-46}$$

The above conclusion can also be obtained from the Riemann-Lebesque lemma on Fourier Integrals [5,23], when the theory of distribution is used (see also Fung [5]).

Hence,

$$F(\infty)=\lim_{z\to\infty}\{\left(\frac{c}{i\lambda}\right)\lim_{\sigma_\infty\to\infty}(\int_c^{\sigma_\infty}e^{-i\frac{\lambda}{c}(\sigma-c)}\frac{(-j)\sqrt{(z-c)z}}{(-2)(z-\sigma)\sqrt{(\sigma-c)\sigma}}d\sigma\ )\}. \tag{4-47}$$

Imposing the condition.

$$\mathrm{IMAG}_j\left[\delta\hat{W}(\infty)\right]=0, \tag{4-48}$$

one obtains,

$$\delta A=-b_0-\frac{2}{\pi}\delta\hat{V}\cos^{-1}\sqrt{\frac{s}{c}}+\frac{1}{2}\frac{\lambda^2}{c^2}\hat{\Gamma}(c)\left(-\frac{c}{i\lambda}\right)\frac{2}{\pi}\lim_{\sigma_\infty\to\infty}\{\int_c^{\sigma_\infty}e^{-i\frac{\lambda}{c}(\sigma-c)}\frac{d\sigma}{2\sqrt{(\sigma-c)\sigma}}\}. \tag{4-49}$$

By inserting δA into $\delta\hat{W}(z)$ and noting the fact that $E_\infty=0$, the equation (4-38) of the complex velocity becomes,

$$\begin{aligned}\delta\hat{W}(z)=&-b_0\left(\sqrt{\frac{c-z}{z}}+j\right)-\frac{2}{\pi}\delta\hat{V}\left[\cosh^{-1}\sqrt{\frac{(c-z)s}{c(s-z)}}+\sqrt{\frac{c-z}{z}}\cos^{-1}\sqrt{\frac{s}{c}}\right],\\&+\frac{1}{2}\frac{\lambda^2}{c^2}\hat{\Gamma}(c)\frac{2}{\pi}\left(-\frac{c}{i\lambda}\right)J(z)\end{aligned} \tag{4-50}$$

where,

$$J(z)=\lim_{\sigma_\infty\to\infty}\{\int_c^{\sigma_\infty}e^{-i\frac{\lambda}{c}(\sigma-c)}\left[\frac{\sqrt{(c-z)z}}{2(\sigma-z)\sqrt{(\sigma-c)\sigma}}+\sqrt{\frac{c-z}{z}}\frac{1}{2\sqrt{(\sigma-c)\sigma}}\right]d\sigma\}. \tag{4-51}$$

Determination of the constant $\delta\hat{\Gamma}(c)$

The reduced circulation around the airfoil $\delta\hat{\Gamma}(c)$ for the prototype problem, is determined by imposing the fact that the reduced bound vortex distribution on the airfoil is related to the complex velocity by the following expression,

$$\hat{\gamma}_b(x) = 2\,\mathrm{REAL}_j\left[\hat{W}(z)\right]_{z=x} = 2\hat{u}(x), \tag{4-52}$$

The reduced circulation at any position x on the airfoil $\hat{\Gamma}(x)$ is related to the reduced bound vortex distribution by,

$$\hat{\Gamma}(x) = \int_0^x \hat{\gamma}_b(x)dx = 2\int_0^x \hat{u}(x)dx = 2\int_0^x \mathrm{REAL}_j\left[\hat{W}(z)\right]_{z=x} dx. \tag{4-53}$$

The expression of $\delta\hat{\Gamma}(x)$ is given by,

$$\begin{aligned}\frac{1}{2}\delta\hat{\Gamma}(x) = -b_0\int_0^x\sqrt{\frac{c-x}{x}}\,dx - \frac{2}{\pi}\delta\hat{V}\int_0^x\left[\cosh^{-1}\sqrt{\frac{(c-x)s}{c(s-x)}} + \sqrt{\frac{c-x}{x}}\cos^{-1}\sqrt{\frac{s}{c}}\right]dx \\ +\frac{1}{2}\frac{\lambda^2}{c^2}\delta\hat{\Gamma}(c)\frac{2}{\pi}\left(-\frac{c}{i\lambda}\right)\int_0^x J(x)dx.\end{aligned} \tag{4-54}$$

To determine $\delta\hat{\Gamma}(c)$, the condition of $x = c$ is introduced in equation (4-54),

$$\begin{aligned}\frac{1}{2}\delta\hat{\Gamma}(c) = -b_0\int_0^c\sqrt{\frac{c-x}{x}}\,dx - \frac{2}{\pi}\delta\hat{V}\int_0^c\left[\cosh^{-1}\sqrt{\frac{(c-x)s}{c(s-x)}} + \sqrt{\frac{c-x}{x}}\cos^{-1}\sqrt{\frac{s}{c}}\right]dx \\ +\frac{1}{2}\frac{\lambda^2}{c^2}\delta\hat{\Gamma}(c)\frac{2}{\pi}\left(-\frac{c}{i\lambda}\right)\int_0^c J(x)dx.\end{aligned} \tag{4-55}$$

The derivation of the various integrals in equation (4-55) is given in Appendix A, and the final formulas of the integrals are obtained as,

$$\int_0^c J(x)dx = -\frac{\pi^2}{8}ce^{i\frac{\lambda}{2}}\left[H_1^{(2)}(\lambda/2) + iH_0^{(2)}(\lambda/2)\right] - \frac{\pi}{2}\left(\frac{c}{i\lambda}\right), \tag{4-56}$$

where $H_1^{(2)}(\lambda/2)$ and $H_0^{(2)}(\lambda/2)$ are the Hankel's integrals of second kind of orders of one and zero [7,20,29], respectively, and

$$\int_0^c \sqrt{\frac{c-x}{x}}\, dx = c\frac{\pi}{2}, \tag{4-57}$$

$$\text{REAL}_j\left[\int_0^c \cosh^{-1}\sqrt{\frac{(c-x)s}{c(s-x)}}\, dx\right] = \frac{\pi}{2}\sqrt{(c-s)s}\,. \tag{4-58}$$

Introducing the above integrals into equation (4-55), one obtains,

$$\delta\hat{\Gamma}(c) = G\left\{-b_0\, c - \frac{2}{\pi}\delta\hat{V}\left[\sqrt{(c-s)s} + c\cos^{-1}\sqrt{\frac{s}{c}}\right]\right\}, \tag{4-59}$$

where,

$$G = -\frac{4i}{\lambda}\frac{e^{-i\frac{\lambda}{2}}}{H_1^{(2)}(\lambda/2) + i H_0^{(2)}(\lambda/2)}. \tag{4-60}$$

Determination of $\delta\hat{C}_p(x)$

The reduced pressure coefficient $\delta\hat{C}_p(x)$ for the prototype oscillating airfoil problem is expressed in terms of the reduced velocity potential $\delta\hat{\varphi}$ as,

$$\delta\hat{C}_p(x) = -\frac{2}{U_\infty}\left[i\frac{\omega}{U_\infty}\delta\hat{\varphi}(x,y) + \frac{\partial(\delta\hat{\varphi})}{\partial x}\right], \tag{4-61}$$

where,

$$\delta\hat{\varphi} = \int_0^x \delta\hat{u}\, dx = \frac{1}{2}\int_0^x 2\,\delta\hat{u}\, dx = \frac{1}{2}\delta\hat{\Gamma}(x). \tag{4-62}$$

The equation of the reduced pressure coefficient $\delta\hat{C}_p(x)$ is then expressed as.

$$\delta\hat{C}_p(x) = -\frac{2}{U_\infty}\left[i\frac{\lambda}{c}\frac{1}{2}\delta\hat{\Gamma}(x) + \delta\hat{u}\right]. \tag{4-63}$$

where λ is the reduced frequency.

The expression of the reduced velocity on the airfoil $\delta\hat{u}$ is given by,

$$\delta\hat{u} = \text{REAL}_j\left\lfloor \delta\hat{W}(z)\right\rfloor_{z=x}, \tag{4-64}$$

where the term REAL $_j$[] represents the real part of the complex function.

By taking the real part of the complex velocity $\delta \hat{W}(z)$, the expression of $\delta \hat{u}$ is given by,

$$\delta \hat{u}(x) = -b_0 \sqrt{\frac{c-x}{c}} - \frac{2}{\pi}\delta\hat{V}\left[\cosh^{-1}\sqrt{\frac{(c-x)s}{c(s-x)}} + \sqrt{\frac{c-x}{x}}\cos^{-1}\sqrt{\frac{s}{c}}\right] + \frac{1}{2}\frac{\lambda^2}{c^2}\delta\hat{\Gamma}(c)\frac{2}{\pi}\left(-\frac{c}{i\lambda}\right)J(x) \quad (4\text{-}65)$$

After inserting the expressions of $\delta \hat{u}$ and $\delta\hat{\Gamma}(x)$ into the expression of the reduced pressure coefficient $\delta \hat{C}_p(x)$, one obtains,

$$\begin{aligned} -\frac{U_\infty}{2}\delta \hat{C}_p(x) = &\left(\frac{i\lambda}{c}\right)\left[-b_0 - \frac{2}{\pi}\delta\hat{V}\cos^{-1}\sqrt{\frac{s}{c}}\right]\sqrt{(c-x)x} \\ &+\left(\frac{i\lambda}{c}\right)\left(-\frac{2}{\pi}\delta\hat{V}\right)\left[(x-s)\cosh^{-1}\sqrt{\frac{(c-x)s}{c(s-x)}}\right] - b_0\sqrt{\frac{c-x}{x}} \\ &-\frac{2}{\pi}\delta\hat{V}\left[\cosh^{-1}\sqrt{\frac{(c-x)s}{c(s-x)}} + \sqrt{\frac{c-x}{x}}\cos^{-1}\sqrt{\frac{s}{c}}\right] \\ &+\left(-\frac{1}{c}\right)\sqrt{\frac{c-x}{x}}(1-C(\lambda/2))\left[-b_0 c - \frac{2}{\pi}\delta\hat{V}\left(c\cos^{-1}\sqrt{\frac{s}{c}} + \sqrt{(c-s)s}\right)\right] \end{aligned} \quad (4\text{-}66)$$

Details of the calculations are shown in Appendix D.

The above equation can be represented after mathematical arrangements as,

$$\begin{aligned} -\frac{U_\infty}{2}\delta \hat{C}_p(x) = &(i\lambda)\sqrt{(c-x)x}\left(\frac{1}{c} - \frac{i}{\lambda x}C(\lambda/2)\right)\left[-b_0 - \frac{2}{\pi}\delta\hat{V}\cos^{-1}\sqrt{\frac{s}{c}}\right] \\ &-\frac{2}{\pi}\delta\hat{V}\cosh^{-1}\sqrt{\frac{(c-x)s}{c(s-x)}}\left[\frac{i\lambda}{c}(x-s)+1\right] \\ &+\left(\frac{1}{c}\right)\sqrt{\frac{c-x}{x}}(1-C(\lambda/2))\frac{2}{\pi}\delta\hat{V}\sqrt{(c-s)s} \end{aligned} \quad (4\text{-}67)$$

where $C(\lambda/2)$ is Theodorsen's function [15,26]. The values of the real and imaginary parts of the Theodorsen function are given in Appendix B.

Determination of $\delta \hat{C}_L$

The reduced lift coefficient $\delta \hat{C}_L$ for the prototype problem is related to the reduced pressure difference coefficient $\delta[\ \Delta\hat{C}_p(x)\ ]$ by the expression,

$$\delta \hat{C}_L = \frac{1}{c}\int_0^c \delta[\ \Delta\hat{C}_p(x)\ ]\,dx = -\frac{2}{c}\int_0^c \delta\hat{C}_p(x)\,dx\,. \tag{4-68}$$

The relation between the reduced pressure coefficient $\delta\hat{C}_p(x)$ and the reduced pressure difference coefficient $\delta[\ \Delta\hat{C}_p(x)\ ]$ is expressed as,

$$\delta[\ \Delta\hat{C}_p(x)\ ] = -2\,\delta\hat{C}_p(x), \tag{4-69}$$

After evaluating the related integrals (see Appendix A), the expression of the reduced lift coefficient is given by,

$$\begin{aligned}\frac{-U_\infty}{i\lambda}\delta\hat{C}_L &= \left(1-\frac{4i}{\lambda}C(\lambda/2)\right)\left[-b_0\frac{\pi}{2}-\delta\hat{V}\cos^{-1}\sqrt{\frac{s}{c}}\right]\\ &\quad -\frac{1}{c}\delta\hat{V}\sqrt{(c-s)s}\left[1-\frac{4i}{\lambda}C(\lambda/2)-\frac{2}{c}s\right],\end{aligned} \tag{4-70}$$

Determination of $\delta \hat{C}_m$

The reduced pitching moment coefficient $\delta\hat{C}_m$ for the prototype problem is defined by,

$$\delta\hat{C}_m = -\frac{2}{c^2}\int_0^c x\,\delta\hat{C}_p(x)\,dx\,. \tag{4-71}$$

The detailed integral derivations related to $\delta\hat{C}_m$ are given in Appendix A, and the expression of the reduced pitching moment coefficient $\delta\hat{C}_m$ is obtained as,

$$\begin{aligned}\frac{-U_\infty}{i\lambda}\delta\hat{C}_m &= \frac{1}{2}\left(1-\frac{2i}{\lambda}C(\lambda/2)\right)\left[-b_0\frac{\pi}{2}-\delta\hat{V}\cos^{-1}\sqrt{\frac{s}{c}}\right]\\ &\quad -\frac{1}{c}\delta\hat{V}\sqrt{(c-s)s}\left[\frac{1}{2}\left(1-\frac{2i}{\lambda}C(\lambda/2)\right)-\left(\frac{1}{3}+\frac{2i}{\lambda}\right)\frac{s}{c}-\frac{2}{3}\frac{s^2}{c^2}\right],\end{aligned} \tag{4-72}$$

where $C(\lambda/2)$ is Theodorsen's [15,26] function.

4.3 The complete oscillating airfoil problem

Let us consider the boundary conditions on the oscillating airfoil in the general form,

$$\hat{V}(x)=\sum_{k=0}^{n} b_k x^k \quad , \tag{4-73}$$

The jump of velocity $\delta\hat{V}$ on the airfoil can be expressed as,

$$\delta\hat{V}=\left[\frac{d\hat{V}}{dx}\right]_{x=s} ds\,, \tag{4-74}$$

and hence,

$$\delta\hat{V}=\sum_{k=1}^{n} k\,b_k\,s^{k-1}\,ds\,. \tag{4-75}$$

where the coefficients b_k are determined for each specific case from the boundary conditions on the oscillating airfoil as it is shown for example in section 4.5.2. The complete motion is obtained by inserting the elementary velocity jump defined by (4-74) into the equations of the prototype problem and then integrating along the chord of the airfoil, as shown in the following:

$$\hat{\Gamma}(c)=G\left\{-b_0\,c-\frac{2}{\pi}\int_0^c\left[\sqrt{(c-s)s}+c\cos^{-1}\sqrt{\frac{s}{c}}\right]\left[\frac{d\hat{V}}{dx}\right]_{x=s}ds\right\}, \tag{4-76}$$

where,

$$G=-\frac{4i}{\lambda}\frac{e^{-i\frac{\lambda}{2}}}{H_1^{(2)}(\lambda/2)+i\,H_0^{(2)}(\lambda/2)}\quad . \tag{4-77}$$

The expression of the reduced pressure coefficient is given by,

$$\begin{aligned}-\frac{U_\infty}{2}\hat{C}_p(x)=&(i\lambda)\sqrt{(c-x)x}\left(\frac{1}{c}-\frac{i}{\lambda x}C(\lambda/2)\right)\left[-b_0-\frac{2}{\pi}\int_0^c\cos^{-1}\sqrt{\frac{s}{c}}\left[\frac{d\hat{V}}{dx}\right]_{x=s}ds\right.\\&\left.-\frac{2}{\pi}\int_0^c\cosh^{-1}\sqrt{\frac{(c-x)s}{c(s-x)}}\left[\frac{i\lambda}{c}(x-s)+1\right]\left[\frac{d\hat{V}}{dx}\right]_{x=s}ds\right]\\&+\left(\frac{1}{c}\right)\sqrt{\frac{c-x}{x}}\left(1-C(\lambda/2)\right)\frac{2}{\pi}\int_0^c\sqrt{(c-s)s}\left[\frac{d\hat{V}}{dx}\right]_{x=s}ds\,.\end{aligned}$$

(4-78)

The reduced lift coefficient is expressed as,

$$\frac{-U_\infty}{i\lambda}\hat{C}_L=\left(1-\frac{4i}{\lambda}C(\lambda/2)\right)\left[-b_0\frac{\pi}{2}-\int_0^c \cos^{-1}\sqrt{\frac{s}{c}}\left[\frac{d\hat{V}}{dx}\right]_{x=s}ds\right]$$
$$-\frac{1}{c}\int_0^c \sqrt{(c-s)s}\left[1-\frac{4i}{\lambda}C(\lambda/2)-\frac{2}{c}s\right]\left[\frac{d\hat{V}}{dx}\right]_{x=s}ds.$$

(4-79)

The reduced pitching moment coefficient is defined by,

$$\frac{-U_\infty}{i\lambda}\hat{C}_m=\frac{1}{2}\left(1-\frac{2i}{\lambda}C(\lambda/2)\right)\left[-b_0\frac{\pi}{2}-\int_0^c \cos^{-1}\sqrt{\frac{s}{c}}\left[\frac{d\hat{V}}{dx}\right]_{x=s}ds\right]$$
$$-\frac{1}{c}\int_0^c \sqrt{(c-s)s}\left[\frac{1}{2}\left(1-\frac{2i}{\lambda}C(\lambda/2)\right)-\left(\frac{1}{3}+\frac{2i}{\lambda}\right)\frac{s}{c}-\frac{2}{3}\frac{s^2}{c^2}\right]\left[\frac{d\hat{V}}{dx}\right]_{x=s}ds.$$

(4-80)

4.3.1 The reduced circulation around the airfoil

The expression of the total reduced circulation around the airfoil $\hat{\Gamma}(c)$ is given by,

$$\hat{\Gamma}(c)=G\left\{-b_0c-\frac{2}{\pi}\sum_{k=1}^{n}b_k\left[k\int_0^c s^{k-1}\sqrt{(c-s)s}\,ds+ck\int_0^c s^{k-1}\cos^{-1}\sqrt{\frac{s}{c}}\,ds\right]\right\}$$

(4-81)

The detailed derivations of the integrals are given in Appendix A.

The resultant expression of the total reduced circulation $\hat{\Gamma}(c)$ is given by,

$$\hat{\Gamma}(c)=\left(-\frac{c}{\pi}\right)G\sum_{k=0}^{n}\left(\frac{2k+1}{k+1}\right)b_k I_k \ , \tag{4-82}$$

where,

$$I_k=\frac{2k-1}{2k}c\,I_{k-1}\quad \text{where, } I_0=\pi \quad I_1=c\frac{\pi}{2}\quad I_2=\frac{3}{8}\pi c^2. \tag{4-83}$$

The detailed derivation of the recurrence formula of I_k is given in Appendix A.

4.3.2 The reduced pressure coefficient

The expression of the total reduced pressure coefficient $\hat{C}_p(x)$ is determined by introducing the expression of the velocity jump $\delta\hat{V}$ into the expression of $\delta\hat{C}_p(x)$. The integral form of the equation is given as,

$$
\begin{aligned}
-\frac{U_\infty}{2}\hat{C}_p(x) = &\left(\frac{i\lambda}{c}\right)\left[-b_0 - \frac{2}{\pi}\sum_{k=1}^{n} b_k\, k \int_0^c s^{k-1}\cos^{-1}\sqrt{\frac{s}{c}}\, ds\right]\sqrt{(c-x)x} \\
&+\left(\frac{i\lambda}{c}\right)\left[-\frac{2}{\pi}\sum_{k=1}^{n} b_k\, k \int_0^c s^{k-1}(x-s)\cosh^{-1}\sqrt{\frac{(c-x)s}{c(s-x)}}\, ds\right] - b_0\sqrt{\frac{c-x}{x}} \\
&-\frac{2}{\pi}\sum_{k=1}^{n} b_k\left[k\int_0^c s^{k-1}\cosh^{-1}\sqrt{\frac{(c-x)s}{c(s-x)}}\, ds + \sqrt{\frac{c-x}{x}}\, k\int_0^c s^{k-1}\cos^{-1}\sqrt{\frac{s}{c}}\, ds\right] \\
&+\left(\frac{-1}{c}\right)\sqrt{\frac{c-x}{x}}(1-C(\lambda/2))[-b_0 c - \frac{2}{\pi}\sum_{k=1}^{n} b_k\left(c\,k\int_0^c s^{k-1}\cos^{-1}\sqrt{\frac{s}{c}}\, ds\right. \\
&\left. + k\int_0^c s^{k-1}\sqrt{(c-s)s}\, ds\right)\ ],
\end{aligned}
$$

(4-84)

The detailed derivations of the integrals related to equation (4-84) are given in Appendix A. The resultant equation of the reduced pressure coefficient $\hat{C}_p(x)$ is expressed as

$$
\begin{aligned}
-\frac{U_\infty}{2}\hat{C}_p(x) = &\left(-\frac{i\lambda}{c\pi}\right)\sqrt{(c-x)c}\left[\sum_{k=0}^{n} b_k\, I_k + \sum_{k=1}^{n}\frac{b_k}{k+1}\left(\sum_{q=0}^{k-1} x^{k-q}\, I_q - k\, I_k\right)\right] \\
&+\frac{1}{\pi}\sqrt{\frac{c-x}{x}}\sum_{k=0}^{n} b_k\left\{[1-C(\lambda/2)]\left(\frac{2k+1}{k+1}\right)I_k - \sum_{q=0}^{k} x^{k-q} I_q\right\},
\end{aligned}
\qquad (4\text{-}85)
$$

Note that the reduced pressure difference coefficient $\Delta\hat{C}_p(x)$, is given by the relation.

$$\Delta\hat{C}_p(x) = -2\ \hat{C}_p(x), \qquad (4\text{-}86)$$

The pressure difference coefficient for the airfoil is expressed by,

$$\Delta C_p(x,t) = \mathrm{Re}\lfloor\Delta\hat{C}_p(x)e^{i\omega t}\rfloor. \qquad (4\text{-}87)$$

4.3.3 The reduced lift and pitching moment coefficients

By inserting the expression of the velocity jump $\delta\hat{V}$ into the reduced lift coefficient $\delta\hat{C}_L$, equation (4-70), and by taking the integrals around the airfoil, the general expression for the total reduced lift coefficient $\hat{C}_L$ is given by,

$$\begin{aligned}\frac{-U_\infty}{i\lambda}\hat{C}_L &= \left(1-\frac{4i}{\lambda}C(\lambda/2)\right)\left[-b_0\frac{\pi}{2}-\sum_{k=1}^{n}b_k\,k\int_0^c s^{k-1}\cos^{-1}\sqrt{\frac{s}{c}}\,ds\right]\\ &-\frac{1}{c}\left(1-\frac{4i}{\lambda}C(\lambda/2)\right)\sum_{k=1}^{n}b_k\,k\int_0^c s^{k-1}\sqrt{(c-s)s}\,ds \\ &+\frac{2}{c^2}\sum_{k=1}^{n}b_k\,k\int_0^c s^{k}\sqrt{(c-s)s}\,ds\,,\end{aligned} \tag{4-88}$$

The detailed derivations of the integrals within equation (4-88), are given in Appendix A. The resultant expression of the total reduced lift coefficient $\hat{C}_L$ is given by,

$$\begin{aligned}\frac{-U_\infty}{i\lambda}\hat{C}_L &= -\frac{1}{2}\left(1-\frac{4i}{\lambda}C(\lambda/2)\right)\left[\sum_{k=0}^{n}b_k\,I_k+\sum_{k=1}^{n}\left(\frac{k}{k+1}\right)b_k\,I_k\right]\\ &+\frac{1}{2}\sum_{k=1}^{n}\frac{k(2k+1)}{(k+1)(k+2)}b_k\,I_k\,,\end{aligned} \tag{4-89}$$

where $C(\lambda/2)$ is Theodorsen's function , λ is the reduced frequency and I_k is a recurrence expression given by equation (4-83) rewritten below as,

$$I_k=\frac{2k-1}{2k}c\,I_{k-1} \quad \text{where, } I_0=\pi \quad I_1=c\frac{\pi}{2} \quad I_2=\frac{3}{8}\pi c^2\,. \tag{4-90}$$

The total reduced pitching moment coefficient $\hat{C}_m$ is derived in the same way and is given by, (see Appendix A for detailed integral calculations),

$$\begin{aligned}\frac{-U_\infty}{i\lambda}\hat{C}_m &= -\frac{1}{4}\left(1-\frac{2i}{\lambda}C(\lambda/2)\right)\sum_{k=0}^{n}b_k\,I_k+\\ &+\sum_{k=1}^{n}\frac{k}{k+1}b_k\,I_k\left\{-\frac{1}{4}\left(1-\frac{2i}{\lambda}C(\lambda/2)\right)+\left(\frac{1}{12}+\frac{i}{2\lambda}\right)\frac{2k+1}{k+2}+\frac{1}{12}\frac{(2k+1)(2k+3)}{(k+2)(k+3)}\right\},\end{aligned}$$

(4-91)

4.4 Method of velocity singularities for unsteady flows past airfoils with oscillating ailerons

The boundary condition on the airfoil with an oscillating aileron is given by the velocity $\hat{V}(x)$ in the form

$$\hat{V}(x)=\begin{Bmatrix} 0 & x\in(0,s_1) \\ \sum_{k=0}^{n}\beta_k x^k & x\in(s_1,c) \end{Bmatrix}, \tag{4-92}$$

The boundary condition on the airfoil at the position of the aileron $(x=s_1)$ is given in terms of the velocity jump $\hat{V}(s_1)$ that is given by,

$$\hat{V}(s_1)=\sum_{k=0}^{n}\beta_k s_1^k . \tag{4-93}$$

where the coefficients β_k are determined from each specific case from the boundary conditions on the airfoil with an oscillating aileron.

4.4.1 Prototype problem for the case of an oscillating aileron

Consider the unsteady flow past an airfoil with an oscillating aileron, as shown in Figure 4.5.

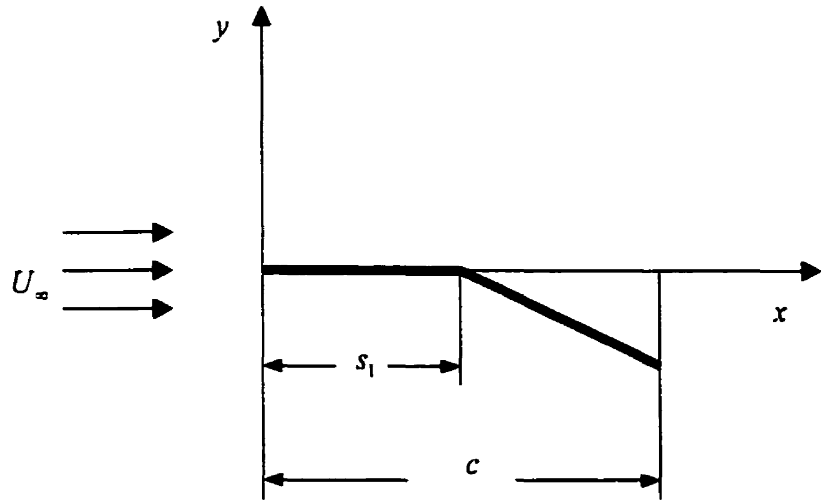

Fig 4.5 Geometry of an oscillating aileron.

The various velocity jumps on the airfoil are represented in Figure 4.6.

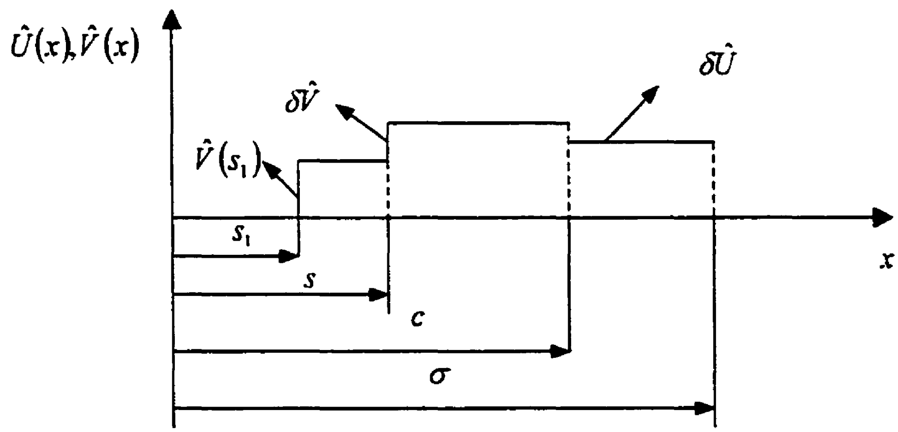

Fig 4.6 Velocity jumps representations in the boundary conditions on an airfoil with an oscillating aileron.

Complex singularity functions

Special singularities are used to determine the complex perturbation velocity $\hat{W}(z)$ (rather than the complex potential) in the airfoil and aileron plane(see Figure 4.6). The velocity singularities are expressed by,

At the leading edge, $z = 0$

$$\sqrt{\frac{c-z}{z}}, \tag{4-94}$$

At the velocity jump on the airfoil, $s \le z \le c$

$$H_1(z,s) = \cosh^{-1}\sqrt{\frac{(c-z)s}{c(s-z)}}, \tag{4-95}$$

At the velocity jump due to the free vortices outside the airfoil, $c < z \le \sigma$

$$A_1(z,\sigma) = \cos^{-1}\sqrt{\frac{(c-z)\sigma}{c(\sigma-z)}}. \tag{4-96}$$

The elementary complex velocity $\delta\hat{W}_e(z)$ is expressed in terms of the velocity jumps, due to the bound and free vortices, and singularities related to the complex variable $z = x + iy$. The expression of the complex velocity $\delta\hat{W}_e(z)$ is given by

$$\begin{aligned}\delta\hat{W}_e(z) = \delta A\sqrt{\frac{c-z}{z}} - \frac{2}{\pi}\hat{V}(s_1)\cosh^{-1}\sqrt{\frac{(c-z)s_1}{c(s_1-z)}} - \frac{2}{\pi}\delta\hat{V}\cosh^{-1}\sqrt{\frac{(c-z)s}{c(s-z)}} + \\ + \frac{2}{\pi}\delta\hat{U}\cos^{-1}\sqrt{\frac{(c-z)\sigma}{c(\sigma-z)}},\end{aligned} \tag{4-97}$$

The velocity $\hat{U}(\sigma)$ is given by,

$$\hat{U}(\sigma) = -\frac{i}{2}\frac{\lambda}{c}\hat{\Gamma}(c)e^{-i\frac{\lambda}{c}(\sigma-c)}, \tag{4-98}$$

The velocity jump $\delta\hat{U}$ due to the free vortices behind the trailing edge is expressed by (see also the analysis in section 4.1),

$$\delta\hat{U} = \frac{d\hat{U}}{d\sigma}\delta\sigma, \tag{4-99}$$

The velocity jump $\delta\hat{V}$ for the airfoil with an oscillating aileron is given by

$$\delta\hat{V}=\sum_{k=1}^{n}k\,\beta_k\,s^{k-1}\,ds. \tag{4-100}$$

From equation (4-98),

$$\frac{d\hat{U}}{d\sigma}=-\frac{1}{2}\frac{\lambda^2}{c^2}\hat{\Gamma}(c)e^{-i\frac{\lambda}{c}(\sigma-c)}. \tag{4-101}$$

Taking the effects of all the free vortices from the trailing edge c to infinity ∞, the complex velocity $\delta\hat{W}(z)$ is expressed by,

$$\begin{aligned}\delta\hat{W}(z)=\delta A\sqrt{\frac{c-z}{z}}-\frac{2}{\pi}\hat{V}(s_1)\cosh^{-1}\sqrt{\frac{(c-z)s_1}{c(s_1-z)}}\\ -\frac{2}{\pi}\delta\hat{V}\cosh^{-1}\sqrt{\frac{(c-z)s}{c(s-z)}}+\frac{2}{\pi}\lim_{\sigma_*\to\infty}\left\{\int_c^{\sigma_*}\left[\frac{d\hat{U}}{d\sigma}d\sigma\right]\cos^{-1}\sqrt{\frac{(c-z)\sigma}{c(\sigma-z)}}\right\},\end{aligned} \tag{4-102}$$

By taking into account equation (4-101), equation (4-102) can be recast as,

$$\begin{aligned}\delta\hat{W}(z)=\delta A\sqrt{\frac{c-z}{z}}-\frac{2}{\pi}\hat{V}(s_1)\cosh^{-1}\sqrt{\frac{(c-z)s_1}{c(s_1-z)}}\\ -\frac{2}{\pi}\delta\hat{V}\cosh^{-1}\sqrt{\frac{(c-z)s}{c(s-z)}}+\frac{2}{\pi}\left[-\frac{1}{2}\frac{\lambda^2}{c^2}\hat{\Gamma}(c)\right]F(z),\end{aligned} \tag{4-103}$$

where,

$$F(z)=\lim_{\sigma_*\to\infty}\left\{\int_c^{\sigma_*}e^{-i\frac{\lambda}{c}(\sigma-c)}\cos^{-1}\sqrt{\frac{(c-z)\sigma}{c(\sigma-z)}}d\sigma\right\}. \tag{4-104}$$

The complex function $F(z)$ is derived in Appendix A and is given by,

$$F(z)=\left(\frac{c}{i\lambda}\right)\lim_{\sigma_*\to\infty}\left\{\int_c^{\sigma_*}e^{-i\frac{\lambda}{c}(\sigma-c)}\frac{\sqrt{(c-z)z}}{2(\sigma-z)\sqrt{(\sigma-c)\sigma}}d\sigma\right\}, \tag{4-105}$$

To determine of the constant δA, we note that at $z\to\infty$ the perturbation velocity vanishes,

$$\delta\hat{W}(\infty)=0, \tag{4-106}$$

The complex velocity at infinity is given by,

$$\delta\hat{W}(\infty) = \delta A(-j) - \frac{2}{\pi}\hat{V}(s_1)\left[j\cos^{-1}\sqrt{\frac{s_1}{c}}\right] - \frac{2}{\pi}\delta\hat{V}\left[j\cos^{-1}\sqrt{\frac{s}{c}}\right] + \frac{2}{\pi}\left[-\frac{1}{2}\frac{\lambda^2}{c^2}\hat{\Gamma}(c)\right]F(\infty) = 0\,, \tag{4-107}$$

where as shown in equation (4-47),

$$F(\infty) = \lim_{z\to\infty}\{\left(\frac{c}{i\lambda}\right)\lim_{\sigma_e\to\infty}\left(\int_c^{\sigma_e} e^{-i\frac{\lambda}{c}(\sigma-c)}\frac{(-j)\sqrt{(z-c)z}}{(-2)(z-\sigma)\sqrt{(\sigma-c)\sigma}}d\sigma\right)\}. \tag{4-108}$$

The real and imaginary parts of the complex velocity, at infinity, are equal to zero. From a similar analysis to that shown in section 4.2, one obtains,

$$\delta A = -\frac{2}{\pi}\hat{V}(s_1)\cos^{-1}\sqrt{\frac{s_1}{c}} - \frac{2}{\pi}\delta\hat{V}\cos^{-1}\sqrt{\frac{s}{c}} + \frac{1}{2}\frac{\lambda^2}{c^2}\hat{\Gamma}(c)\left(-\frac{c}{i\lambda}\right)\frac{2}{\pi}\lim_{\sigma_e\to\infty}\left[\int_c^{\sigma_e} e^{-i\frac{\lambda}{c}(\sigma-c)}\frac{d\sigma}{2\sqrt{(\sigma-c)\sigma}}\right]. \tag{4-109}$$

By inserting δA into $\delta\hat{W}(z)$, the equation of the complex velocity becomes,

$$\delta\hat{W}(z) = -\frac{2}{\pi}\hat{V}(s_1)\left[\sqrt{\frac{c-z}{z}}\cos^{-1}\sqrt{\frac{s_1}{c}} + \cosh^{-1}\sqrt{\frac{(c-z)s_1}{c(s_1-z)}}\right] - \frac{2}{\pi}\delta\hat{V}\left[\cosh^{-1}\sqrt{\frac{(c-z)s}{c(s-z)}} + \sqrt{\frac{c-z}{z}}\cos^{-1}\sqrt{\frac{s}{c}}\right] + \frac{1}{2}\frac{\lambda^2}{c^2}\hat{\Gamma}(c)\frac{2}{\pi}\left(-\frac{c}{i\lambda}\right)J(z) \tag{4-110}$$

where,

$$J(z) = \lim_{\sigma_e\to\infty}\{\int_c^{\sigma_e} e^{-i\frac{\lambda}{c}(\sigma-c)}\left[\frac{\sqrt{(c-z)z}}{2(\sigma-z)\sqrt{(\sigma-c)\sigma}} + \sqrt{\frac{c-z}{z}}\frac{1}{2\sqrt{(\sigma-c)\sigma}}\right]d\sigma\}. \tag{4-111}$$

Determination of $\delta\hat{\Gamma}(c)$ for the prototype problem of the airfoil with an oscillating aileron

The circulation for the prototype aileron problem around the airfoil is given by,

$$\delta\hat{\Gamma}(c) = 2\int_0^c \mathrm{REAL}_j\left[\delta\hat{W}(z)\right]_{z=x} dx, \tag{4-112}$$

By taking the real part of the complex velocity and performing the integration around the airfoil, one obtains,

$$\frac{1}{2}\delta\hat{\Gamma}(c) = -\frac{2}{\pi}\hat{V}(s_1)\left[\cos^{-1}\sqrt{\frac{s_1}{c}}\cdot\int_0^c\sqrt{\frac{c-x}{x}}dx + \int_0^c \cosh^{-1}\sqrt{\frac{(c-x)s_1}{c(s_1-x)}}dx\right]$$
$$-\frac{2}{\pi}\delta\hat{V}\int_0^c\left[\cosh^{-1}\sqrt{\frac{(c-x)s}{c(s-x)}} + \sqrt{\frac{c-x}{x}}\cos^{-1}\sqrt{\frac{s}{c}}\right]dx + \frac{1}{2}\frac{\lambda^2}{c^2}\delta\hat{\Gamma}(c)\frac{2}{\pi}\left(-\frac{c}{i\lambda}\right)\int_0^c J(x)dx \tag{4-113}$$

The derivations of the above integrals are given in Appendix A.

The resultant equation of the reduced circulation for the airfoil with an oscillating aileron is given by,

$$\delta\hat{\Gamma}(c) = G\left\{-\frac{2}{\pi}\hat{V}(s_1)\left[\sqrt{(c-s_1)s_1} + c\cos^{-1}\sqrt{\frac{s_1}{c}}\right] - \frac{2}{\pi}\delta\hat{V}\left[\sqrt{(c-s)s} + c\cos^{-1}\sqrt{\frac{s}{c}}\right]\right\} \tag{4-114}$$

where,

$$G = -\frac{4i}{\lambda}\frac{e^{-i\frac{\lambda}{2}}}{H_1^{(2)}(\lambda/2) + i H_0^{(2)}(\lambda/2)}. \tag{4-115}$$

where $H_1^{(2)}(\lambda/2)$ and $H_0^{(2)}(\lambda/2)$ are the Hankel's integrals of second kind of orders of one and zero [7,20,29], respectively.

Determination of $\delta\hat{C}_p(x)$

The reduced pressure coefficient $\delta\hat{C}_p(x)$ for the prototype aileron problem is expressed in terms of the reduced velocity potential $\delta\hat{\varphi}$ as,

$$\delta\hat{C}_p(x) = -\frac{2}{U_\infty}\left[i\frac{\omega}{U_\infty}\delta\hat{\varphi}(x,y) + \frac{\partial(\delta\hat{\varphi})}{\partial x}\right], \tag{4-116}$$

where,

$$\delta\hat{\varphi} = \int_0^x \delta\hat{u}\,dx = \frac{1}{2}\int_0^x 2\,\delta\hat{u}\,dx = \frac{1}{2}\delta\hat{\Gamma}(x). \tag{4-117}$$

The equation of the reduced pressure coefficient $\delta\hat{C}_p(x)$ is then expressed as,

$$\delta\hat{C}_p(x) = -\frac{2}{U_\infty}\left[i\frac{\lambda}{c}\frac{1}{2}\delta\hat{\Gamma}(x) + \delta\hat{u}\right]. \tag{4-118}$$

where λ is the reduced frequency.

The expression of the reduced velocity on the airfoil $\delta\hat{u}$ is given by,

$$\delta\hat{u} = \mathrm{REAL}_j\left[\delta\hat{W}(z)\right]_{z=x}. \tag{4-119}$$

By taking the real part of the complex velocity $\delta\hat{W}(z)$, the expression of $\delta\hat{u}$ is given by,

$$\begin{aligned}\delta\hat{u}(x) = &-\frac{2}{\pi}\hat{V}(s_1)\left[\sqrt{\frac{c-x}{x}}\cos^{-1}\sqrt{\frac{s_1}{c}} + \cosh^{-1}\sqrt{\frac{(c-x)s_1}{c(s_1-x)}}\right] \\ &-\frac{2}{\pi}\delta\hat{V}\left[\cosh^{-1}\sqrt{\frac{(c-x)s}{c(s-x)}} + \sqrt{\frac{c-x}{x}}\cos^{-1}\sqrt{\frac{s}{c}}\right] + \frac{1}{2}\frac{\lambda^2}{c^2}\delta\hat{\Gamma}(c)\frac{2}{\pi}\left(-\frac{c}{i\lambda}\right)J(x)\end{aligned} \tag{4-120}$$

The expression of the partial reduced circulation at any position x is given by,

$$\begin{aligned}\frac{1}{2}\delta\hat{\Gamma}(x) = &-\frac{2}{\pi}\hat{V}(s_1)\left[\cos^{-1}\sqrt{\frac{s_1}{c}}\cdot\int_0^x\sqrt{\frac{c-x}{x}}dx + \int_0^x\cosh^{-1}\sqrt{\frac{(c-x)s_1}{c(s_1-x)}}dx\right] \\ &-\frac{2}{\pi}\delta\hat{V}\int_0^x\left[\cosh^{-1}\sqrt{\frac{(c-x)s}{c(s-x)}} + \sqrt{\frac{c-x}{x}}\cos^{-1}\sqrt{\frac{s}{c}}\right]dx + \frac{1}{2}\frac{\lambda^2}{c^2}\delta\hat{\Gamma}(c)\frac{2}{\pi}\left(-\frac{c}{i\lambda}\right)\int_0^x J(x)dx\end{aligned}$$

(4-121)

The above integrals are evaluated in Appendix A.

By inserting the above equations into the expression of the reduced pressure coefficient, one obtains,

$$-\frac{U_\infty}{2}\delta\hat{C}_p(x)=\left(\frac{i\lambda}{c}\right)\left[-\frac{2}{\pi}\hat{V}(s_1)\cos^{-1}\sqrt{\frac{s_1}{c}}-\frac{2}{\pi}\delta\hat{V}\cos^{-1}\sqrt{\frac{s}{c}}\right]\sqrt{(c-x)x}$$

$$+\left(-\frac{1}{c}\right)\sqrt{\frac{c-x}{x}}(1-C(\lambda/2))\{\ -\frac{2}{\pi}\hat{V}(s_1)\left[\sqrt{(c-s_1)s_1}+c\cos^{-1}\sqrt{\frac{s_1}{c}}\right]-$$

$$-\frac{2}{\pi}\delta\hat{V}\left[\sqrt{(c-s)s}+c\cos^{-1}\sqrt{\frac{s}{c}}\right]\ \}$$

$$-\frac{2}{\pi}\left(\frac{i\lambda}{c}\right)\hat{V}(s_1)\left[(x-s_1)\cosh^{-1}\sqrt{\frac{(c-x)s_1}{c(s_1-x)}}\right]-\frac{2}{\pi}\left(\frac{i\lambda}{c}\right)\delta\hat{V}\left[(x-s)\cosh^{-1}\sqrt{\frac{(c-x)s}{c(s-x)}}\right]-$$

$$-\frac{2}{\pi}\hat{V}(s_1)\left[\sqrt{\frac{c-x}{x}}\cos^{-1}\sqrt{\frac{s_1}{c}}+\cosh^{-1}\sqrt{\frac{(c-x)s_1}{c(s_1-x)}}\right]-$$

$$-\frac{2}{\pi}\delta\hat{V}\left[\cosh^{-1}\sqrt{\frac{(c-x)s}{c(s-x)}}+\sqrt{\frac{c-x}{x}}\cos^{-1}\sqrt{\frac{s}{c}}\right]$$

(4-122)

Detailed calculations are shown in Appendix D.

Determination of $\delta\hat{C}_L$

The reduced lift coefficient $\delta\hat{C}_L$ for the prototype aileron problem is related to the reduced pressure difference coefficient $\delta[\ \Delta\hat{C}_p(x)\ ]$ by the expression.

$$\delta\hat{C}_L=\frac{1}{c}\int_0^c\delta[\ \Delta\hat{C}_p(x)\ ]dx=-\frac{2}{c}\int_0^c\delta\hat{C}_p(x)\,dx. \tag{4-123}$$

After evaluating the related integrals (see Appendix A), the expression of the reduced lift coefficient is given by,

$$\begin{aligned}-\frac{U_\infty c}{4}\delta\hat{C}_L&=-\hat{V}(s_1)\cdot\sqrt{(c-s_1)s_1}\left\{C(\lambda/2)+\frac{1}{2}\left(\frac{i\lambda}{c}\right)\left(\frac{c}{2}-s_1\right)\right\}-\\&-\delta\hat{V}\cdot\sqrt{(c-s)s}\left\{C(\lambda/2)+\frac{1}{2}\left(\frac{i\lambda}{c}\right)\left(\frac{c}{2}-s\right)\right\}-\\&-\left[\hat{V}(s_1)\cos^{-1}\sqrt{\frac{s_1}{c}}+\delta\hat{V}\cos^{-1}\sqrt{\frac{s}{c}}\right]\cdot\left\{\left(\frac{i\lambda c}{4}\right)+cC(\lambda/2)\right\}\end{aligned} \tag{4-124}$$

Determination of $\delta \hat{C}_m$

The reduced pitching moment coefficient $\delta \hat{C}_m$ for the prototype aileron problem is evaluated by

$$\delta \hat{C}_m = -\frac{2}{c^2}\int_0^c x\,\delta \hat{C}_p(x)\,dx, \tag{4-125}$$

The detailed integral derivations related to $\delta \hat{C}_m$ are given in Appendix A, the expression of the reduced pitching moment coefficient $\delta \hat{C}_m$ is given by,

$$\begin{aligned}
-\frac{U_\infty c^2}{4}\delta\hat{C}_m = & -\hat{V}(s_1)\sqrt{(c-s_1)s_1}\left\{\frac{c}{4}C(\lambda/2)+\left(\frac{i\lambda}{c}\right)\left(\frac{3}{24}c^2-\frac{c}{12}s_1-\frac{s_1^2}{6}\right)+\frac{s_1}{2}\right\}- \\
& -\left[\hat{V}(s_1)\cos^{-1}\sqrt{\frac{s_1}{c}}+\delta\hat{V}\cos^{-1}\sqrt{\frac{s}{c}}\right]\left\{\frac{3}{24}\left(\frac{i\lambda}{c}\right)c^3+\frac{c^2}{4}C(\lambda/2)\right\}- \quad . \\
& -\delta\hat{V}\sqrt{(c-s)s}\left\{\frac{c}{4}C(\lambda/2)+\left(\frac{i\lambda}{c}\right)\left(\frac{3}{24}c^2-\frac{c}{12}s-\frac{s^2}{6}\right)+\frac{s}{2}\right\}
\end{aligned} \tag{4-126}$$

where $C(\lambda/2)$ is Theodorsen's [15,26] function.

4.4.2 The complete problem for the airfoil with an oscillating aileron

In the equations derived in the previous section, the velocity jump $\delta\hat{V}$ can be obtained from equations (4-92) and (4-100) in the form,

$$\delta\hat{V} = \left[\frac{d\hat{V}}{dx}\right]_{x=s} ds = \begin{cases} 0 & \text{for } x \in (0, s_1) \\ \sum_{k=1}^{n} k\,\beta_k s^{k-1} ds & \text{for } x \in (s_1, c). \end{cases} \tag{4-127}$$

The reduced circulation is given in the general form as.

$$\begin{aligned}
\hat{\Gamma}(c) = G\Bigg\{ & -\frac{2}{\pi}\hat{V}(s_1)\left[\sqrt{(c-s_1)s_1}+c\cos^{-1}\sqrt{\frac{s_1}{c}}\right]- \\
& -\frac{2}{\pi}\int_{s_1}^{c}\left[\sqrt{(c-s)s}+c\cos^{-1}\sqrt{\frac{s}{c}}\right]\left[\frac{d\hat{V}}{dx}\right]_{x=s} ds.
\end{aligned} \tag{4-128}$$

By using the above expression and performing the integration from $x = s_1$ to the trailing edge of the airfoil $x = c$, the reduced circulation can be expressed as,

$$\hat{\Gamma}(c) = G\left\{ -\frac{2}{\pi}\hat{V}(s_1)\left[\sqrt{(c-s_1)s_1} + c\cos^{-1}\sqrt{\frac{s_1}{c}}\right] - \right.$$
$$\left. -\frac{2}{\pi}\sum_{k=1}^{n} k\,\beta_k \int_{s_1}^{c} s^{k-1}\left[\sqrt{(c-s)s} + c\cos^{-1}\sqrt{\frac{s}{c}}\right] ds \right\}. \tag{4-129}$$

Details of the integrals calculations are shown in Appendix A.

After performing the integration in equation (4-129), the expression of the reduced circulation for the airfoil with an oscillating aileron $\hat{\Gamma}(c)$ is given by,

$$\hat{\Gamma}(c) = G\left\{ -\frac{2}{\pi}\hat{V}(s_1)\left[\sqrt{(c-s_1)s_1} + c\cos^{-1}\sqrt{\frac{s_1}{c}}\right] - \right.$$
$$\left. -\frac{2}{\pi}\sum_{k=1}^{n} \beta_k\left[\left(\frac{2k+1}{k+1}\right)\frac{c}{2}I_k - s_1^k\left(\frac{k}{k+1}\sqrt{(c-s_1)s_1} + c\cos^{-1}\sqrt{\frac{s_1}{c}}\right)\right] \right\} \tag{4-130}$$

where the recurrence formula I_k for the airfoil with an oscillating aileron is given by.

$$I_k = \frac{s_1^{k-1}}{k}\sqrt{(c-s_1)s_1} + \frac{2k-1}{2k}c\,I_{k-1} \qquad ,k \geq 1. \tag{4-131}$$

where,

$$I_0 = 2\cos^{-1}\sqrt{\frac{s_1}{c}} \quad , \quad I_1 = \sqrt{(c-s_1)s_1} + c\cos^{-1}\sqrt{\frac{s_1}{c}}. \tag{4-132}$$

The reduced pressure coefficient $\hat{C}_p(x)$ for the airfoil with an aileron

The general expression of the reduced pressure coefficient for the airfoil with an aileron is obtained by substituting the expression of the velocity jump $\delta\hat{V}$ into the equation obtained for the reduced pressure coefficient of the prototype aileron problem, $\delta\hat{C}_p(x)$. The expression is given in general form as,

$$
\begin{aligned}
-\frac{U_\infty}{2}\hat{C}_p(x) &= \left(\frac{i\lambda}{c}\right)\left[-\frac{2}{\pi}\hat{V}(s_1)\cos^{-1}\sqrt{\frac{s_1}{c}} - \frac{2}{\pi}\int_{s_1}^{c}\cos^{-1}\sqrt{\frac{s}{c}}\left[\frac{d\hat{V}}{dx}\right]_{x=s} ds\right]\sqrt{(c-x)x} + \\
&+\left(-\frac{1}{c}\right)\sqrt{\frac{c-x}{x}}\left(1-C(\lambda/2)\right)\Big\{-\frac{2}{\pi}\hat{V}(s_1)\left[\sqrt{(c-s_1)s_1}+c\cos^{-1}\sqrt{\frac{s_1}{c}}\right]- \\
&\qquad -\frac{2}{\pi}\int_{s_1}^{c}\left[\sqrt{(c-s)s}+c\cos^{-1}\sqrt{\frac{s}{c}}\right]\left[\frac{d\hat{V}}{dx}\right]_{x=s} ds\Big\} \\
&-\frac{2}{\pi}\left(\frac{i\lambda}{c}\right)\hat{V}(s_1)\left[(x-s_1)\cosh^{-1}\sqrt{\frac{(c-x)s_1}{c(s_1-x)}}\right]- \\
&-\frac{2}{\pi}\left(\frac{i\lambda}{c}\right)\int_{s_1}^{c}\left[(x-s)\cosh^{-1}\sqrt{\frac{(c-x)s}{c(s-x)}}\right]\left[\frac{d\hat{V}}{dx}\right]_{x=s} ds- \\
&-\frac{2}{\pi}\hat{V}(s_1)\left[\sqrt{\frac{c-x}{x}}\cos^{-1}\sqrt{\frac{s_1}{c}}+\cosh^{-1}\sqrt{\frac{(c-x)s_1}{c(s_1-x)}}\right]- \\
&-\frac{2}{\pi}\int_{s_1}^{c}\left[\cosh^{-1}\sqrt{\frac{(c-x)s}{c(s-x)}}+\sqrt{\frac{c-x}{x}}\cos^{-1}\sqrt{\frac{s}{c}}\right]\left[\frac{d\hat{V}}{dx}\right]_{x=s} ds.
\end{aligned}
\tag{4-133}
$$

By integrating from $x = s_1$ to the trailing edge of the airfoil $x = c$ one obtains the reduced pressure coefficient $\hat{C}_p(x)$ in the general integral form,

$$
\begin{aligned}
-\frac{U_\infty}{2}\hat{C}_p(x) = &\left(\frac{i\lambda}{c}\right)\left[-\frac{2}{\pi}\hat{V}(s_1)\cos^{-1}\sqrt{\frac{s_1}{c}} - \frac{2}{\pi}\sum_{k=1}^{n} k\beta_k \int_{s_1}^{c} s^{k-1}\cos^{-1}\sqrt{\frac{s}{c}}\,ds\right]\sqrt{(c-x)x} + \\
&+\left(-\frac{1}{c}\right)\sqrt{\frac{c-x}{x}}\left(1 - C(\lambda/2)\right)\Bigg\{ -\frac{2}{\pi}\hat{V}(s_1)\left[\sqrt{(c-s_1)s_1} + c\cos^{-1}\sqrt{\frac{s_1}{c}}\right] - \\
&\qquad -\frac{2}{\pi}\sum_{k=1}^{n} k\,\beta_k \int_{s_1}^{c} s^{k-1}\left[\sqrt{(c-s)s} + c\cos^{-1}\sqrt{\frac{s}{c}}\right]ds \Bigg\} \\
&-\frac{2}{\pi}\left(\frac{i\lambda}{c}\right)\hat{V}(s_1)\left[(x-s_1)\cosh^{-1}\sqrt{\frac{(c-x)s_1}{c(s_1-x)}}\right] - \\
&-\frac{2}{\pi}\left(\frac{i\lambda}{c}\right)\sum_{k=1}^{n} k\,\beta_k \int_{s_1}^{c} s^{k-1}\left[(x-s)\cosh^{-1}\sqrt{\frac{(c-x)s}{c(s-x)}}\right]ds - \\
&-\frac{2}{\pi}\hat{V}(s_1)\left[\sqrt{\frac{c-x}{x}}\cos^{-1}\sqrt{\frac{s_1}{c}} + \cosh^{-1}\sqrt{\frac{(c-x)s_1}{c(s_1-x)}}\right] - \\
&-\frac{2}{\pi}\sum_{k=1}^{n} k\,\beta_k \int_{s_1}^{c} s^{k-1}\left[\cosh^{-1}\sqrt{\frac{(c-x)s}{c(s-x)}} + \sqrt{\frac{c-x}{x}}\cos^{-1}\sqrt{\frac{s}{c}}\right]ds
\end{aligned}
\tag{4-134}
$$

The resultant expression of the reduced pressure coefficient $\hat{C}_p(x)$ for the airfoil with an oscillating aileron is given by,

$$
\begin{aligned}
-\frac{U_\infty}{2}\hat{C}_p(x) = & \left(\frac{i\lambda}{c}\right)\left[-\frac{2}{\pi}\hat{V}(s_1)\cos^{-1}\sqrt{\frac{s_1}{c}}-\frac{2}{\pi}\zeta_1\right]\sqrt{(c-x)x}+ \\
& +\left(-\frac{1}{c}\right)\sqrt{\frac{c-x}{x}}(1-C(\lambda/2))\left\{-\frac{2}{\pi}\hat{V}(s_1)\zeta_6-\frac{2}{\pi}\zeta_2-\frac{2}{\pi}c\zeta_1\right\}- \\
& -\frac{2}{\pi}\left(\frac{i\lambda}{c}\right)\hat{V}(s_1)\zeta_7(x)-\frac{2}{\pi}\zeta_3(x)\left(1+\frac{i\lambda}{c}x\right)+\frac{2}{\pi}\left(\frac{i\lambda}{c}\right)\zeta_4(x)- \\
& -\frac{2}{\pi}\hat{V}(s_1)\zeta_5(x)-\frac{2}{\pi}\sqrt{\frac{c-x}{x}}\zeta_1
\end{aligned}, \tag{4-135}
$$

where,

$$\zeta_1=\sum_{k=1}^{n}\beta_k\left(\frac{1}{2}I_k-s_1^k\cos^{-1}\sqrt{\frac{s_1}{c}}\right), \tag{4-136}$$

$$\zeta_2=\sum_{k=1}^{n}\left(\frac{k}{k+1}\right)\beta_k\left(\frac{c}{2}I_k-s_1^k\sqrt{(c-s_1)s_1}\right), \tag{4-137}$$

$$\zeta_3(x)=\sum_{k=1}^{n}\beta_k\left[\left(x^k-s_1^k\right)H(x)+\frac{1}{2}\sqrt{\frac{c-x}{x}}\sum_{q=0}^{k-1}x^{k-q}I_q\right], \tag{4-138}$$

$$\zeta_4(x)=\sum_{k=1}^{n}\left(\frac{k}{k+1}\right)\beta_k\left[\left(x^{k+1}-s_1^{k+1}\right)H(x)+\frac{1}{2}\sqrt{(c-x)x}\sum_{q=0}^{k}x^{k-q}I_q\right], \tag{4-139}$$

$$\zeta_5(x)=\sqrt{\frac{c-x}{x}}\cos^{-1}\sqrt{\frac{s_1}{c}}+H(x), \tag{4-140}$$

$$\zeta_6=\sqrt{(c-s_1)s_1}+c\cos^{-1}\sqrt{\frac{s_1}{c}}. \tag{4-141}$$

$$\zeta_7(x)=(x-s_1)H(x). \tag{4-142}$$

where,

$$H(x)=\left\{\begin{array}{ll}\cosh^{-1}\sqrt{\dfrac{(c-x)s_1}{c(s_1-x)}} & 0<x<s_1\\ \sinh^{-1}\sqrt{\dfrac{(c-x)s_1}{c(x-s_1)}} & s_1<x<c\end{array}\right\}. \tag{4-143}$$

The recurrence expression I_k is given by equations (4-131) and (4-132),

$$I_k = \frac{s_1^{k-1}}{k}\sqrt{(c-s_1)s_1} + \frac{2k-1}{2k} c\, I_{k-1} \qquad ,k \geq 1, \tag{4-144}$$

where,

$$I_0 = 2\cos^{-1}\sqrt{\frac{s_1}{c}} \quad , \quad I_1 = \sqrt{(c-s_1)s_1} + c\,\cos^{-1}\sqrt{\frac{s_1}{c}}. \tag{4-145}$$

The values of the coefficients$(\beta_k,\ \ k = 0 \rightarrow n)$can be determined from the specific boundary conditions on the airfoil with an oscillating aileron.

The reduced lift coefficient $\hat{C}_L$ for the airfoil with an aileron

The general expression for the reduced lift coefficient $\hat{C}_L$ is obtained by inserting the equation of the velocity jump $\delta\hat{V}$ into the expression obtained for $\delta\hat{C}_L$ and performing the integration from the aileron position $x = s_1$ to the trailing edge of the airfoil $x = c$. The expression is given by.

$$\begin{aligned}
-\frac{U_\infty c}{4}\hat{C}_L = &-\hat{V}(s_1)\sqrt{(c-s_1)s_1}\left\{C(\lambda/2) + \frac{1}{2}\left(\frac{i\lambda}{c}\right)\left(\frac{c}{2}-s_1\right)\right\} - \\
&-\int_{s_1}^{c} \sqrt{(c-s)s}\left\{C(\lambda/2) + \frac{1}{2}\left(\frac{i\lambda}{c}\right)\left(\frac{c}{2}-s\right)\right\}\left[\frac{d\hat{V}}{dx}\right]_{x=s} ds - \\
&-\left[\hat{V}(s_1)\cos^{-1}\sqrt{\frac{s_1}{c}} + \int_{s_1}^{c} \cos^{-1}\sqrt{\frac{s}{c}}\left[\frac{d\hat{V}}{dx}\right]_{x=s} ds\right]\left\{\left(\frac{i\lambda c}{4}\right) + c\,C(\lambda/2)\right\}.
\end{aligned}$$

(4-146)

The resultant expression of the reduced lift coefficient $\hat{C}_L$ for the airfoil with an oscillating aileron is given in an integral form by,

$$
\begin{aligned}
-\frac{U_\infty c}{4}\hat{C}_L = & -\hat{V}(s_1)\sqrt{(c-s_1)s_1}\left\{C(\lambda/2)+\frac{1}{2}\left(\frac{i\lambda}{c}\right)\left(\frac{c}{2}-s_1\right)\right\}- \\
& -\sum_{k=1}^{n} k\,\beta_k \int_{s_1}^{c} s^{k-1}\sqrt{(c-s)s}\left\{C(\lambda/2)+\frac{1}{2}\left(\frac{i\lambda}{c}\right)\left(\frac{c}{2}-s\right)\right\}ds- \\
& -\left[\hat{V}(s_1)\cos^{-1}\sqrt{\frac{s_1}{c}}+\sum_{k=1}^{n} k\,\beta_k \int_{s_1}^{c} s^{k-1}\cos^{-1}\sqrt{\frac{s}{c}}\,ds\right]\left\{\left(\frac{i\lambda c}{4}\right)+cC(\lambda/2)\right\}
\end{aligned}
$$

(4-147)

Detailed calculations of the integrals are given in Appendix A.

The expression of the reduced lift coefficient $\hat{C}_L$ for the airfoil with an oscillating aileron is then given in the form

$$
\begin{aligned}
-\frac{U_\infty c}{4}\hat{C}_L = & -\hat{V}(s_1)\sqrt{(c-s_1)s_1}\left\{C(\lambda/2)+\frac{1}{2}\left(\frac{i\lambda}{c}\right)\left(\frac{c}{2}-s_1\right)\right\}- \\
& -\left[C(\lambda/2)+\frac{i\lambda}{4}\right]\sum_{k=1}^{n}\beta_k\left(\frac{ck}{2(k+1)}I_k-\frac{k}{k+1}s_1^k\sqrt{(c-s_1)s_1}\right)+ \\
& +\frac{1}{2}\left(\frac{i\lambda}{c}\right)\sum_{k=1}^{n}k\,\beta_k\left(\frac{c^2(2k+1)}{4(k+1)(k+2)}I_k+\frac{s_1^k}{k+2}\sqrt{(c-s_1)s_1}\left(\frac{c}{2(k+1)}-s_1\right)\right)- \\
& -\left\{\left(\frac{i\lambda c}{4}\right)+cC(\lambda/2)\right\}\left[\hat{V}(s_1)\cos^{-1}\sqrt{\frac{s_1}{c}}+\sum_{k=1}^{n}\beta_k\left(\frac{1}{2}I_k-s_1^k\cos^{-1}\sqrt{\frac{s_1}{c}}\right)\right]
\end{aligned}
$$

(4-148)

The same analytical steps used to obtain the reduced lift coefficient $\hat{C}_L$ for the airfoil with an oscillating aileron are repeated for the reduced pitching moment coefficient $\hat{C}_m$. The general expression is defined by,

$$
\begin{aligned}
-\frac{U_\infty c^2}{4}\hat{C}_m = & -\hat{V}(s_1)\sqrt{(c-s_1)s_1}\left\{\frac{c}{4}C(\lambda/2)+\left(\frac{i\lambda}{c}\right)\left(\frac{3}{24}c^2-\frac{c}{12}s_1-\frac{s_1^2}{6}\right)+\frac{s_1}{2}\right\}- \\
& -\left[\hat{V}(s_1)\cos^{-1}\sqrt{\frac{s_1}{c}}+\int_{s_1}^{c}\cos^{-1}\sqrt{\frac{s}{c}}\left[\frac{d\hat{V}}{dx}\right]_{x=s}ds\right]\left\{\frac{3}{24}\left(\frac{i\lambda}{c}\right)c^3+\frac{c^2}{4}C(\lambda/2)\right\}- \\
& -\int_{s_1}^{c}\sqrt{(c-s)s}\left\{\frac{c}{4}C(\lambda/2)+\left(\frac{i\lambda}{c}\right)\left(\frac{3}{24}c^2-\frac{c}{12}s-\frac{s^2}{6}\right)+\frac{s}{2}\right\}\left[\frac{d\hat{V}}{dx}\right]_{x=s}ds.
\end{aligned}
$$

(4-149)

The resultant expression of the reduced pitching moment coefficient for the airfoil with an aileron is expressed in an integral form as

$$
\begin{aligned}
-\frac{U_\infty c^2}{4}\hat{C}_m = & -\hat{V}(s_1)\sqrt{(c-s_1)s_1}\left\{\frac{c}{4}C(\lambda/2)+\left(\frac{i\lambda}{c}\right)\left(\frac{3}{24}c^2-\frac{c}{12}s_1-\frac{s_1^2}{6}\right)+\frac{s_1}{2}\right\}- \\
& -\left[\hat{V}(s_1)\cos^{-1}\sqrt{\frac{s_1}{c}}+\sum_{k=1}^{n}k\,\beta_k\int_{s_1}^{c}s^{k-1}\cos^{-1}\sqrt{\frac{s}{c}}\,ds\right]\left\{\frac{3}{24}\left(\frac{i\lambda}{c}\right)c^3+\frac{c^2}{4}C(\lambda/2)\right\}- \\
& -\sum_{k=1}^{n}k\,\beta_k\int_{s_1}^{c}s^{k-1}\sqrt{(c-s)s}\left\{\frac{c}{4}C(\lambda/2)+\left(\frac{i\lambda}{c}\right)\left(\frac{3}{24}c^2-\frac{c}{12}s-\frac{s^2}{6}\right)+\frac{s}{2}\right\}ds.
\end{aligned}
$$

(4-150)

Detailed calculations of the integrals are given in Appendix A.

The expression of the reduced pitching moment coefficient for the airfoil with an oscillating aileron is then expressed as,

$$
\begin{aligned}
-\frac{U_\infty c^2}{4}\hat{C}_m =& -\hat{V}(s_1)\sqrt{(c-s_1)s_1}\left\{\frac{c}{4}C(\lambda/2)+\left(\frac{i\lambda}{c}\right)\left(\frac{3}{24}c^2-\frac{c}{12}s_1-\frac{s_1^2}{6}\right)+\frac{s_1}{2}\right\}- \\
& -\left\{\frac{3}{24}\left(\frac{i\lambda}{c}\right)c^3+\frac{c^2}{4}C(\lambda/2)\right\}\left[\hat{V}(s_1)\cos^{-1}\sqrt{\frac{s_1}{c}}+\sum_{k=1}^{n}\beta_k\left(\frac{1}{2}I_k-s_1^k\cos^{-1}\sqrt{\frac{s_1}{c}}\right)\right] \\
& -\left[\frac{c}{4}C(\lambda/2)+\frac{3}{24}(i\lambda c)\right]\sum_{k=1}^{n}\frac{k}{k+1}\beta_k\left(\frac{c}{2}I_k-s_1^k\sqrt{(c-s_1)s_1}\right)- \\
& -\left(\frac{1}{2}-\frac{i\lambda}{12}\right)\sum_{k=1}^{n}\frac{k}{k+2}\beta_k\left(\frac{c}{2}I_{k+1}-s_1^{k+1}\sqrt{(c-s_1)s_1}\right) \\
& +\left(\frac{i\lambda}{6c}\right)\sum_{k=1}^{n}\frac{k}{k+3}\beta_k\left(\frac{c}{2}I_{k+2}-s_1^{k+2}\sqrt{(c-s_1)s_1}\right)
\end{aligned}
\tag{4-151}
$$

The recurrence expression I_k is given by equations (4-131) and (4-132),

$$I_k=\frac{s_1^{k-1}}{k}\sqrt{(c-s_1)s_1}+\frac{2k-1}{2k}c\,I_{k-1} \qquad ,k\geq 1. \tag{4-152}$$

where,

$$I_0=2\cos^{-1}\sqrt{\frac{s_1}{c}} \quad , \quad I_1=\sqrt{(c-s_1)s_1}+c\cos^{-1}\sqrt{\frac{s_1}{c}}. \tag{4-153}$$

The values of the coefficients (β_k for $k\geq 0$) can be determined from the specific boundary conditions on the airfoil with an oscillating aileron.

4.5 Unsteady flow solutions for airfoils executing oscillatory translations and rotations

4.5.1 Boundary conditions on the oscillating airfoil and aileron

Consider an airfoil executing vertical oscillatory translation $h(t)$ and oscillatory pitching rotation $\theta(t)$, while the aileron executes oscillatory rotational motion $\beta(t)$, as shown in Figure 4.7.

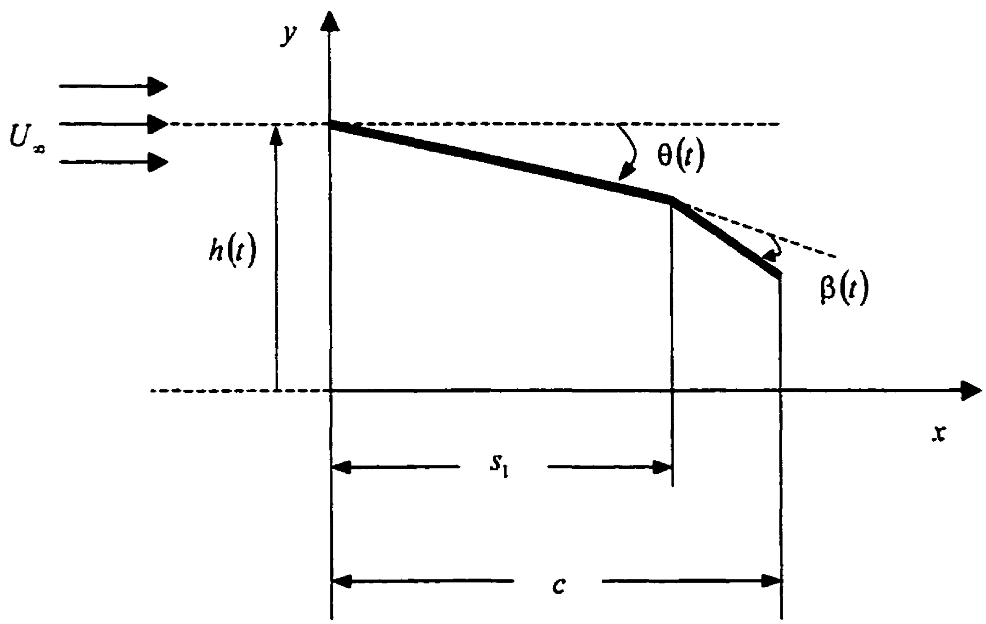

Fig 4.7 Geometry of an airfoil and aileron under unsteady oscillations.

The vertical oscillatory translation $h(t)$, the pitching oscillatory rotation $\theta(t)$ and the oscillatory rotation of the aileron $\beta(t)$, are denoted by (as shown in Chapter 2),

$$h(t)=\hat{h}e^{i\omega t}, \tag{4-154}$$

$$\theta(t)=\hat{\theta}e^{i\omega t}, \tag{4-155}$$

$$\beta(t)=\hat{\beta}e^{i\omega t}, \tag{4-156}$$

The corresponding boundary conditions are,

$$V(x,t)=\begin{Bmatrix} \left(-U_\infty\hat{\theta}+i\omega\left(\hat{h}-\hat{\theta}x\right)\right)e^{i\omega t} & \text{for } x\in(0,s_1) \\ \left(-U_\infty\hat{\theta}+i\omega\left(\hat{h}-\hat{\theta}x\right)-i\omega\hat{\beta}(x-s_1)-U_\infty\hat{\beta}\right)e^{i\omega t} & \text{for } x\in(s_1,c) \end{Bmatrix},$$

(4-157)

The vertical disturbance velocity $V(x,t)$ can be expressed as,

$$V(x,t)=\hat{V}(x)e^{i\omega t}, \tag{4-158}$$

where $\hat{V}(x)$ is the reduced vertical disturbance velocity given by,

$$\hat{V}(x)=\begin{Bmatrix} \left(-U_\infty\hat{\theta}+i\omega\left(\hat{h}-\hat{\theta}x\right)\right) & \text{for } x\in(0,s_1) \\ \left(-U_\infty\hat{\theta}+i\omega\left(\hat{h}-\hat{\theta}x\right)-i\omega\hat{\beta}(x-s_1)-U_\infty\hat{\beta}\right) & \text{for } x\in(s_1,c) \end{Bmatrix}. \tag{4-159}$$

4.5.2 Unsteady flow solution past an airfoil in oscillatory translation

Consider an airfoil executing vertical oscillatory translation $h(t)$, as shown in Figure 4.8.

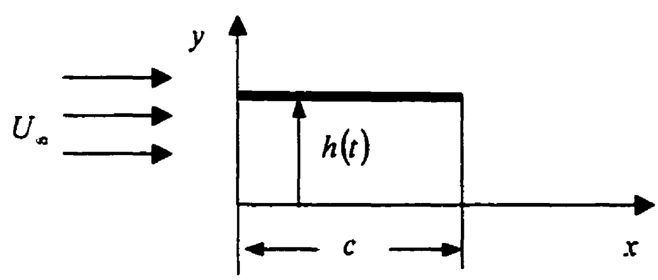

Fig 4.8 Geometry of an airfoil executing vertical oscillatory translation $h(t)$.

The vertical oscillatory translation $h(t)$ is expressed as,

$$h(t)=\hat{h}e^{i\omega t}, \tag{4-160}$$

where ω and t are the frequency and time, respectively.

The boundary condition on the oscillating airfoil is given from equation (4-159) by,

$$\hat{V}(x)=i\omega\hat{h}, \tag{4-161}$$

From the method of velocity singularity for unsteady flows, the polynomial representation of the vertical velocity on the airfoil is given by,

$$\hat{V}(x)=\sum_{k=1}^{n} b_k\, x^k\,, \tag{4-162}$$

By comparing the two vertical velocities on the airfoil, one concludes the values of the constants b_k,

$$b_0 = i\omega\,\hat{h} \qquad \text{and} \quad b_k = 0,\ \text{for}\ k \ge 1. \tag{4-163}$$

Reduced pressure difference coefficient for oscillatory translation

The expression of the reduced pressure coefficient $\hat{C}_p(x)$ for an airfoil executing oscillatory translational motion, after substituting the values of the constants b_k in the general expression of the reduced pressure coefficient equation (4-85), is given by,

$$-\frac{U_\infty}{2}\,\hat{C}_p(x)=\left(-\frac{i\lambda}{c\pi}\right)\sqrt{(c-x)c}\,\left[b_0\, I_0\right]+\frac{1}{\pi}\sqrt{\frac{c-x}{x}}\, b_0\,\{(1-C(\lambda/2))I_0 - I_0\}, \tag{4-164}$$

where

$$b_0 = i\omega\,\hat{h} \ \text{and} \ I_0 = \pi. \tag{4-165}$$

The general expression of the reduced pressure coefficient $\hat{C}_p(x)$ for an airfoil executing oscillatory translation after arrangements, is given by,

$$\frac{U_\infty^2}{\hat{h}\,\omega^2 c}\,\hat{C}_p(x)=-2\,\sqrt{(c-x)x}\left[\frac{1}{c}-\frac{i}{\lambda x}\,C(\lambda/2)\right]. \tag{4-166}$$

The reduced pressure difference coefficient $\Delta\hat{C}_p(x)$ is given by,

$$\Delta\hat{C}_p(x) = -2\,\hat{C}_p(x), \tag{4-167}$$

The pressure difference coefficient $\Delta C_p(x)$ is expressed as,

$$\Delta C_p(x,t)=\Delta\hat{C}_p(x)\,e^{i\omega t}. \tag{4-168}$$

Reduced lift and pitching moment coefficients for oscillatory translation

The reduce lift coefficient is calculated in the same manner as the reduced pressure coefficient. From equation (4-89) $\hat{C}_L$ is given by,

$$\frac{-U_\infty}{i\lambda}\hat{C}_L = -\frac{1}{2}\left(1-\frac{4i}{\lambda}C(\lambda/2)\right)[b_0\, I_0], \tag{4-169}$$

The expression of the lift L for an airfoil executing oscillatory translation can be calculated by,

$$C_L = \hat{C}_L e^{i\omega t}, \tag{4-170}$$

$$C_L = \frac{L}{\frac{1}{2}\rho U_\infty^2 c}. \tag{4-171}$$

where ρ is the density. The general expression of the lift is given by,

$$\frac{4}{\rho\omega^2 c^2 \pi h}L = -\left[1-\frac{4i}{\lambda}C(\lambda/2)\right]. \tag{4-172}$$

The reduced pitching moment coefficient $\hat{C}_m$ for an airfoil executing oscillatory translation is given from equation (4-91) as,

$$\frac{-U_\infty}{i\lambda}\hat{C}_m = -\frac{1}{4}\left(1-\frac{2i}{\lambda}C(\lambda/2)\right)b_0\, I_0, \tag{4-173}$$

The pitching moment coefficient C_m is expressed as.

$$C_m = \hat{C}_m e^{i\omega t}, \tag{4-174}$$

$$C_m = \frac{M}{\frac{1}{2}\rho U_\infty^2 c^2}, \tag{4-175}$$

The pitching moment around the leading edge of the airfoil is expressed as,

$$\frac{8}{\rho\omega^2 c^3 \pi h}M = -\left[1-\frac{2i}{\lambda}C(\lambda/2)\right]. \tag{4-176}$$

where the reduced frequency is given by,

$$\lambda = \frac{\omega c}{U_\infty}. \tag{4-177}$$

4.5.3 Unsteady flow solution past an airfoil in oscillatory rotation

Consider a thin airfoil executing oscillatory rotation $\theta(t)$, as shown in Figure 4.9.

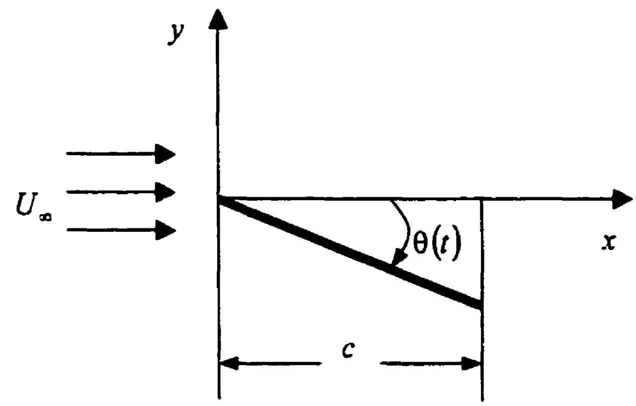

Fig 4.9 Geometry of an airfoil executing oscillatory rotation $\theta(t)$.

The oscillatory rotation $\theta(t)$, is expressed as,

$$\theta(t) = \hat{\theta} e^{i\omega t}, \tag{4-178}$$

The boundary condition on the oscillating airfoil in pure rotation $\theta(t)$ is expressed (from equation (4-159)) as,

$$\hat{V}(x) = -U_\infty \hat{\theta} - i\omega\hat{\theta} x. \tag{4-179}$$

By comparing the terms in the polynomial representation of the vertical velocity $V(x)$ given by,

$$\hat{V}(x) = \sum_{k=1}^{n} b_k x^k . \tag{4-180}$$

one obtains,

$$b_0 = -U_\infty \hat{\theta} \quad , \quad b_1 = -i\omega\hat{\theta} \quad \text{and} \quad b_k = 0 \ \text{for}\, k \geq 2. \tag{4-181}$$

Reduced pressure coefficient for oscillatory rotation

By inserting the constants (obtained from the boundary condition on the airfoil) into the general expression of the reduced pressure coefficient for the airfoil, equation (4-85), one obtains the reduced pressure coefficient $\hat{C}_p(x)$ for an airfoil executing oscillatory rotation,

$$\frac{U_\infty^2}{2\omega^2\hat{\theta}c}\hat{C}_p(x) = -\sqrt{(c-x)x}\left(\frac{2i}{\lambda}-\frac{x}{2c}-\frac{1}{4}\right)+\frac{ic}{\lambda}\sqrt{\frac{c-x}{x}}\left(\frac{1}{4}+\left(-\frac{3}{4}+\frac{i}{\lambda}\right)C(\lambda/2)\right).$$

(4-182)

where the pressure coefficient $C_p(x,t)$ is given by,

$$C_p(x,t) = \hat{C}_p(x)e^{i\omega t}, \tag{4-183}$$

The pressure difference coefficient $\Delta C_p(x,t) = \Delta\hat{C}_p \exp(i\omega t)$ is given by,

$$\Delta C_p(x,t) = -2C_p(x,t), \tag{4-184}$$

$$\Delta\hat{C}_p(x) = -2\hat{C}_p(x). \tag{4-185}$$

Reduced lift and pitching moment coefficients for oscillatory rotation

By inserting the values of the constants b_k into the general equations of the reduced lift and moment coefficients, equations (4-89) and (4-91) respectively, one obtains,

$$\hat{C}_L = \frac{\pi}{4}\hat{\theta}\lambda^2\left[1-\frac{2i}{\lambda}-\frac{8}{\lambda^2}C(\lambda/2)-\frac{6i}{\lambda}C(\lambda/2)\right], \tag{4-186}$$

$$\hat{C}_m = \frac{\pi}{8}\hat{\theta}\lambda^2\left[\frac{9}{8}-\frac{3i}{\lambda}-\frac{3i}{\lambda}C(\lambda/2)-\frac{4}{\lambda^2}C(\lambda/2)\right]. \tag{4-187}$$

The general expressions of the lift L and pitching moment M around the leading edge of the airfoil are given, respectively, as,

$$L = \frac{\pi}{8}\rho c^3\theta\omega^2\left[1-\frac{2i}{\lambda}-\frac{8}{\lambda^2}C(\lambda/2)-\frac{6i}{\lambda}C(\lambda/2)\right], \tag{4-188}$$

$$M = \frac{\pi}{16}\rho c^4\theta\omega^2\left[\frac{9}{8}-\frac{3i}{\lambda}-\frac{3i}{\lambda}C(\lambda/2)-\frac{4}{\lambda^2}C(\lambda/2)\right]. \tag{4-189}$$

4.5.4 Unsteady flow solution past an airfoil executing flexural oscillations

Consider an airfoil executing flexural oscillation of a parabolic type, as shown in Figure 4.10.

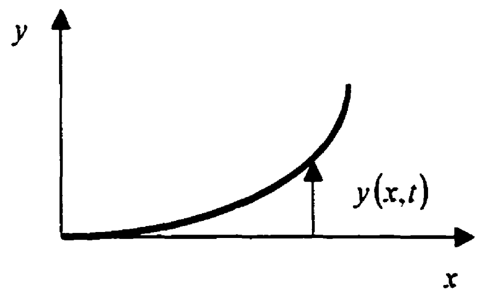

Fig 4.10 Geometry of flexural oscillations on an airfoil.

The parabolic flexural oscillation $y(x,t)$ is assumed in the form,

$$y(x,t) = \mathrm{Re}\left[\varepsilon_0\, c\left(\frac{x}{c}\right)^2 e^{i\omega t}\right]. \tag{4-190}$$

where ε_0 is a constant.

From equations (4-1) and (4-2) one obtains,

$$\hat{e}(x) = \varepsilon_0\, c\left(\frac{x}{c}\right)^2. \tag{4-191}$$

By substituting in equation (4-10), the equation of the reduced vertical velocity $\hat{V}(x)$ for an airfoil under flexural oscillations is given by,

$$\hat{V}(x) = \varepsilon_0 U_\infty\left[2\frac{x}{c} + i\lambda\left(\frac{x}{c}\right)^2\right], \tag{4-192}$$

By comparing the terms in the polynomial representation of the vertical velocity on the airfoil, one obtains,

$b_0 = 0$, $b_1 = 2U_\infty\, \varepsilon_0 / c$, $b_2 = i\omega\varepsilon_0 / c$ and $b_k = 0$ for $k \geq 3$. (4-193)

Reduced pressure coefficient for parabolic flexural oscillations

By substituting the above constants into the general expression of the reduced pressure coefficient (equation (4-85)), one obtains the expression of the reduced pressure coefficient $\hat{C}_p(x)$ for an airfoil executing parabolic flexural oscillations,

$$\hat{C}_p(x)=\frac{2\varepsilon_0\,\omega^2}{U_\infty^2}\Big[\;\sqrt{(c-x)x}\left\{\frac{i}{\lambda}\left(x+\frac{c}{2}\right)-\frac{1}{c}\left(\frac{x^2}{3}+\frac{xc}{6}+\frac{c^2}{8}\right)\right\}+ \\ +\sqrt{\frac{c-x}{x}}\Big\{\;\frac{c^2}{\lambda^2}\left(2\frac{x}{c}-\frac{1}{2}+\frac{3}{2}C(\lambda/2)\right)+ \\ +\frac{i}{\lambda}\left(x^2+\frac{xc}{2}-\frac{c^2}{4}+\frac{5}{8}c^2\,C(\lambda/2)\right)\Big\}\;\Big] \quad . \tag{4-194}$$

where the pressure coefficient $C_p(x,t)$ is given by,

$$C_p(x,t)=\hat{C}_p(x)e^{i\omega t}\;. \tag{4-195}$$

The pressure difference coefficient $\Delta C_p(x,t)$ is given by,

$$\Delta C_p(x,t)=-2C_p(x,t), \tag{4-196}$$

Reduced lift and pitching moment coefficients for parabolic flexural oscillations

By inserting the values of the coefficients b_k into the general equations of the reduced lift and moment coefficients, equations (4-89) and (4-91) respectively, one obtains after mathematical simplifications,

$$\hat{C}_L=\frac{3}{8}\varepsilon_0\,\lambda^2\,\pi\left[-\frac{5}{12}+\frac{4}{3}\frac{i}{\lambda}+\frac{10}{3}\frac{i}{\lambda}C(\lambda/2)+\frac{8}{\lambda^2}C(\lambda/2)\right], \tag{4-197}$$

$$\hat{C}_m=-\frac{3}{8}\varepsilon_0\,\lambda^2\,\pi\left[\frac{1}{4}-\frac{7}{6}\frac{i}{\lambda}-\frac{2}{3}\frac{1}{\lambda^2}-\frac{5}{6}\frac{i}{\lambda}C(\lambda/2)-\frac{2}{\lambda^2}C(\lambda/2)\right]. \tag{4-198}$$

where $C(\lambda/2)$ is Theodorsen's function and λ is the reduced frequency.

4.6 Unsteady flow past an airfoil with an oscillating aileron

Consider an airfoil having an aileron that is executing oscillatory rotation $\beta(t)$, as shown in Figure 4.11.

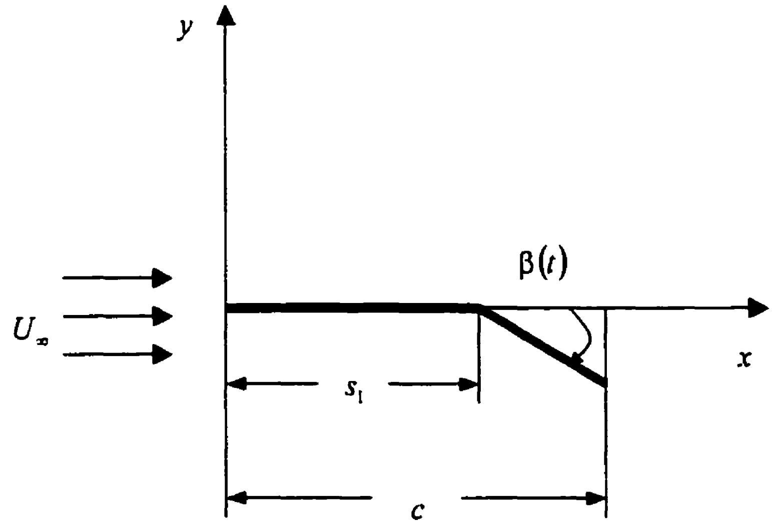

Fig 4.11 Geometry of an airfoil and aileron executing oscillatory rotation $\beta(t)$.

The aileron oscillatory rotation $\beta(t)$ is given by,

$$\beta(t)=\hat{\beta}e^{i\omega t}, \tag{4-199}$$

The boundary condition is represented in terms of the reduced vertical velocity $\hat{V}(x)$, which in the case of aileron oscillations is given by,

$$\hat{V}(x)=-i\omega\hat{\beta}(x-s_1)-U_\infty\hat{\beta}. \tag{4-200}$$

The boundary condition on the airfoil with an oscillating aileron is given by,

$$\hat{V}(x)=\begin{cases}0 & \text{for } x\in(0,s_1)\\ \sum_{k=1}^{n}\beta_k x^k & \text{for } x\in(s_1,c)\end{cases}, \tag{4-201}$$

From the above conditions one obtains the values of the boundary constants,

$$\beta_0=-U_\infty\hat{\beta}+i\omega\hat{\beta}s_1 \quad , \quad \beta_1=-i\omega\hat{\beta} \quad \text{and} \quad \beta_k=0 \;\; \text{for } k\geq 2 \quad . \tag{4-202}$$

In this case, the value of $\hat{V}(s_1)$ is,

$$\hat{V}(s_1)=-\hat{\beta}U_\infty, \tag{4-203}$$

The resultant expression of the pressure difference coefficient for an airfoil with an aileron executing pitching oscillations is given by,

$$
\begin{aligned}
-\frac{U_\infty}{2}\hat{C}_p(x) = {} & \left(\frac{i\lambda}{c}\right)\left[-\frac{2}{\pi}\hat{V}(s_1)\cos^{-1}\sqrt{\frac{s_1}{c}}-\frac{2}{\pi}\zeta_1\right]\sqrt{(c-x)x}+ \\
& +\left(-\frac{1}{c}\right)\sqrt{\frac{c-x}{x}}(1-C(\lambda/2))\left\{-\frac{2}{\pi}\hat{V}(s_1)\zeta_6-\frac{2}{\pi}\zeta_2-\frac{2}{\pi}c\zeta_1\right\}- \\
& -\frac{2}{\pi}\left(\frac{i\lambda}{c}\right)\hat{V}(s_1)\zeta_7(x)-\frac{2}{\pi}\zeta_3(x)\left(1+\frac{i\lambda}{c}x\right)+\frac{2}{\pi}\left(\frac{i\lambda}{c}\right)\zeta_4(x)- \\
& -\frac{2}{\pi}\hat{V}(s_1)\zeta_5(x)-\frac{2}{\pi}\sqrt{\frac{c-x}{x}}\zeta_1
\end{aligned}
\qquad (4\text{-}204)
$$

where,

$$\zeta_1 = \beta_1\left(\frac{1}{2}I_1 - s_1\cos^{-1}\sqrt{\frac{s_1}{c}}\right), \qquad (4\text{-}205)$$

$$\zeta_2 = \frac{1}{2}\beta_1\left(\frac{c}{2}I_1 - s_1\sqrt{(c-s_1)s_1}\right), \qquad (4\text{-}206)$$

$$\zeta_3(x) = \beta_1\left[(x-s_1)H(x)+\frac{1}{2}\sqrt{(c-x)x}\,I_0\right], \qquad (4\text{-}207)$$

$$\zeta_4(x) = \frac{1}{2}\beta_1\left[(x^2-s_1^2)H(x)+\frac{1}{2}\sqrt{(c-x)x}(xI_0+I_1)\right], \qquad (4\text{-}208)$$

$$\zeta_5(x) = \sqrt{\frac{c-x}{x}}\cos^{-1}\sqrt{\frac{s_1}{c}}+H(x), \qquad (4\text{-}209)$$

$$\zeta_6 = \sqrt{(c-s_1)s_1}+c\cos^{-1}\sqrt{\frac{s_1}{c}}. \qquad (4\text{-}210)$$

$$\zeta_7(x) = (x-s_1)H(x). \qquad (4\text{-}211)$$

where,

$$H(x) = \left\{\begin{array}{ll} \cosh^{-1}\sqrt{\dfrac{(c-x)s_1}{c(s_1-x)}} & 0<x<s_1 \\ \sinh^{-1}\sqrt{\dfrac{(c-x)s_1}{c(x-s_1)}} & s_1<x<c \end{array}\right\}. \qquad (4\text{-}212)$$

The resultant expression of the lift coefficient for an airfoil with an aileron executing pitching oscillations is given by,

$$
\begin{aligned}
-\frac{U_\infty c}{4}\hat{C}_L = &-\hat{V}(s_1)\sqrt{(c-s_1)s_1}\left\{C(\lambda/2)+\frac{1}{2}\left(\frac{i\lambda}{c}\right)\left(\frac{c}{2}-s_1\right)\right\}- \\
&-\left[C(\lambda/2)+\frac{i\lambda}{4}\right]\beta_1\left(\frac{c}{4}I_1-\frac{1}{2}s_1\sqrt{(c-s_1)s_1}\right)+ \\
&+\frac{1}{2}\left(\frac{i\lambda}{c}\right)\beta_1\left(\frac{3}{24}I_1+\frac{s_1}{3}\sqrt{(c-s_1)s_1}\left(\frac{c}{4}-s_1\right)\right)- \\
&-\left\{\left(\frac{i\lambda c}{4}\right)+cC(\lambda/2)\right\}\left[\hat{V}(s_1)\cos^{-1}\sqrt{\frac{s_1}{c}}+\beta_1\left(\frac{1}{2}I_1-s_1\cos^{-1}\sqrt{\frac{s_1}{c}}\right)\right]
\end{aligned}
$$

(4-213)

The resultant expression of the pitching moment coefficient for an airfoil with an aileron executing pitching oscillations is given by,

$$
\begin{aligned}
-\frac{U_\infty c^2}{4}\hat{C}_m = &-\hat{V}(s_1)\sqrt{(c-s_1)s_1}\left\{\ \frac{c}{4}C(\lambda/2)+\left(\frac{i\lambda}{c}\right)\left(\frac{3}{24}c^2-c\frac{s_1}{12}-\frac{s_1^2}{6}\right)+\frac{s_1}{2}\ \right\} \\
&-c^2\left\{\frac{3}{24}i\lambda+\frac{1}{4}C(\lambda/2)\right\}\left[\hat{V}(s_1)\cos^{-1}\sqrt{\frac{s_1}{c}}+\beta_1\left(\frac{1}{2}I_1-s_1\cos^{-1}\sqrt{\frac{s_1}{c}}\right)\right]- \\
&-\frac{c}{2}\beta_1\left[\frac{1}{4}C(\lambda/2)+i\frac{3}{24}\lambda\right]\left(\frac{c}{2}I_1-s_1\sqrt{(c-s_1)s_1}\right)- \\
&-\frac{\beta_1}{3}\left(\frac{1}{2}-i\frac{\lambda}{12}\right)\left(\frac{c}{2}I_2-s_1^2\sqrt{(c-s_1)s_1}\right)+\left(\frac{i\lambda}{24c}\right)\beta_1\left(\frac{c}{2}I_3-s_1^3\sqrt{(c-s_1)s_1}\right)
\end{aligned}
$$

(4-214)

where,

$$
I_0=2\cos^{-1}\sqrt{\frac{s_1}{c}}\quad,\quad I_1=\sqrt{(c-s_1)s_1}+c\cos^{-1}\sqrt{\frac{s_1}{c}},
$$

$$
I_2=\frac{s_1}{2}\sqrt{(c-s_1)s_1}+\frac{3}{4}cI_1\quad,\quad I_3=\frac{s_1^2}{3}\sqrt{(c-s_1)s_1}+\frac{5}{6}cI_2. \tag{4-215}
$$

4.7 Unsteady flow past an airfoil with an aileron executing flexural oscillations

Consider an airfoil having an aileron under parabolic flexural oscillations $y(x,t)$. The parabolic flexural oscillation $y(x,t)$ on the aileron is assumed in the form,

$$y(x,t) = \mathrm{Re}\left[\kappa_0 c\left(\frac{x-s_1}{c}\right)^2 e^{i\omega t}\right]. \tag{4-216}$$

where κ_0 is a constant.

From equation (4-2), one obtains,

$$\hat{e}(x) = \kappa_0\, c\left(\frac{x-s_1}{c}\right)^2, \tag{4-217}$$

From the above analysis and from equation (4-10), the equation of the reduced vertical velocity $\hat{V}(x)$ for an airfoil with an aileron executing flexural oscillations is given by,

$$\hat{V}(x) = 2U_\infty \kappa_0\left(\frac{x-s_1}{c}\right) + i\omega\kappa_0 c\left(\frac{x-s_1}{c}\right)^2, \tag{4-218}$$

where,

$$\hat{V}(x) = \begin{cases} 0 & \text{for } x \in (0, s_1) \\ \sum\limits_{k=1}^{n} \beta_k x^k & \text{for } x \in (s_1, c) \end{cases}. \tag{4-219}$$

By comparing the terms in the polynomial representation of the boundary conditions on the airfoil, one obtains,

$$\beta_0 = (\ -2U_\infty \kappa_0 s_1 + i\omega\kappa_0 s_1^2\ )/c\ ,\quad \beta_1 = (\ 2U_\infty \kappa_0 - i2\omega\kappa_0 s_1\ )/c\ ,\quad \beta_2 = i\omega\kappa_0/c$$

and $\beta_k = 0$ for $k \geq 3$.

(4-220)

In this case, the value of $\hat{V}(s_1)$ is,

$$\hat{V}(s_1) = 0, \tag{4-221}$$

The resultant expression of the pressure difference coefficient for an airfoil with an aileron executing parabolic flexural oscillations is given by,

$$
\begin{aligned}
-\frac{U_\infty}{2}\hat{C}_p(x) = & \left(\frac{i\lambda}{c}\right)\left[-\frac{2}{\pi}\zeta_1\right]\sqrt{(c-x)x} + \left(\frac{2}{\pi c}\right)\sqrt{\frac{c-x}{x}}(1-C(\lambda/2))\{\zeta_2 + c\zeta_1\} - \\
& -\frac{2}{\pi}\zeta_3(x)\left(1+\frac{i\lambda}{c}x\right) + \frac{2}{\pi}\left(\frac{i\lambda}{c}\right)\zeta_4(x) - \frac{2}{\pi}\sqrt{\frac{c-x}{x}}\zeta_1
\end{aligned}
$$

(4-222)

where,

$$\zeta_1 = \beta_1\left(\frac{1}{2}I_1 - s_1\cos^{-1}\sqrt{\frac{s_1}{c}}\right) + \beta_2\left(\frac{1}{2}I_2 - s_1^2\cos^{-1}\sqrt{\frac{s_1}{c}}\right), \tag{4-223}$$

$$\zeta_2 = \frac{1}{2}\beta_1\left(\frac{c}{2}I_1 - s_1\sqrt{(c-s_1)s_1}\right) + \frac{2}{3}\beta_2\left(\frac{c}{2}I_2 - s_1^2\sqrt{(c-s_1)s_1}\right), \tag{4-224}$$

$$\zeta_3(x) = \beta_1\left[(x-s_1)H(x) + \frac{1}{2}\sqrt{(c-x)x}\,I_0\right] + \beta_2\left[(x^2-s_1^2)H(x) + \frac{1}{2}\sqrt{(c-x)x}(xI_0 + I_1)\right]$$

(4-225)

$$
\begin{aligned}
\zeta_4(x) = & \frac{1}{2}\beta_1\left[(x^2-s_1^2)H(x) + \frac{1}{2}\sqrt{(c-x)x}(xI_0 + I_1)\right] + \\
& + \frac{2}{3}\beta_2\left[(x^3-s_1^3)H(x) + \frac{1}{2}\sqrt{(c-x)x}(x^2I_0 + xI_1 + I_2)\right],
\end{aligned} \tag{4-226}
$$

where,

$$H(x) = \left\{\begin{array}{ll} \cosh^{-1}\sqrt{\dfrac{(c-x)s_1}{c(s_1-x)}} & 0 < x < s_1 \\ \sinh^{-1}\sqrt{\dfrac{(c-x)s_1}{c(x-s_1)}} & s_1 < x < c \end{array}\right\}. \tag{4-227}$$

$$I_0 = 2\cos^{-1}\sqrt{\frac{s_1}{c}}\ , \quad I_1 = \sqrt{(c-s_1)s_1} + c\cos^{-1}\sqrt{\frac{s_1}{c}},$$

$$I_2 = \frac{s_1}{2}\sqrt{(c-s_1)s_1} + \frac{3}{4}cI_1\ , \quad I_3 = \frac{s_1^2}{3}\sqrt{(c-s_1)s_1} + \frac{5}{6}cI_2. \tag{4-228}$$

The resultant expression of the lift coefficient for an airfoil with an aileron executing parabolic flexural oscillations is given by,

$$-\frac{U_\infty c}{4}\hat{C}_L = -\left[C(\lambda/2)+\frac{i\lambda}{4}\right]Z_1 + \frac{1}{2}\left(\frac{i\lambda}{c}\right)Z_2 - \left[\frac{i\lambda c}{4}+cC(\lambda/2)\right]Z_3, \tag{4-229}$$

where,

$$Z_1 = \beta_1\left(\frac{c}{4}I_1 - \frac{1}{2}s_1\sqrt{(c-s_1)s_1}\right) + \beta_2\left(\frac{c}{3}I_2 - \frac{2}{3}s_1^2\sqrt{(c-s_1)s_1}\right), \tag{4-230}$$

$$Z_2 = \beta_1\left(\frac{3c^2}{24}I_1 + \frac{s_1}{3}\left(\frac{c}{4}-s_1\right)\sqrt{(c-s_1)s_1}\right) + 2\beta_2\left(\frac{5c^2}{48}I_2 + \frac{s_1^2}{4}\left(\frac{c}{6}-s_1\right)\sqrt{(c-s_1)s_1}\right), \tag{4-231}$$

$$Z_3 = \beta_1\left(\frac{1}{2}I_1 - s_1\cos^{-1}\sqrt{\frac{s_1}{c}}\right) + \beta_2\left(\frac{1}{2}I_2 - s_1^2\cos^{-1}\sqrt{\frac{s_1}{c}}\right), \tag{4-232}$$

The resultant expression of the pitching moment coefficient for an airfoil with an aileron executing parabolic flexural oscillations is given by,

$$-\frac{U_\infty c^2}{4}\hat{C}_m = -\left[i\frac{3}{24}\lambda + \frac{1}{4}C(\lambda/2)\right]\left(c^2Y_1 + cY_2\right) - \left(\frac{1}{2} - \frac{i\lambda}{12}\right)Y_3 + \left(\frac{i\lambda}{6c}\right)Y_4, \tag{4-233}$$

where,

$$Y_1 = Z_3, \tag{4-234}$$

$$Y_2 = Z_1, \tag{4-235}$$

$$Y_3 = \frac{1}{3}\beta_1\left(\frac{c}{2}I_2 - s_1^2\sqrt{(c-s_1)s_1}\right) + \frac{1}{2}\beta_2\left(\frac{c}{2}I_3 - s_1^3\sqrt{(c-s_1)s_1}\right), \tag{4-236}$$

$$Y_4 = \frac{1}{4}\beta_1\left(\frac{c}{2}I_3 - s_1^3\sqrt{(c-s_1)s_1}\right) + \frac{2}{5}\beta_2\left(\frac{c}{2}I_4 - s_1^4\sqrt{(c-s_1)s_1}\right), \tag{4-237}$$

where,

$$I_1 = \sqrt{(c-s_1)s_1} + c\cos^{-1}\sqrt{\frac{s_1}{c}}, \qquad I_2 = \frac{s_1}{2}\sqrt{(c-s_1)s_1} + \frac{3}{4}cI_1, \tag{4-238}$$

$$I_3 = \frac{s_1^2}{3}\sqrt{(c-s_1)s_1} + \frac{5}{6}cI_2, \qquad I_4 = \frac{s_1^3}{4}\sqrt{(c-s_1)s_1} + \frac{7}{8}cI_3. \tag{4-239}$$

Chapter 5

Results and discussion

The present method has been validated by comparison with the results obtained by Theodorsen [15,26] and Postel and Leppert [24] for the case of an airfoil executing oscillatory translation and rotation and for the case of an airfoil with an aileron executing oscillatory rotations.

After validation, the present method has been used to obtain solutions for airfoils executing flexural oscillations and for airfoils with ailerons executing flexural oscillations.

No comparisons were presented for the case of flexural oscillations since there are no previous results known.

For the sake of comparison, the following coefficients have been introduced:

$$\Delta K_p^* = \frac{1}{\lambda^2}\Delta\hat{C}_p = \frac{\Delta\hat{p}}{\frac{1}{2}\rho\omega^2c^2}\,. \tag{5-1}$$

which is the reduced oscillatory pressure difference coefficient, and

$$K_L^* = \frac{1}{\lambda^2}\hat{C}_L = \frac{\hat{L}}{\frac{1}{2}\rho\omega^2c^3}\,. \tag{5-2}$$

$$K_L = \mathrm{REAL}\left(K_L^* e^{i\omega t}\right). \tag{5-3}$$

which are the reduced oscillatory lift coefficient and the oscillatory lift coefficient, respectively, and

$$K_m^* = \frac{1}{\lambda^2}\hat{C}_m = \frac{\hat{M}}{\frac{1}{2}\rho\omega^2c^4}\,. \tag{5-4}$$

$$K_m = \mathrm{REAL}\left(\mathrm{K}_\mathrm{m}^* e^{i\omega t}\right). \tag{5-5}$$

which are the reduced oscillatory pitching moment coefficient and the oscillatory pitching moment coefficient, respectively.

5.1 Case of airfoils executing oscillatory translations

The numerical results were obtained for various values of the reduced frequency λ ,such as $\lambda = 0.48, 0.60, 0.68$. The results are presented in Figure 5.1 and in Figures 5.2, 5.3, for the real and imaginary parts of the reduced oscillatory pressure difference coefficient $(-c/(2h_0))\Delta K_p^*$, where $h_0 = \hat{h}$, represents the complex amplitude of oscillations, and for the real and imaginary parts of the reduced oscillatory lift and pitching moment coefficients, $(2c/(\pi h_0))K_L^*$ and $(4c/(\pi h_0))K_m^*$, respectively. The corresponding typical variations in time of the oscillatory lift and pitching moment coefficients have been calculated for several values of λ , such as $\lambda = 0.48, 0.68$, as shown in Figure 5.4.

The results of the real and imaginary parts of the pressure difference coefficient are in very good agreement with the previous results obtained by Postel & Leppert [24]. The results of the lift and pitching moment coefficients obtained by the present method are in excellent agreement with Theodorsen's solution [15,26].

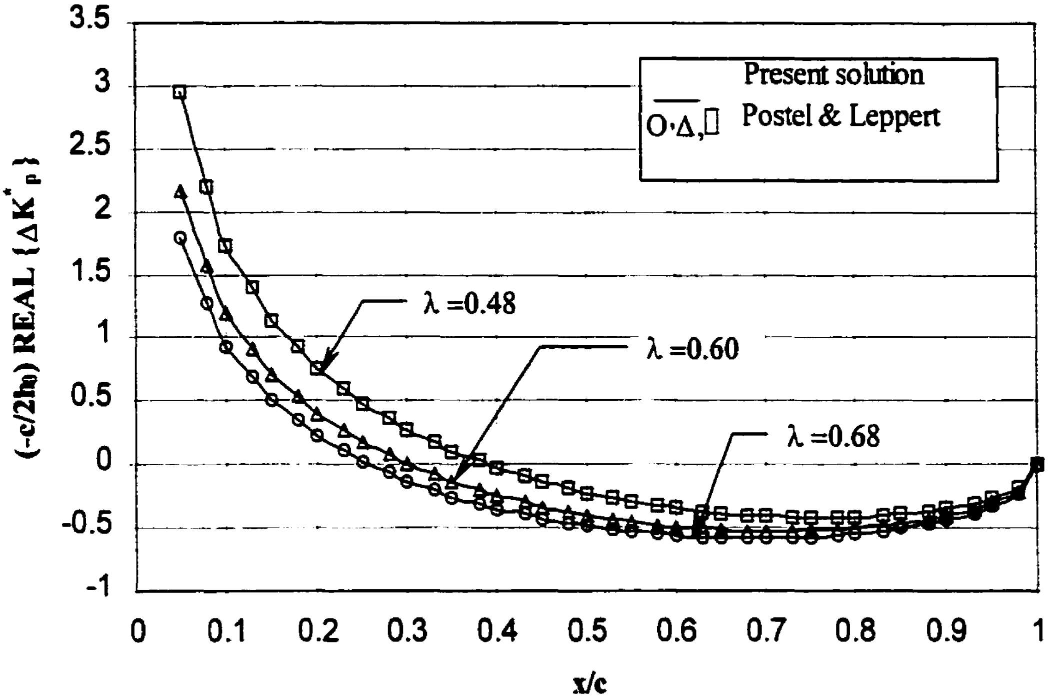

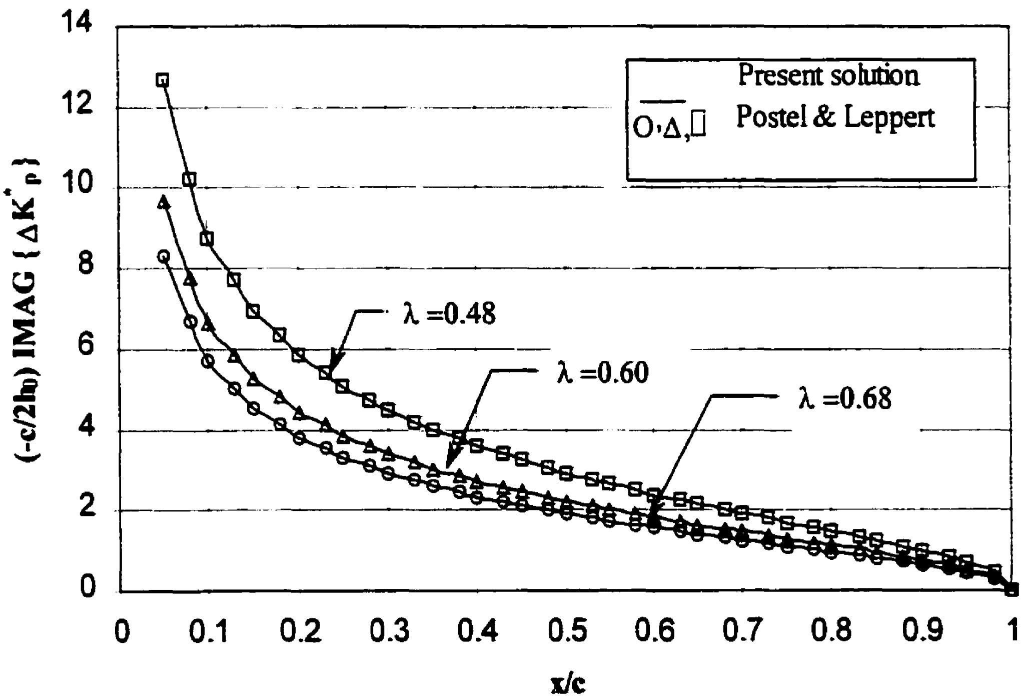

Fig 5.1 Real and imaginary parts of the pressure difference for an airfoil *executing oscillatory translation.*

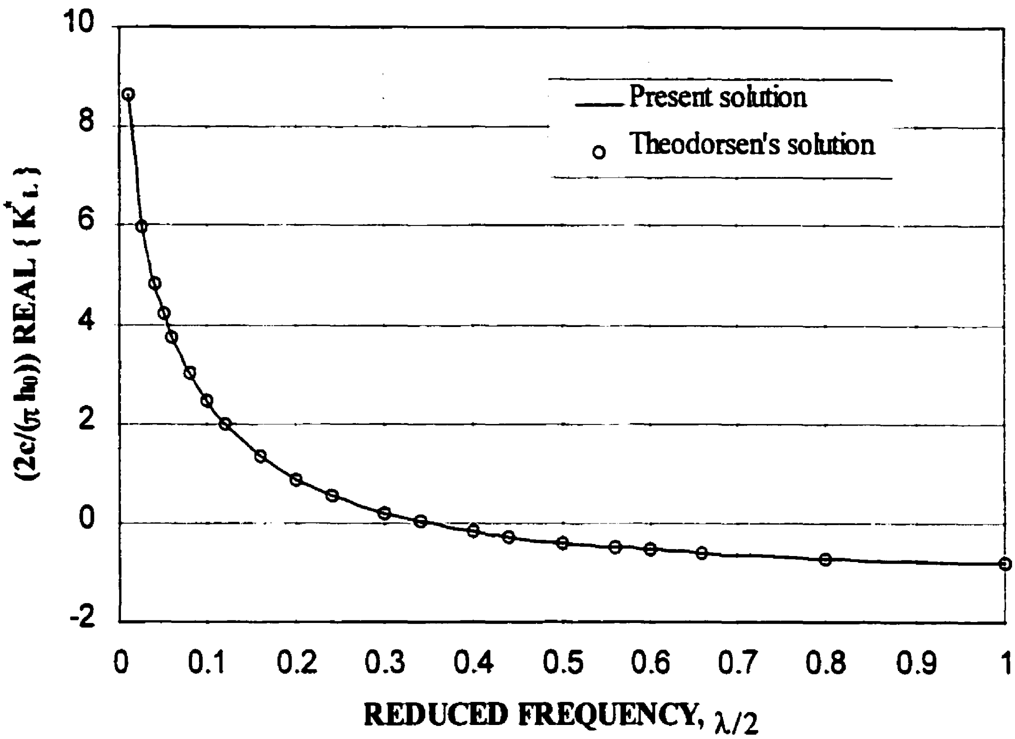

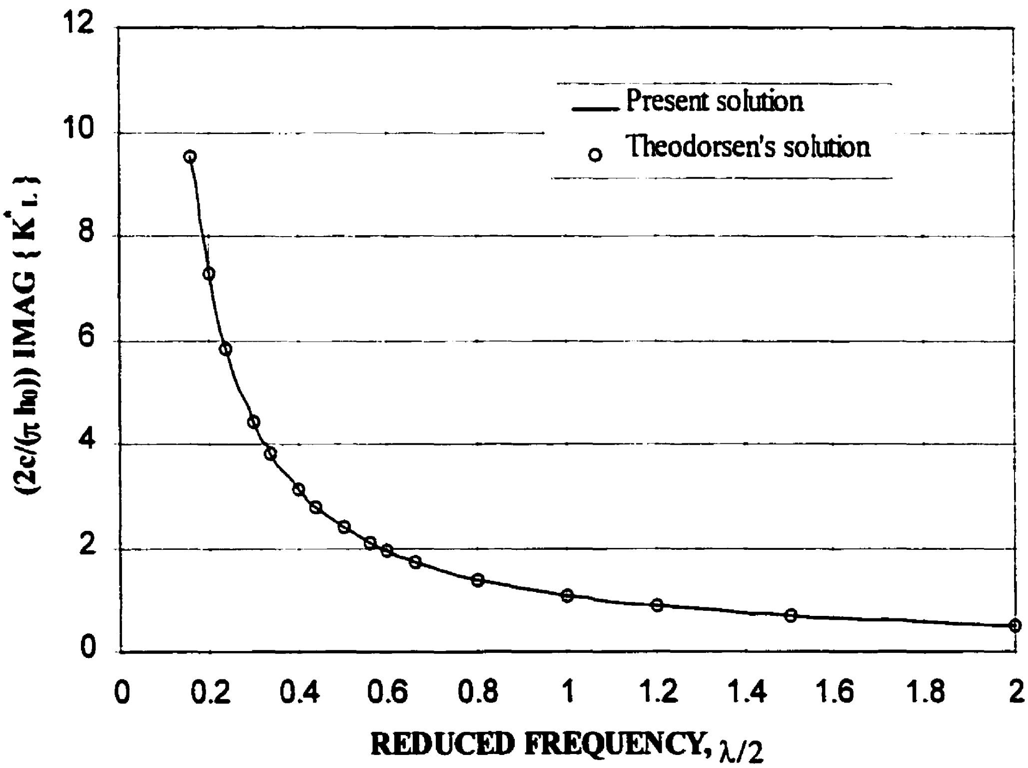

Fig 5.2 Real and imaginary parts of the lift coefficient for an airfoil *executing oscillatory translation.*

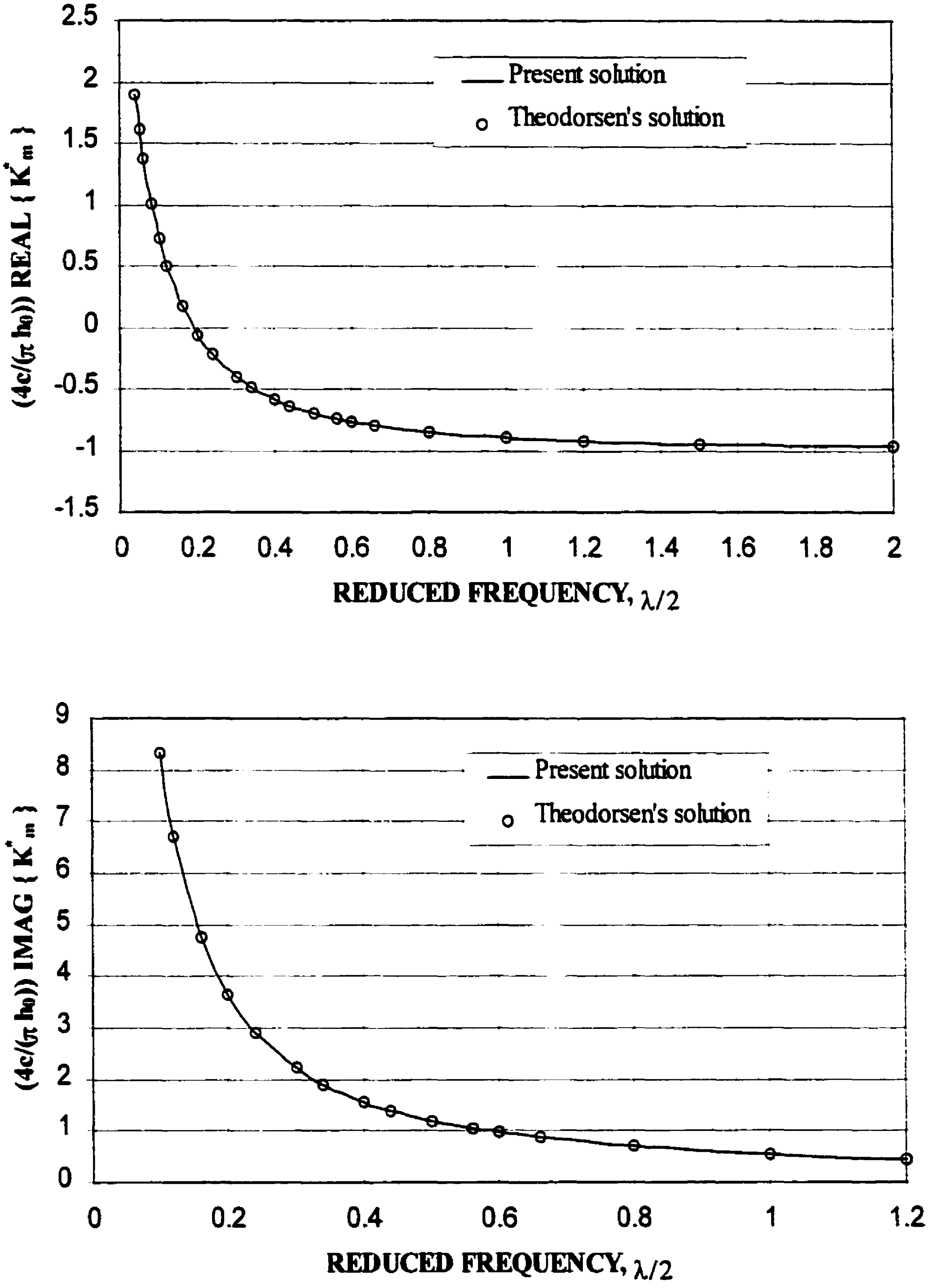

Fig 5.3 Real and imaginary parts of the pitching moment coefficient for an airfoil *executing oscillatory translation.*

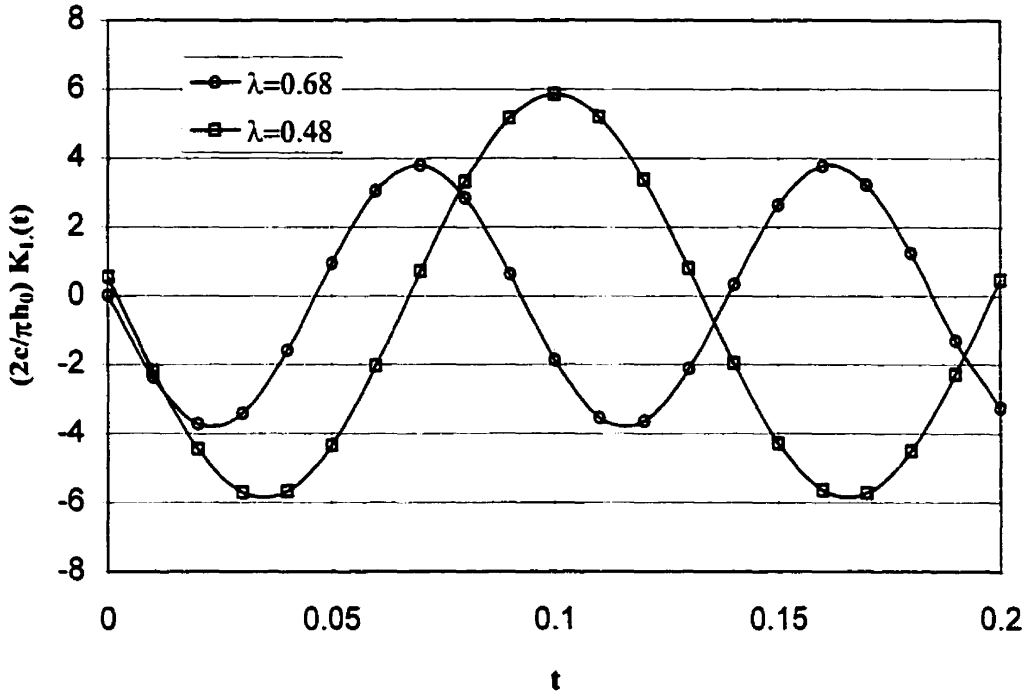

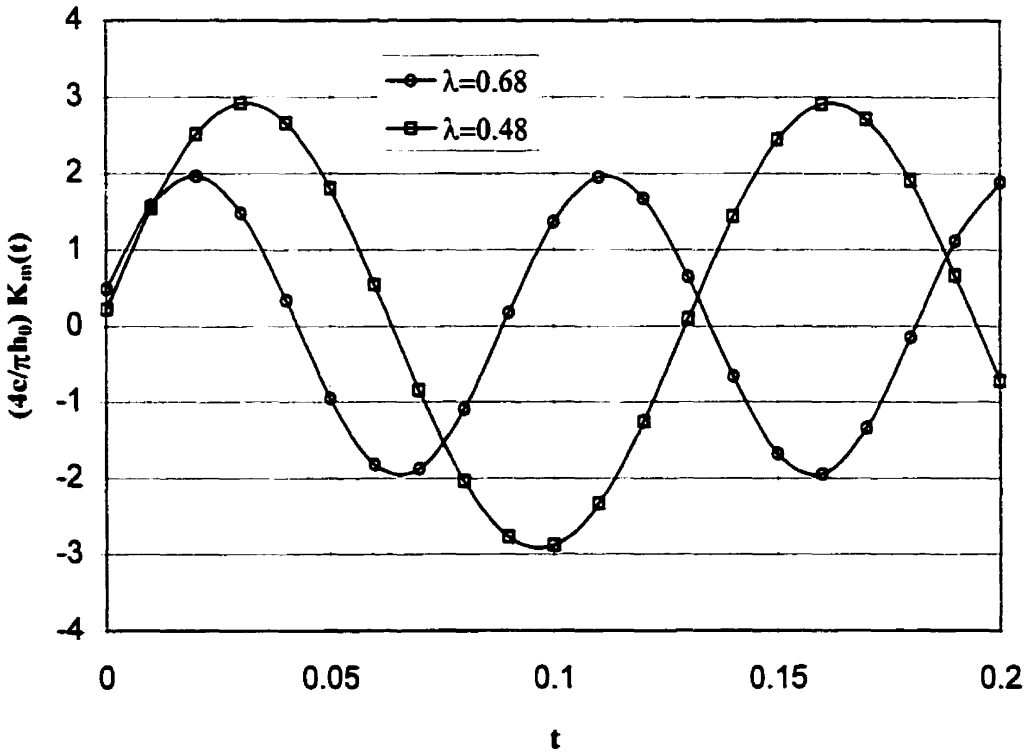

Fig 5.4 Typical variations in time of the lift and pitching moment coefficients for an airfoil *executing oscillatory translation.*

5.2 Case of airfoils executing oscillatory rotations

The numerical results were obtained for various values of the reduced frequency λ ,such as $\lambda = 0.48, 0.60, 0.68$. The results are presented in Figure 5.5 and in Figures 5.6, 5.7 for the real and imaginary parts of the reduced oscillatory pressure difference coefficient $(1/\theta_0)\Delta K_p^*$, where $\theta_0 = \hat{\theta}$ represents the complex amplitude of oscillations, and for the real and imaginary parts of the reduced oscillatory lift and pitching moment coefficients, $(-4/(\pi\theta_0))K_L^*$ and $(-8/(\pi\theta_0))K_m^*$, respectively. The corresponding typical variations in time of the oscillatory lift and pitching moment coefficients have been calculated for various values of λ , such as $\lambda = 0.48, 0.68$, as shown in Figure 5.8.

The results of the real and imaginary parts of the pressure difference coefficient are in very good agreement with the previous results obtained by Postel & Leppert [24]. The results of the lift and pitching moment coefficients obtained by the present method are in excellent agreement with Theodorsen's solution [15,26].

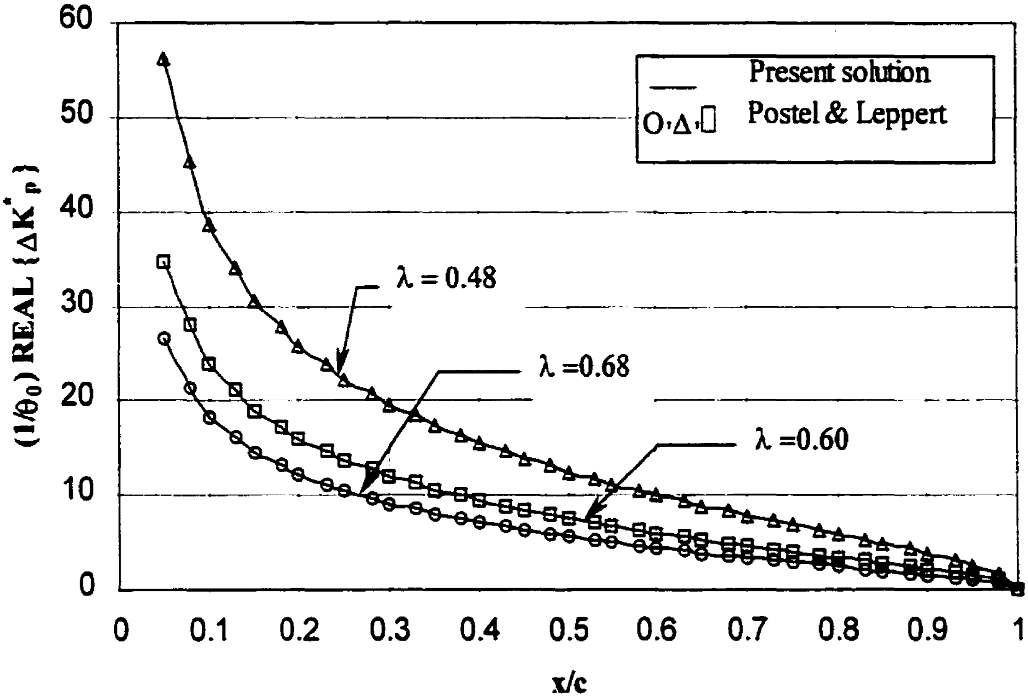

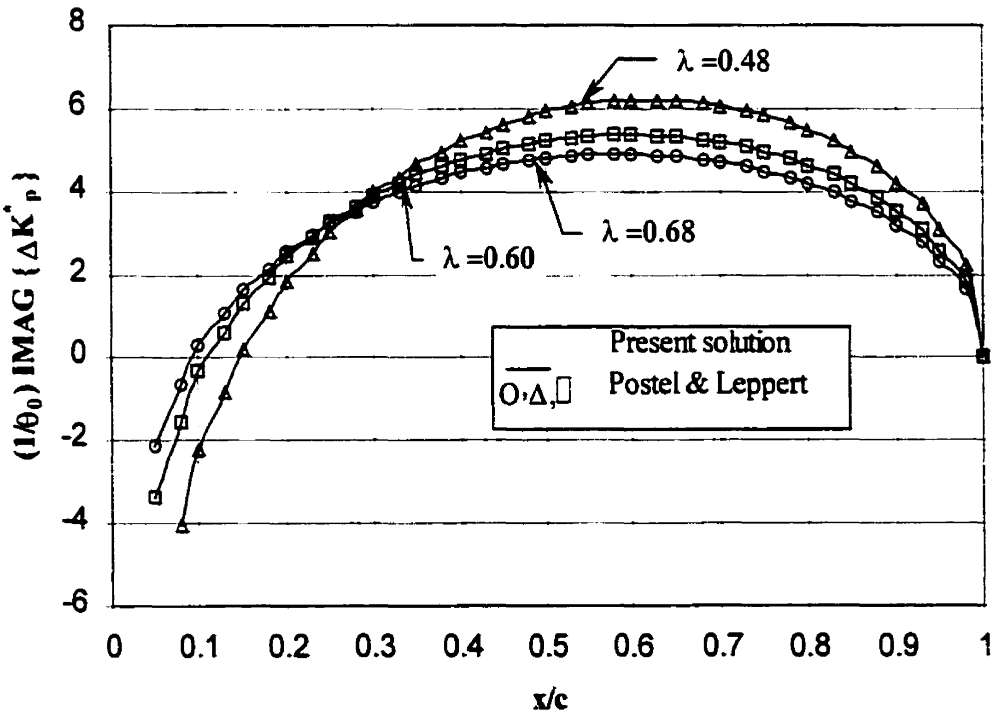

Fig 5.5 Real and imaginary parts of the pressure difference for an airfoil *executing oscillatory rotation.*

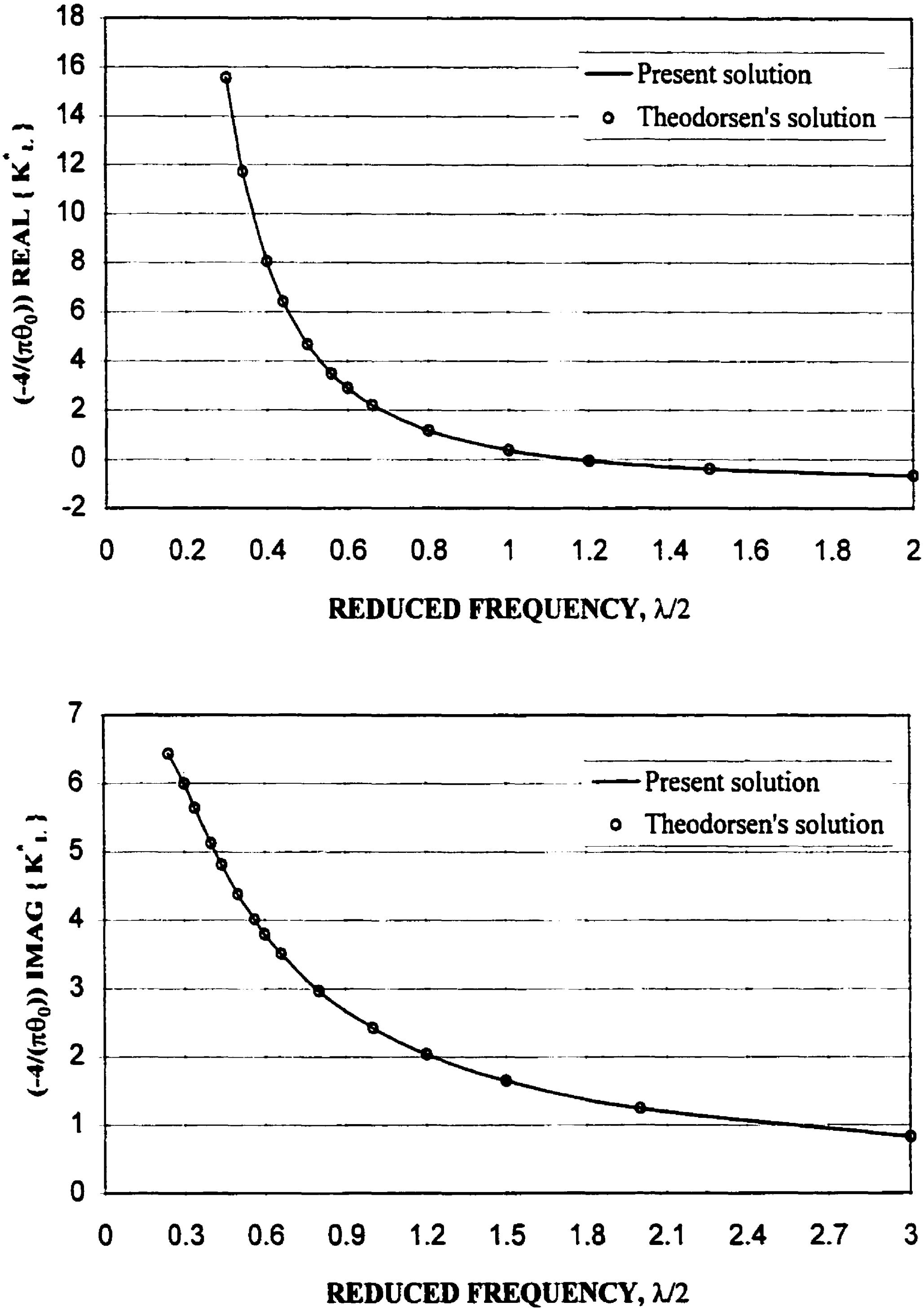

Fig 5.6 Real and imaginary parts of the lift coefficient for an airfoil *executing oscillatory rotation.*

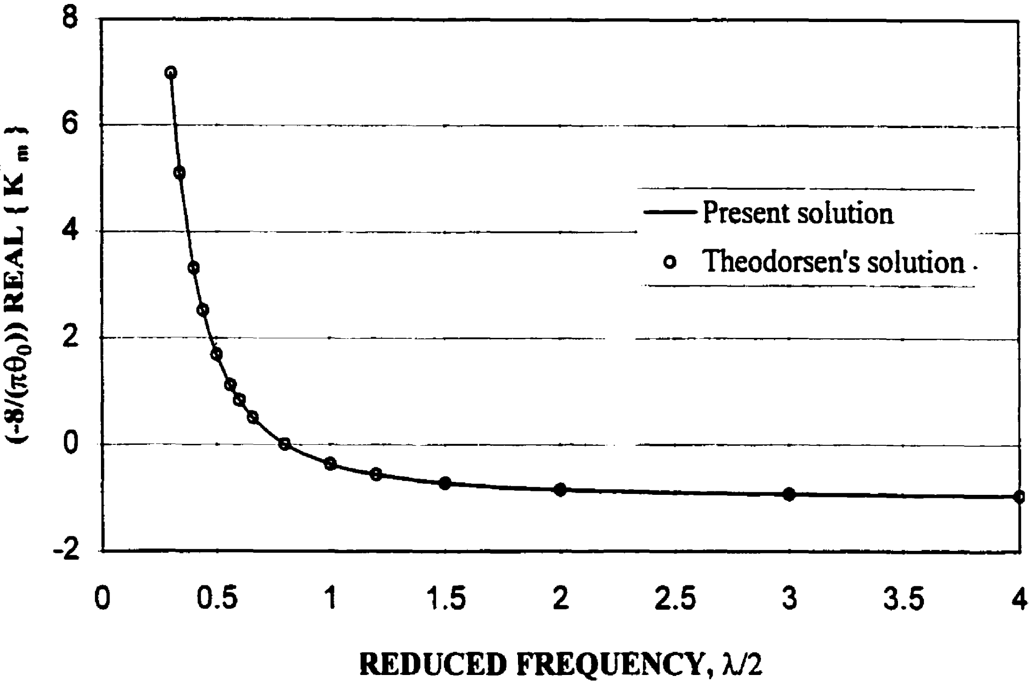

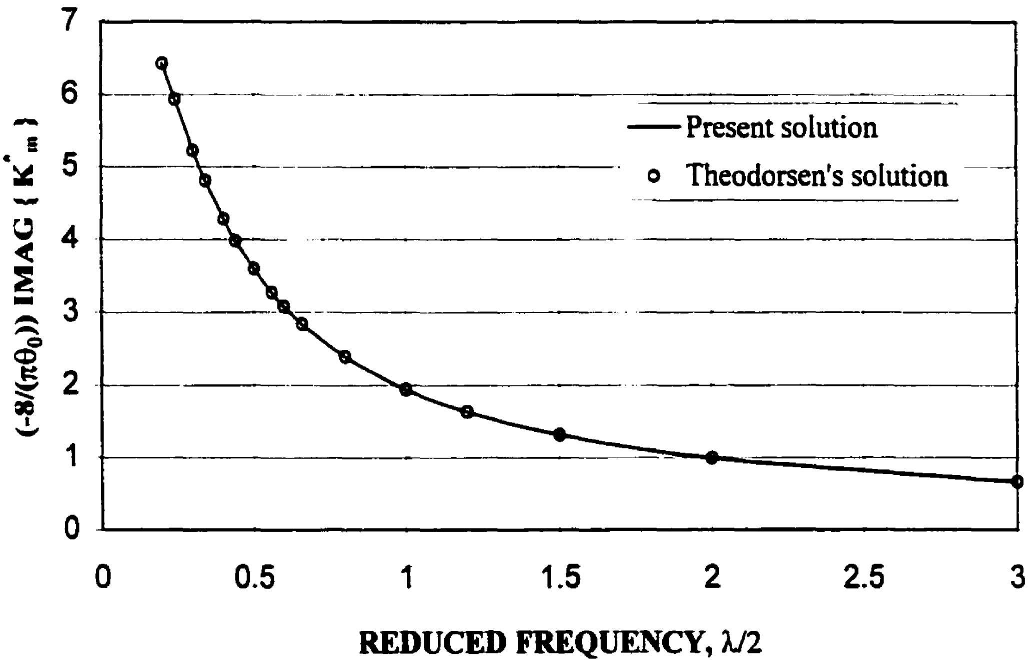

Fig 5.7 Real and imaginary parts of the pitching moment coefficient for an airfoil *executing oscillatory rotation.*

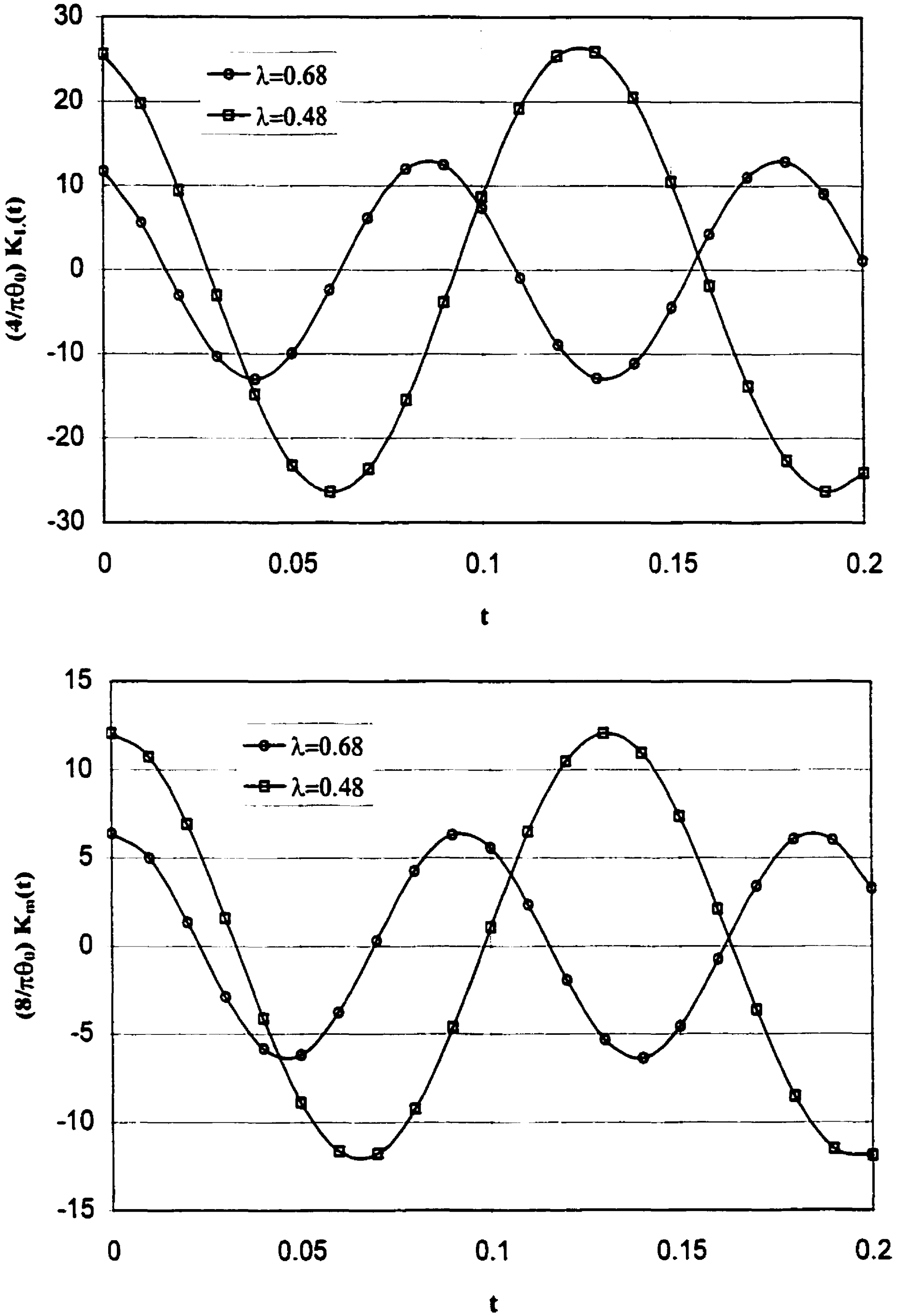

Fig 5.8 Typical variations in time of the lift and pitching moment coefficients for an airfoil *executing oscillatory rotation.*

5.3 Case of airfoils executing flexural oscillations

The numerical results were obtained for various values of the reduced frequency λ ,such as $\lambda = 0.48, 0.60, 0.68$. The results are presented in Figure 5.9 and in Figures 5.10, 5.11 for the real and imaginary parts of the reduced oscillatory pressure difference coefficient $\left(-c^2/4\varepsilon_0\right)\Delta K_p^{\bullet}$, and for the real and imaginary parts of the reduced oscillatory lift and pitching moment coefficients, $\left(8/(3\pi\varepsilon_0)\right)K_L^{\bullet}$ and $\left(8/(3\pi\varepsilon_0)\right)K_m^{\bullet}$, respectively. The corresponding typical variations in time of the oscillatory lift and pitching moment coefficients have been calculated for various values of λ , such as $\lambda = 0.48, 0.68$ as shown in Figure 5.12. No comparisons were presented for the case of flexural oscillations since there are no previous results known.

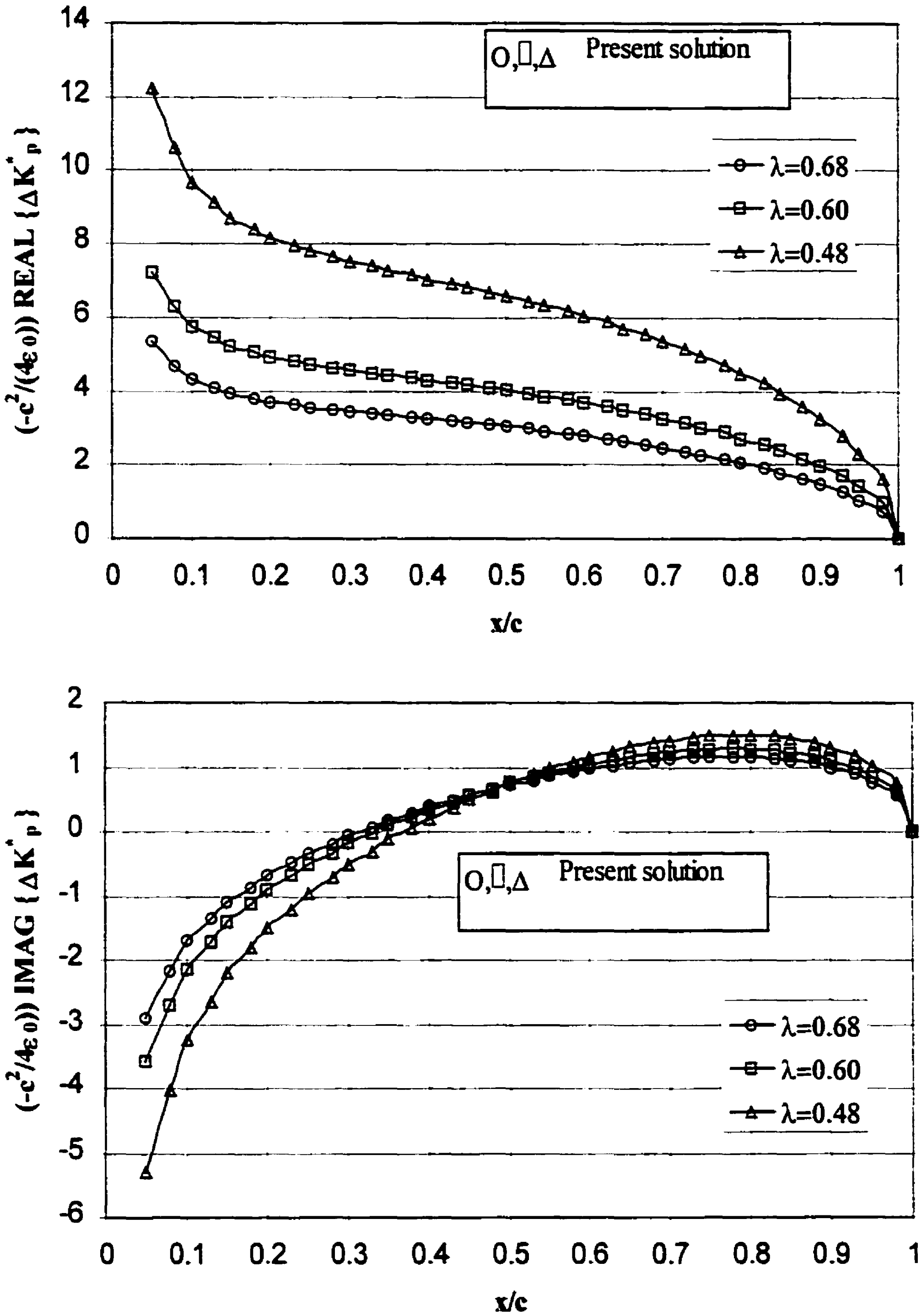

Fig 5.9 Real and imaginary parts of the pressure difference for an airfoil *executing parabolic flexural oscillations.*

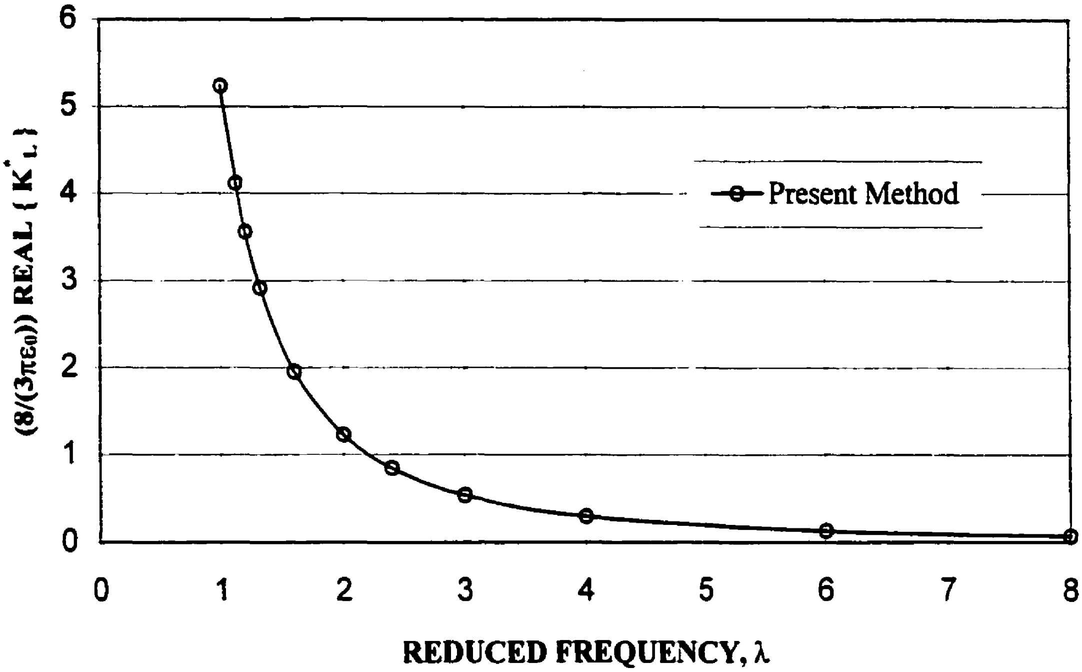

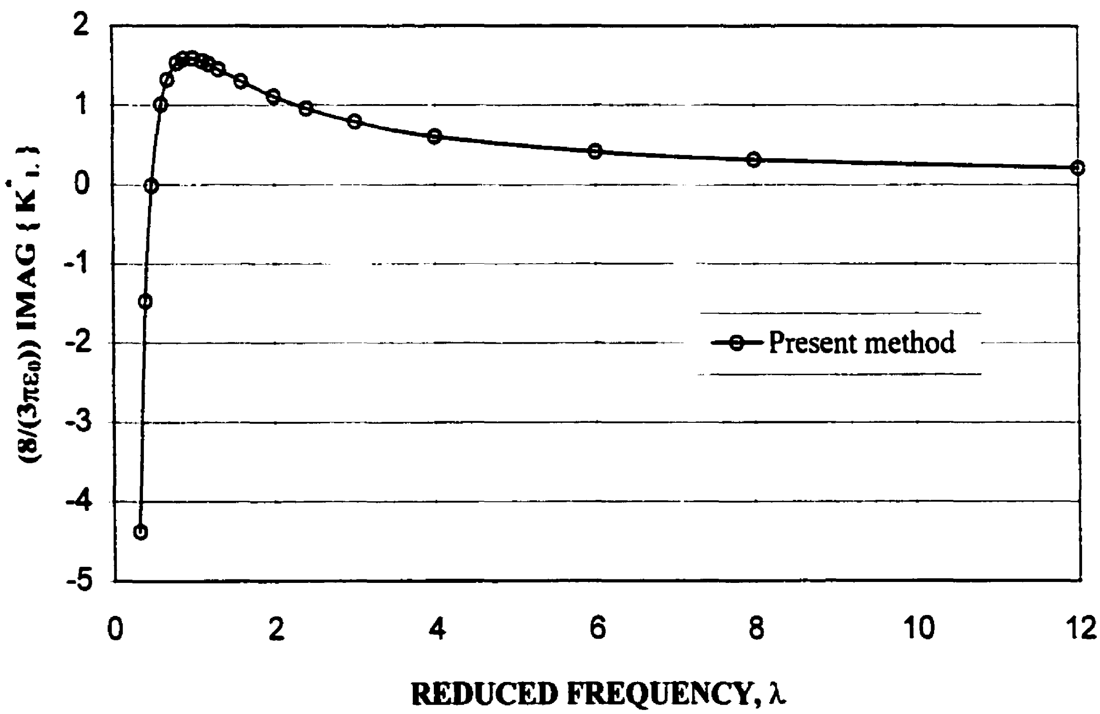

Fig 5.10 Real and imaginary parts of the lift coefficient for an airfoil *executing parabolic flexural oscillations.*

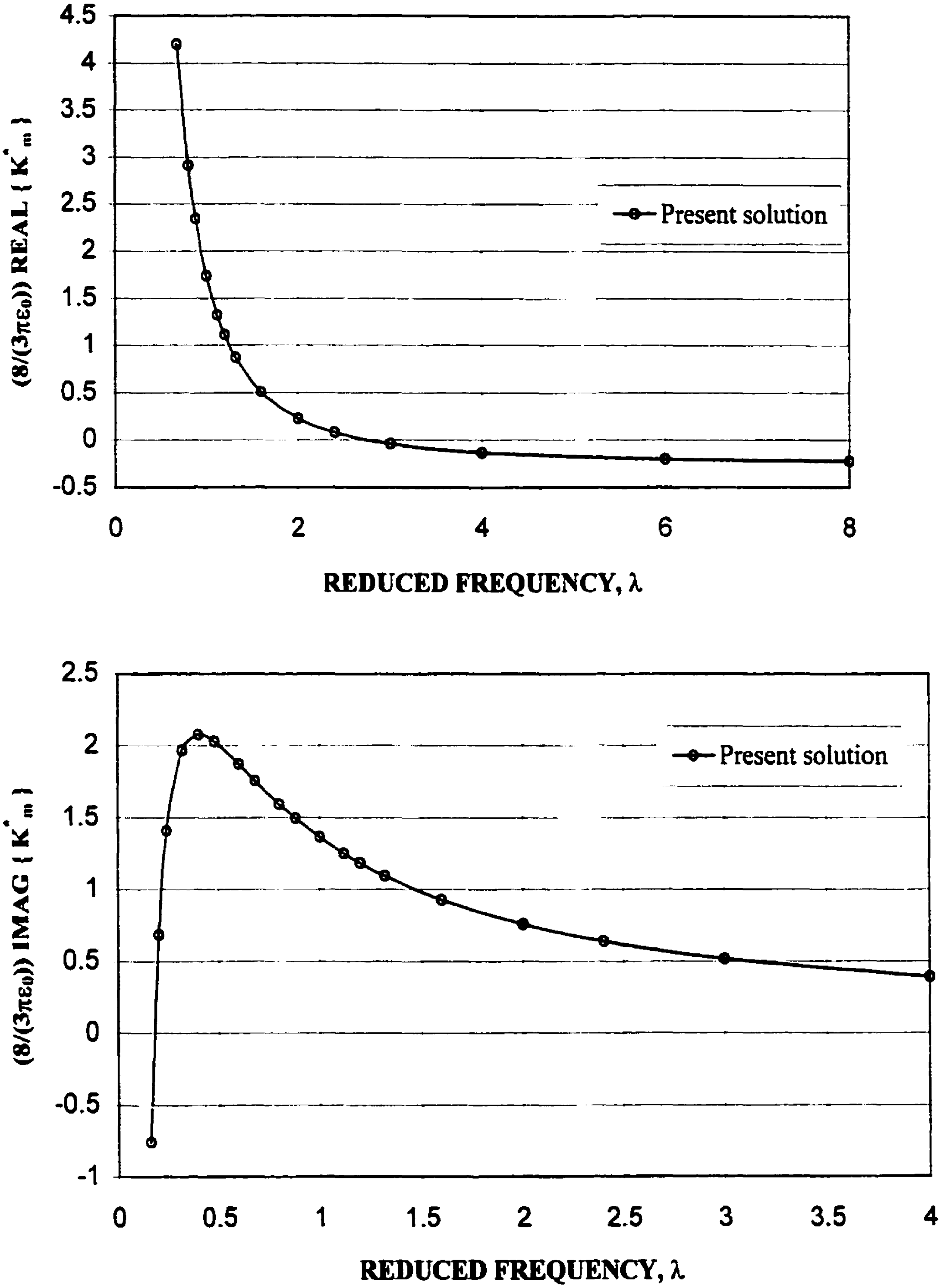

Fig 5.11 Real and imaginary parts of the pitching moment coefficient for an airfoil *executing parabolic flexural oscillations.*

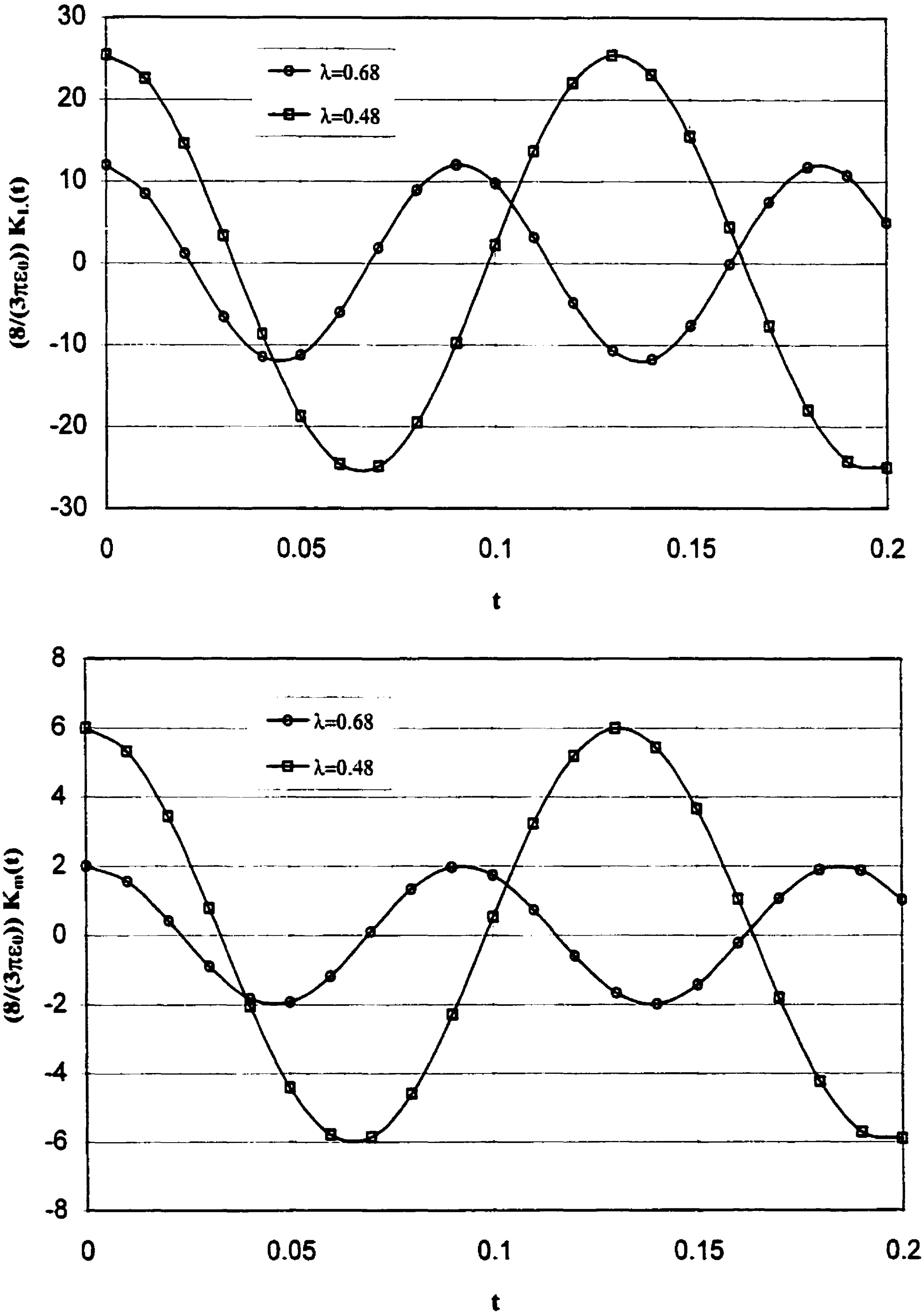

Fig 5.12 Typical variations in time of the lift and pitching moment coefficients for an airfoil *executing parabolic flexural oscillations.*

5.4 Case of an airfoil with an aileron executing pitching oscillations

The numerical results were obtained for various values of the reduced frequency λ ,such as $\lambda = 0.48, 0.60, 0.68$. The results are presented in Figure 5.13 and in Figures 5.14, 5.15 for the real and imaginary parts of the reduced oscillatory pressure difference coefficient $(1/\beta_0)\Delta K_p^{*}$, where $\beta_0 = \hat{\beta}$ represents the complex amplitude of oscillations, and for the real and imaginary parts of the reduced oscillatory lift and pitching moment coefficients, $(-4/\beta_0)K_L^{*}$ and $(-8/\beta_0)K_m^{*}$, respectively.

The results of the real and imaginary parts of the pressure difference coefficient for an airfoil with an aileron $(s_1/c = 0.75)$, were found to be in very good agreement with the previous results obtained by Postel & Leppert [24]. The results of the lift and pitching moment coefficients obtained by the present method for an airfoil with an aileron located at $(s_1/c = 0.70)$ were in excellent agreement with Theodorsen's solution [15,26].

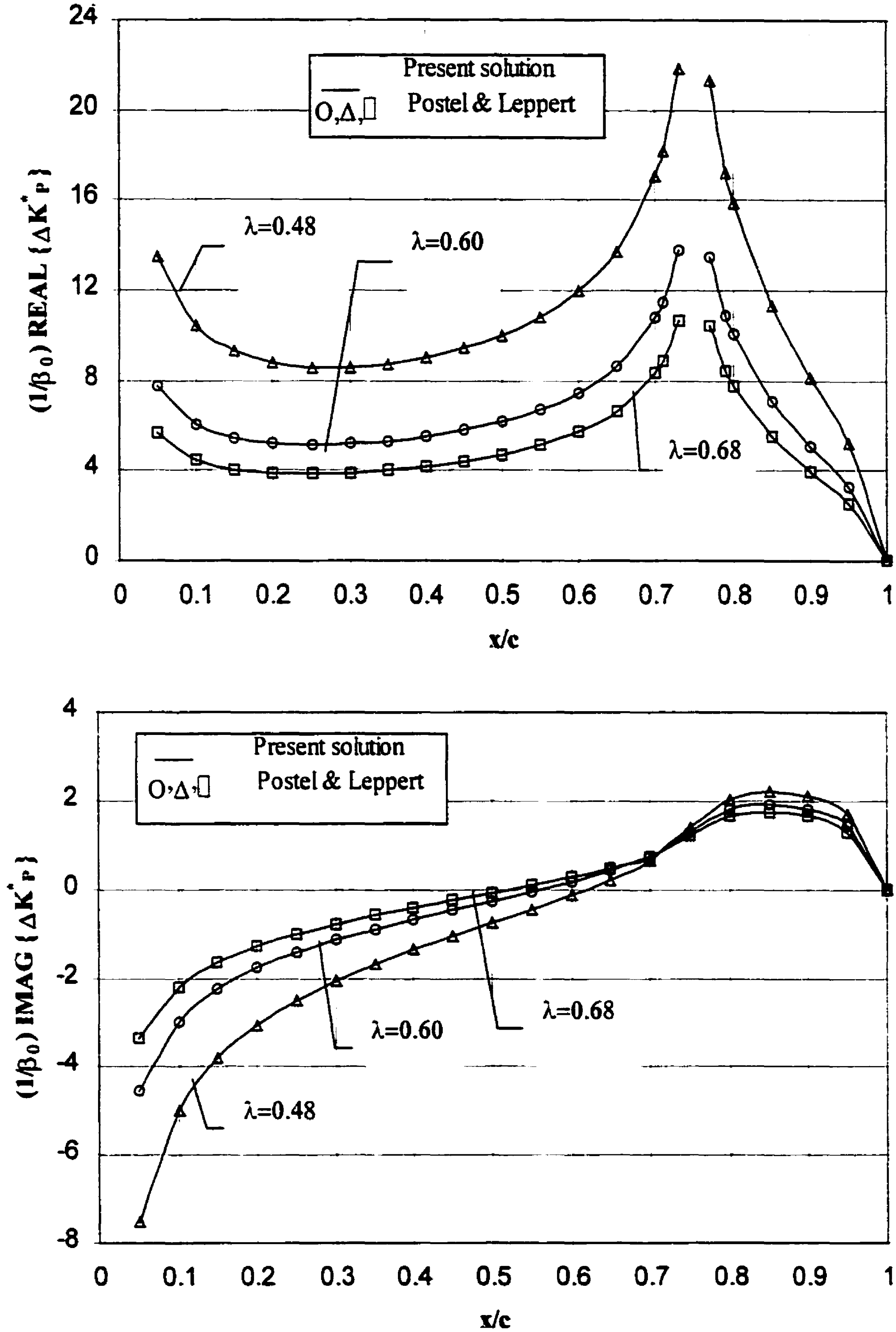

Fig 5.13 Real and imaginary parts of the pressure difference coefficient for an airfoil with *an aileron* $(s_1 / c = 0.75)$ *executing oscillatory rotations.*

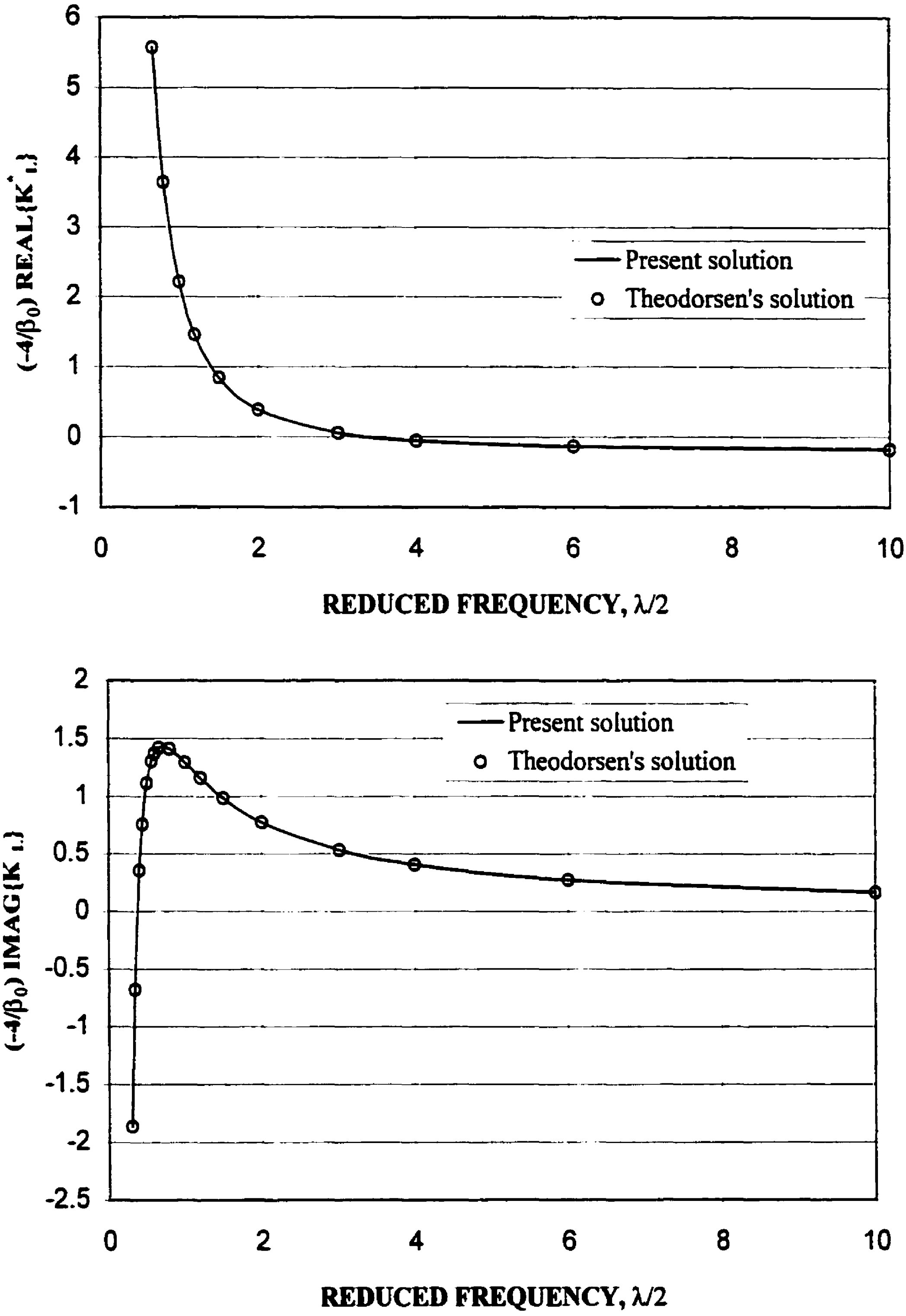

Fig 5.14 Real and imaginary parts of the reduced lift coefficient for an airfoil with an *aileron* $(s_1 / c = 0.70)$ *executing oscillatory rotations.*

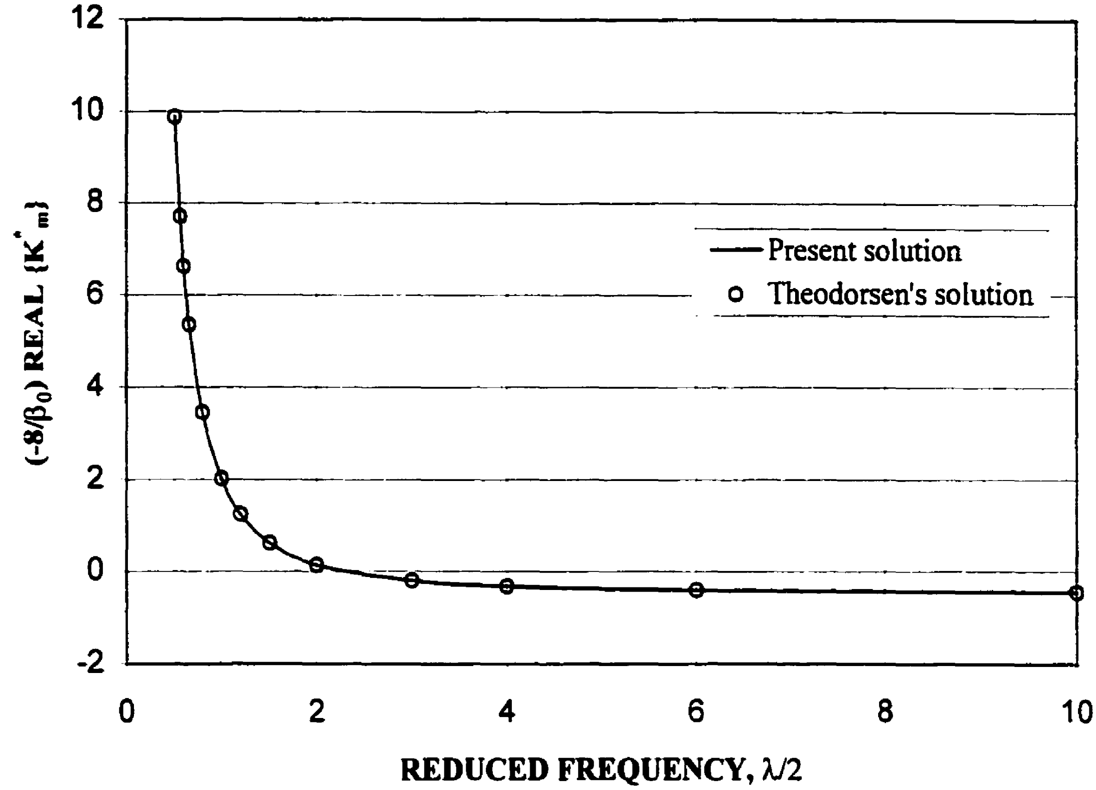

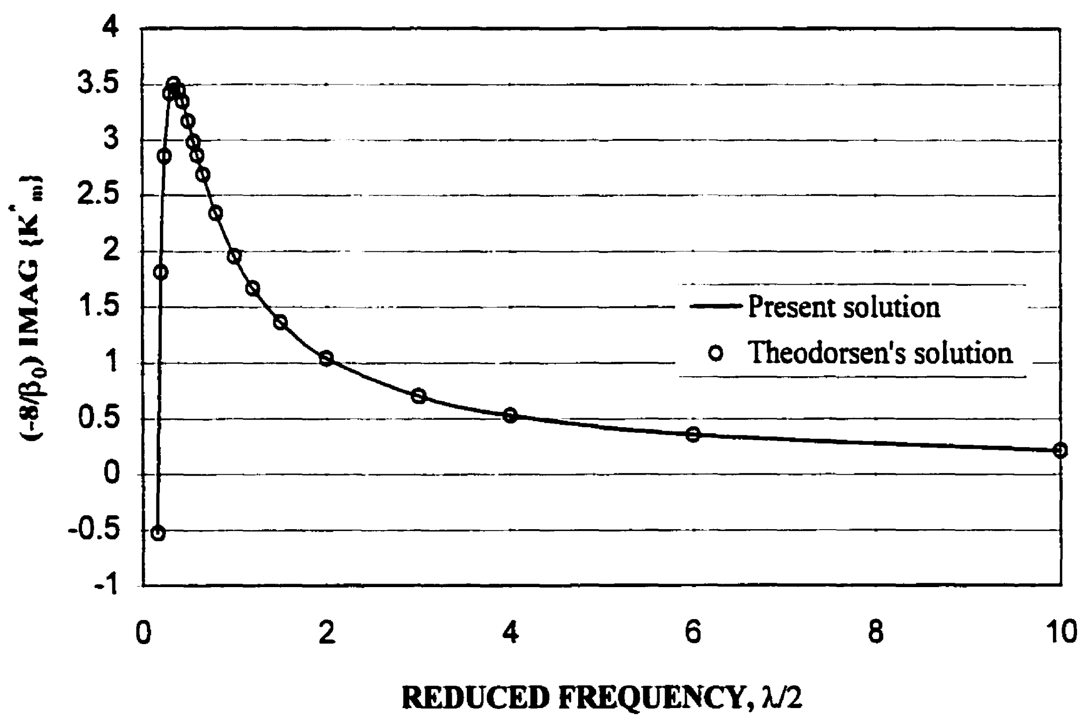

Fig 5.15 Real and imaginary parts of the reduced pitching moment coefficient for an airfoil with an *aileron* $(s_1 / c = 0.70)$ *executing oscillatory rotations.*

5.5 Case of an airfoil with an aileron executing flexural oscillations

The numerical results were obtained for various values of the reduced frequency λ ,such as $\lambda = 0.48, 0.60, 0.68$. The results are presented in Figures 5.16, 5.19, 5.22 and in Figures 5.17, 5.18, 5.20, 5.21, 5.23,5.24, for the real and imaginary parts of the reduced oscillatory pressure difference coefficient $(-c/\kappa_0)\Delta K_p^*$, and for the real and imaginary parts of the reduced oscillatory lift and pitching moment coefficients, $(4c/\kappa_0)K_L^*$ and $(8c/\kappa_0)K_m^*$, respectively. The results were performed for various aileron positions such as $s_1/c = 0.60, 0.75, 0.80$. No comparisons were presented for the case of flexural oscillations since there are no previous results known.

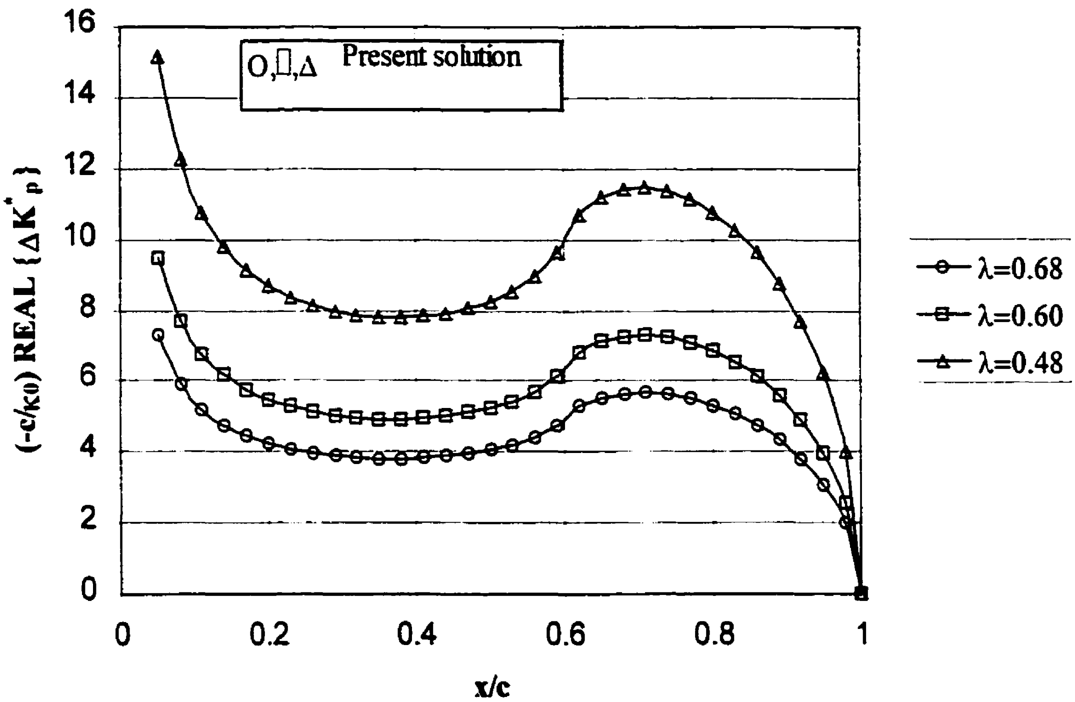

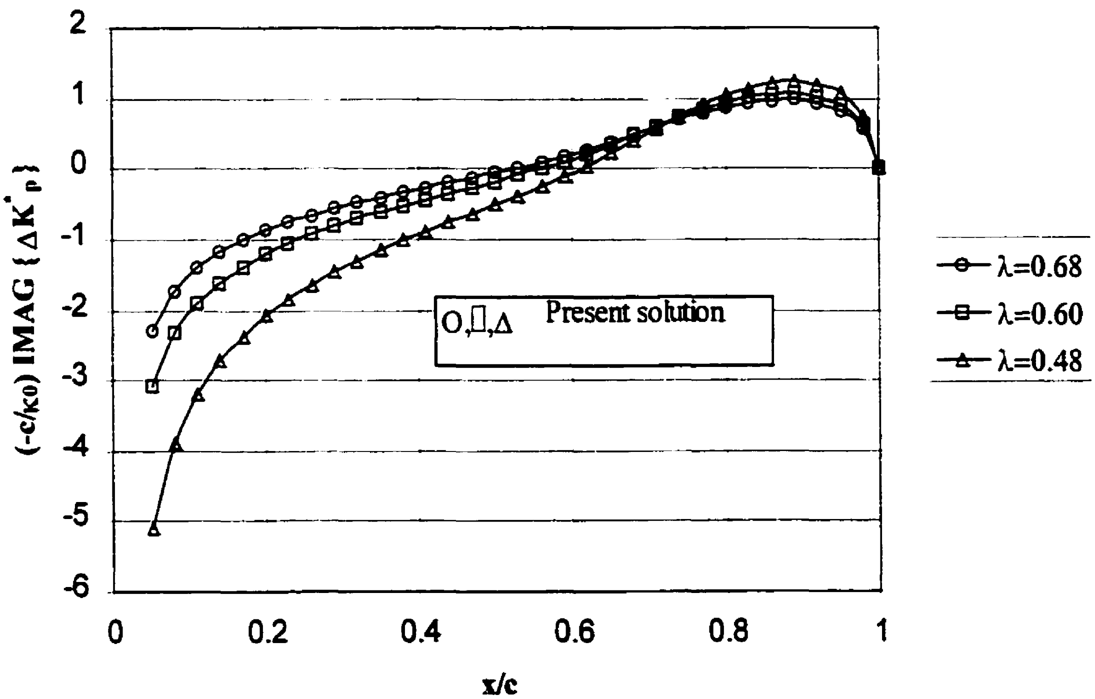

Fig 5.16 Real and imaginary parts of the pressure difference coefficient for an airfoil with an *aileron* $(s_1 / c = 0.60)$ *executing parabolic flexural oscillations.*

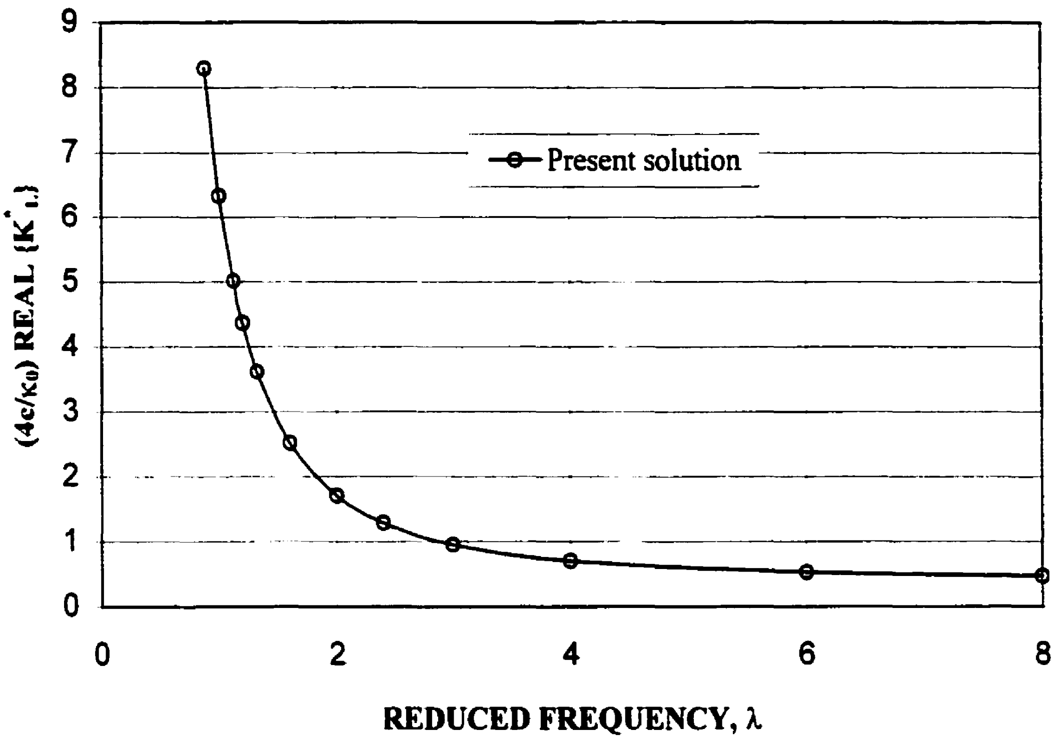

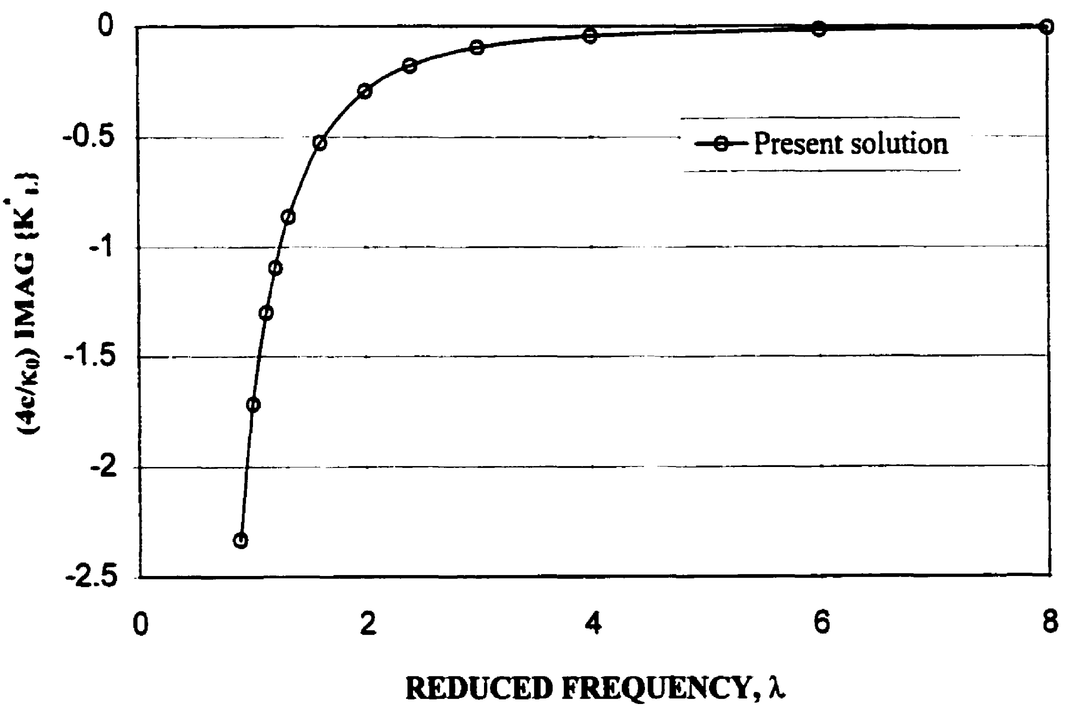

Fig 5.17 Real and imaginary parts of the reduced lift coefficient for an airfoil with an *aileron* $(s_1 / c = 0.60)$ *executing parabolic flexural oscillations.*

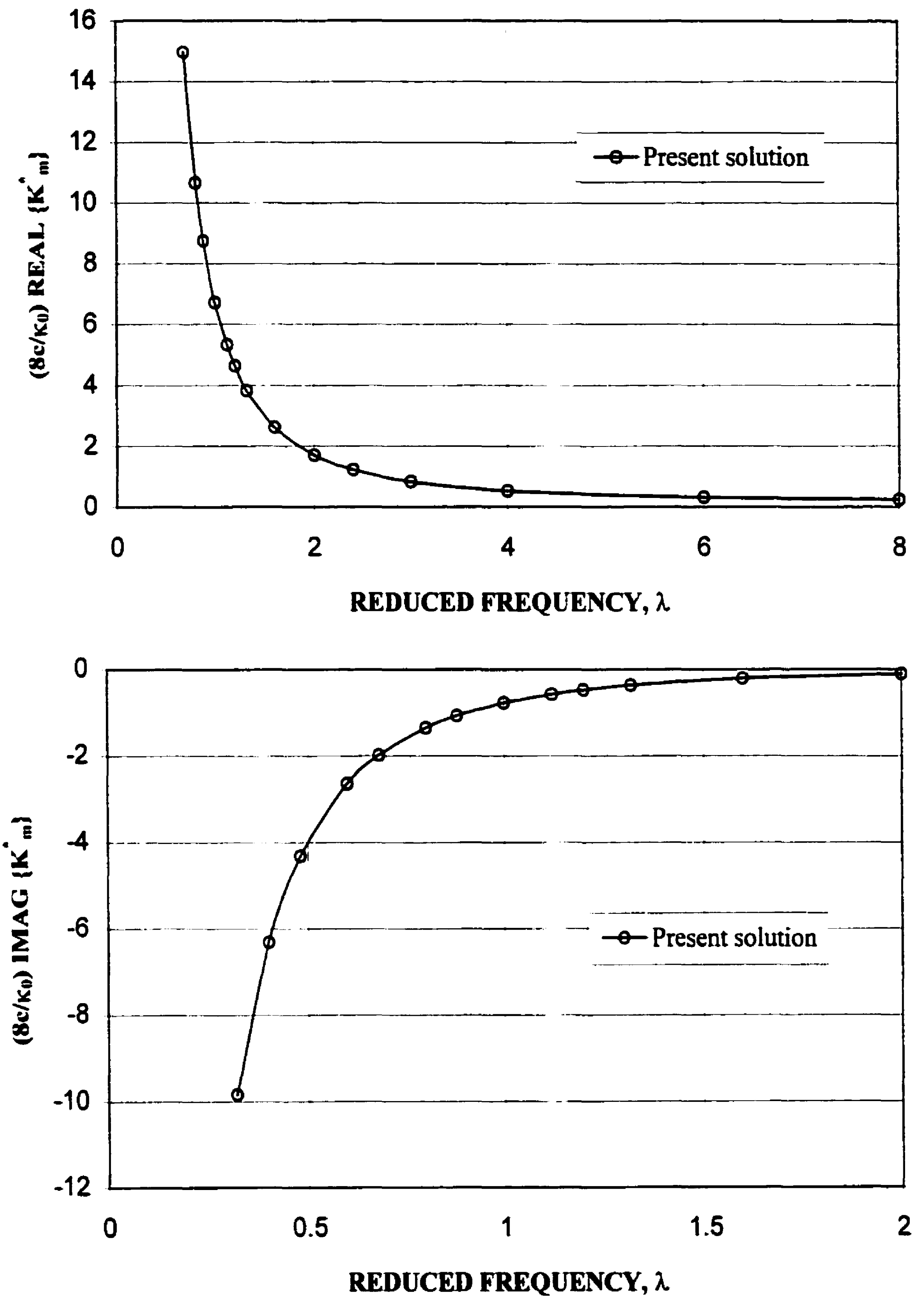

Fig 5.18 Real and imaginary parts of the reduced pitching moment coefficient for an airfoil with an *aileron* $(s_1 / c = 0.60)$ *executing parabolic flexural oscillations*

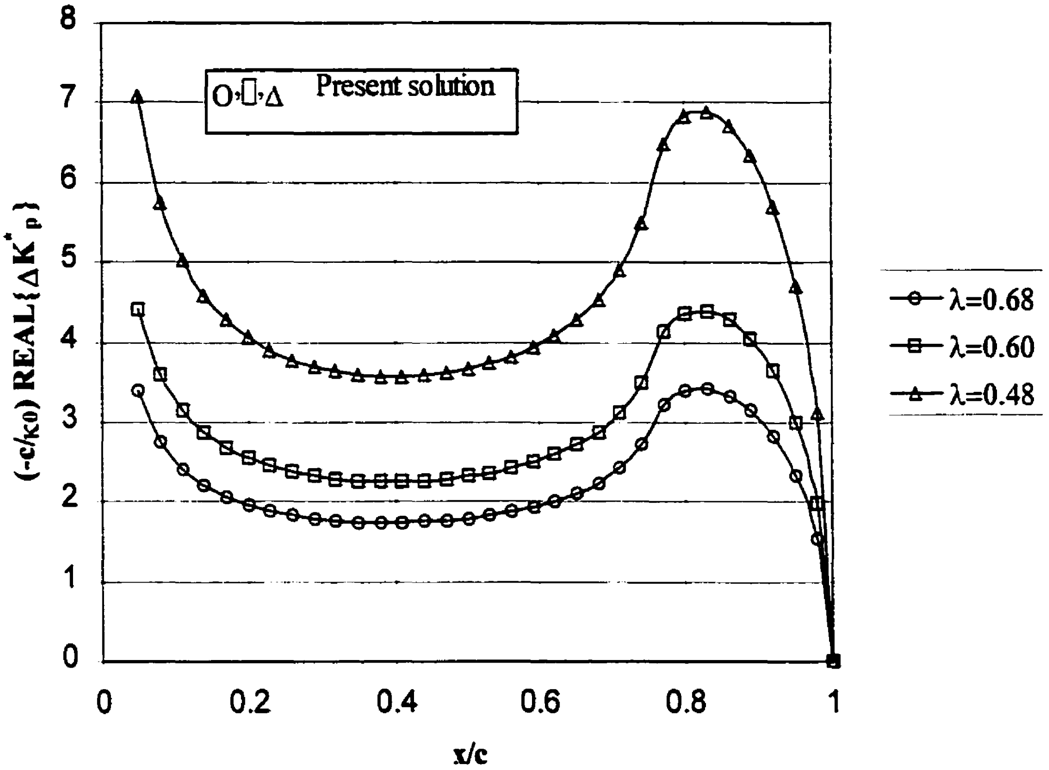

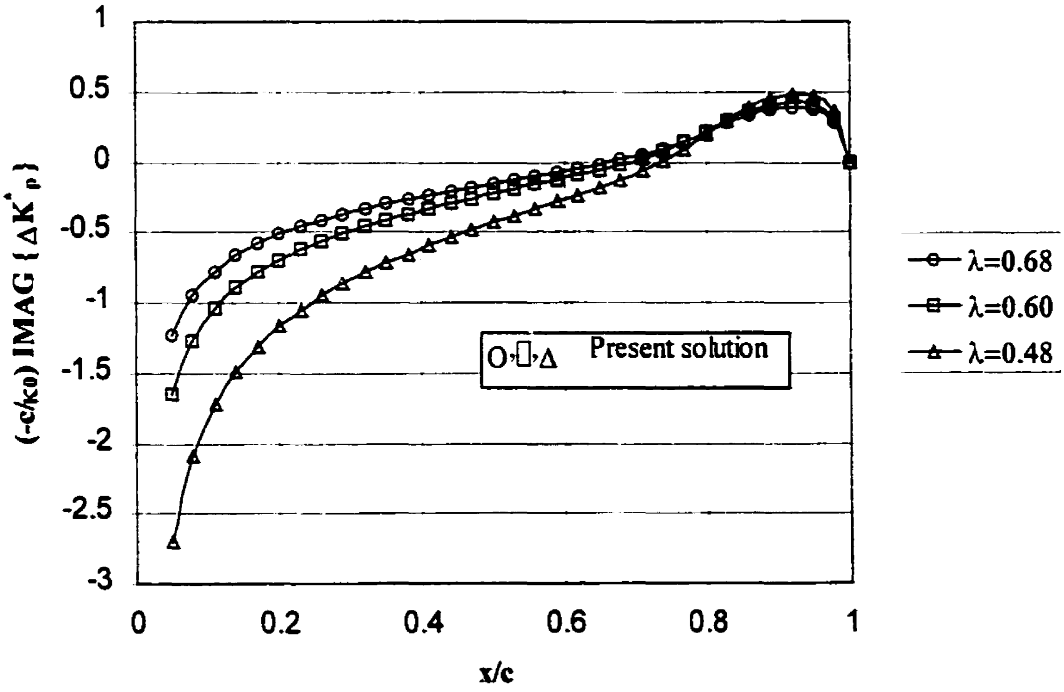

Fig 5.19 Real and imaginary parts of the pressure difference coefficient for an airfoil with an *aileron* $(s_1 / c = 0.75)$ *executing parabolic flexural oscillations.*

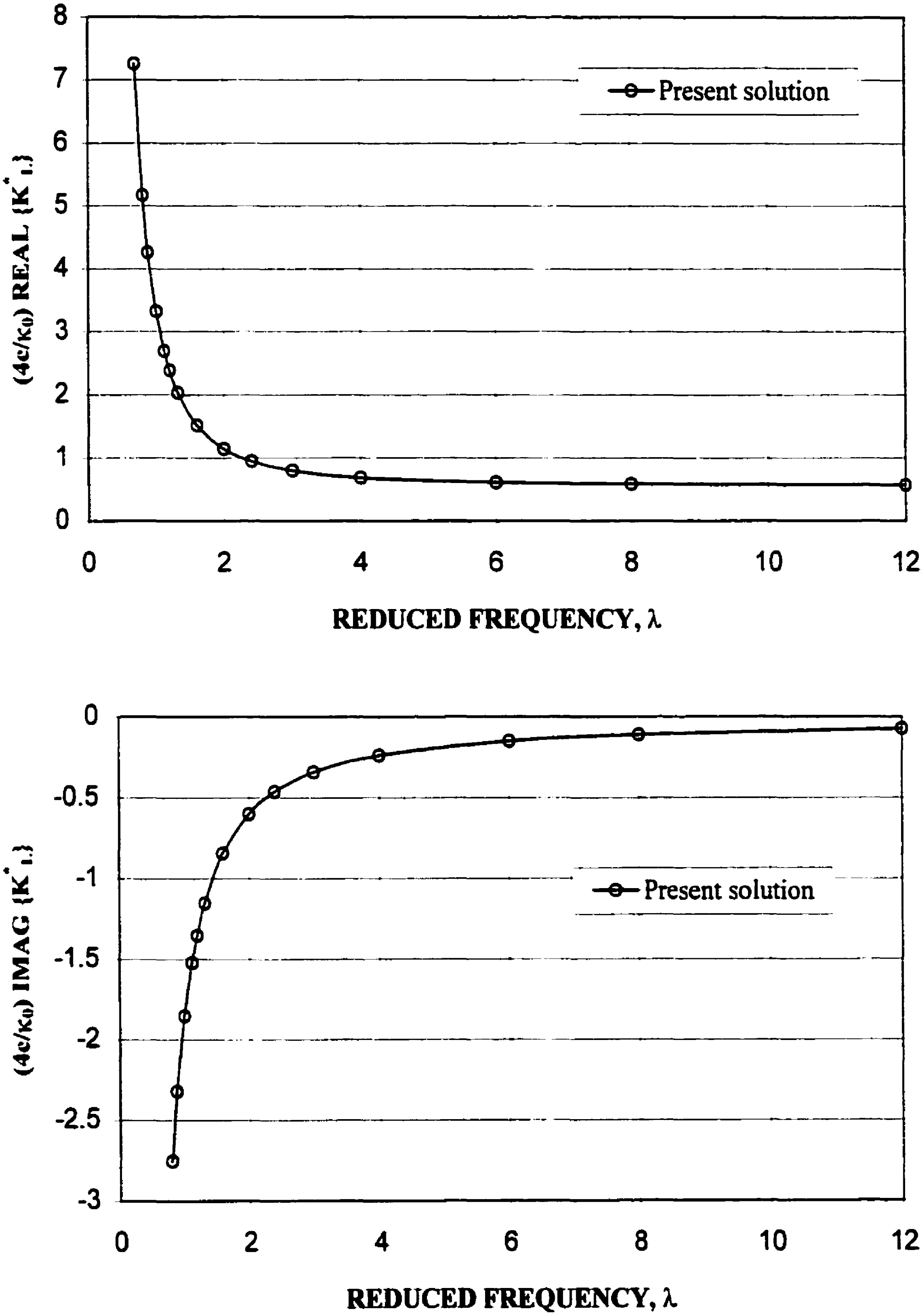

Fig 5.20 Real and imaginary parts of the reduced lift coefficient for an airfoil with an *aileron* $(s_1 / c = 0.75)$ *executing parabolic flexural oscillations.*

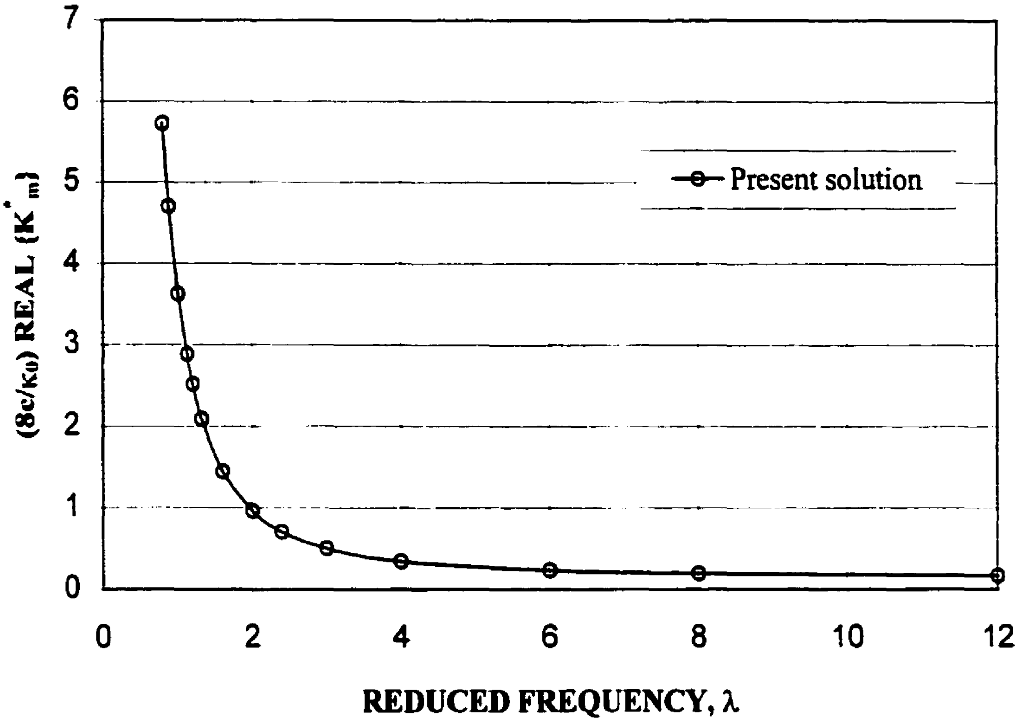

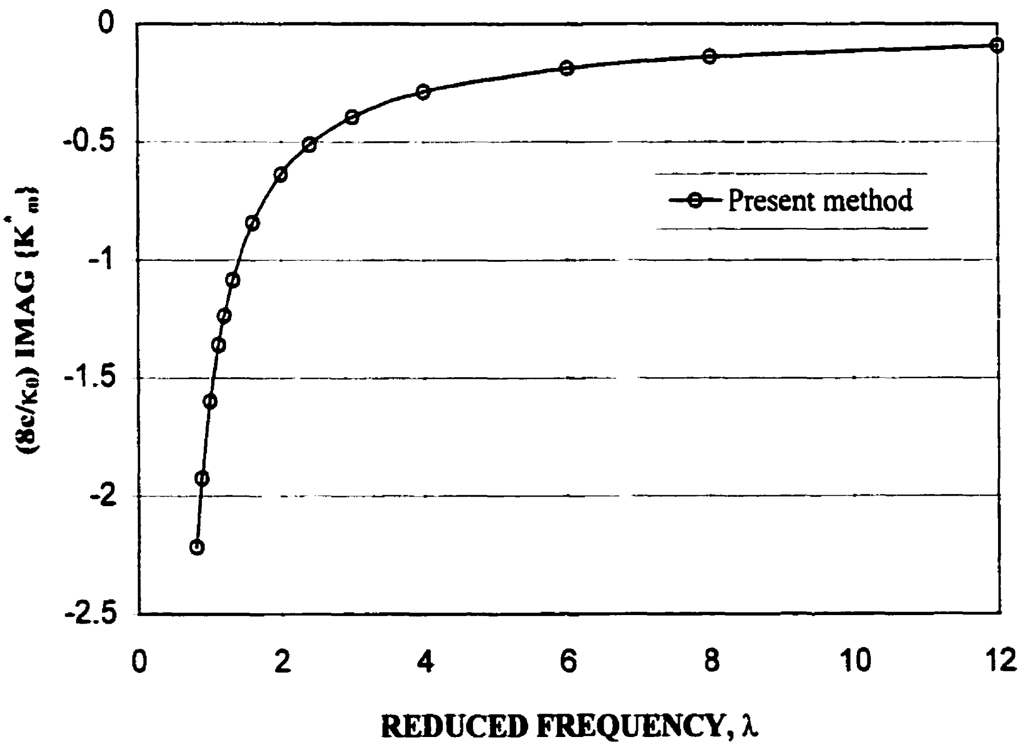

Fig 5.21 Real and imaginary parts of the reduced pitching moment coefficient for an airfoil with an *aileron* $(s_1 / c = 0.75)$ *executing parabolic flexural oscillations*

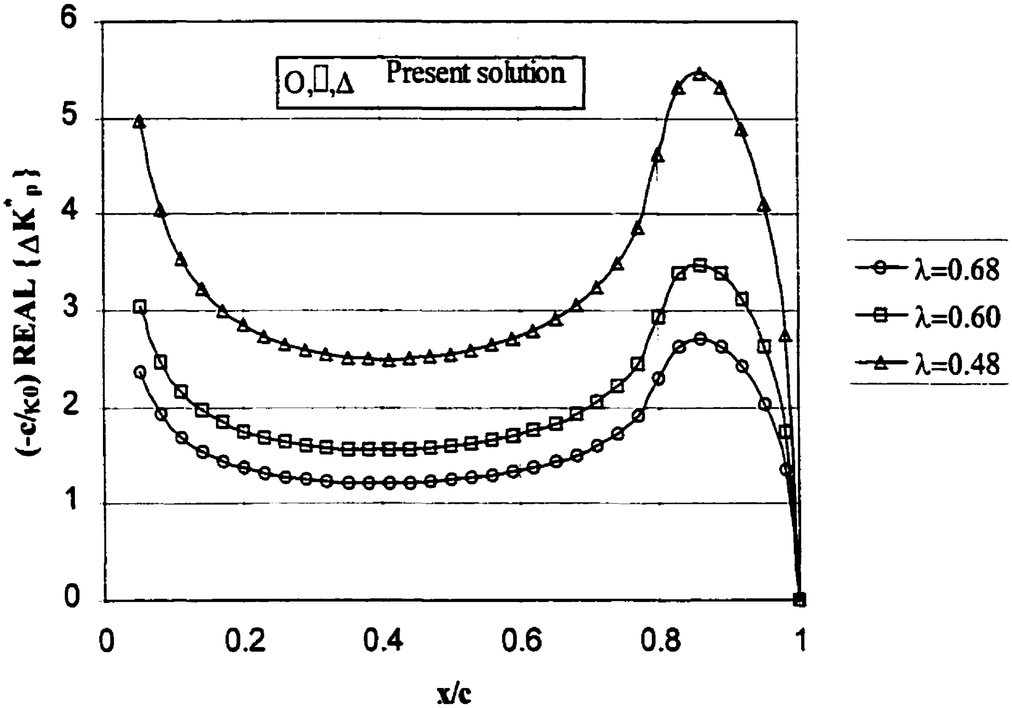

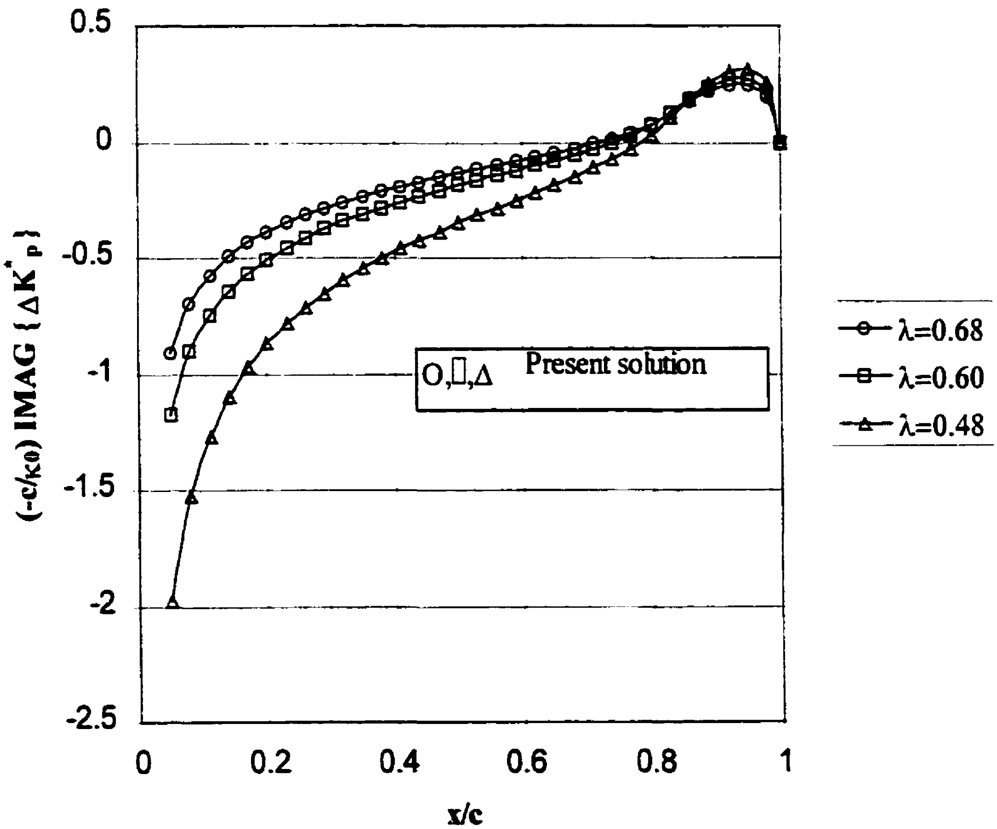

Fig 5.22 Real and imaginary parts of the pressure difference coefficient for an airfoil with an *aileron* $(s_1 / c = 0.80)$ *executing parabolic flexural oscillations*.

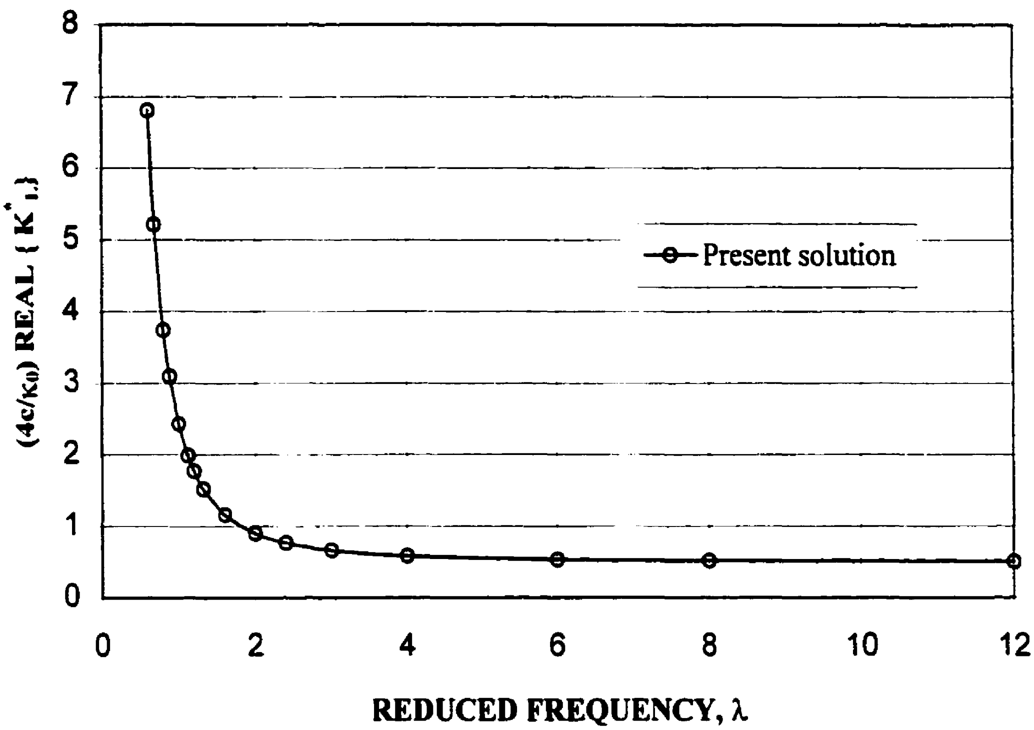

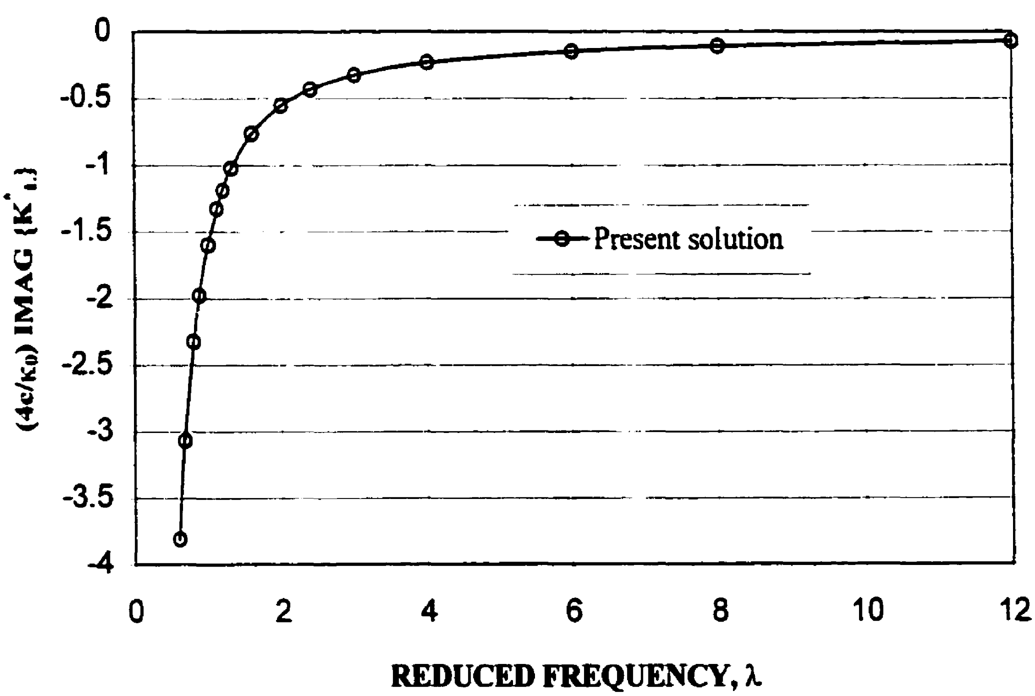

Fig 5.23 Real and imaginary parts of the reduced lift coefficient for an airfoil with an *aileron* $(s_1 / c = 0.80)$ *executing parabolic flexural oscillations.*

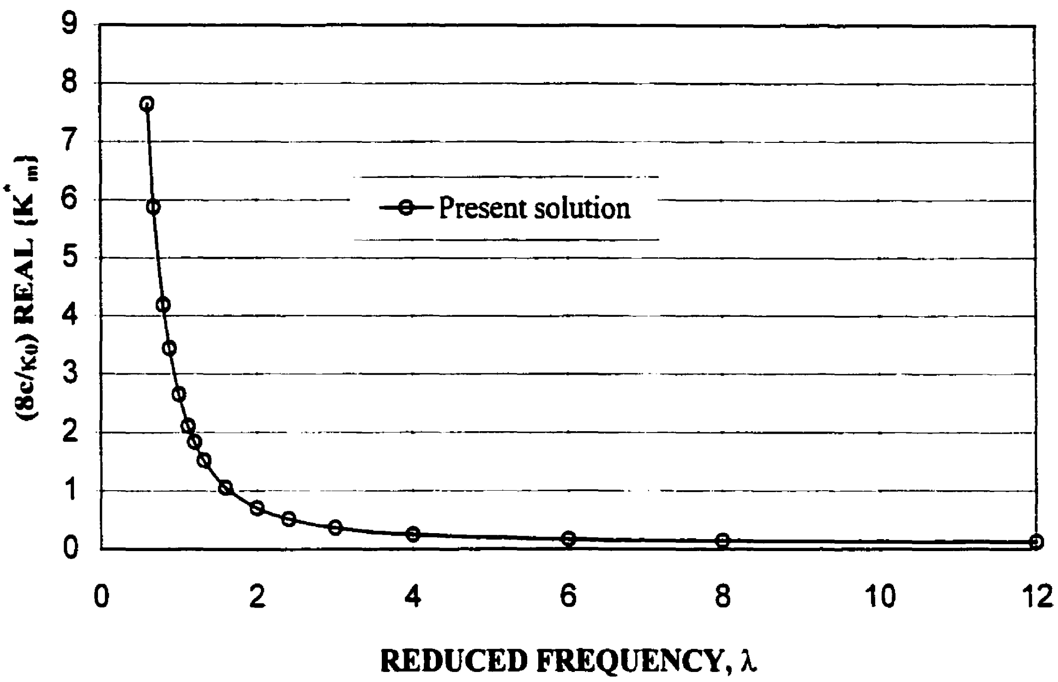

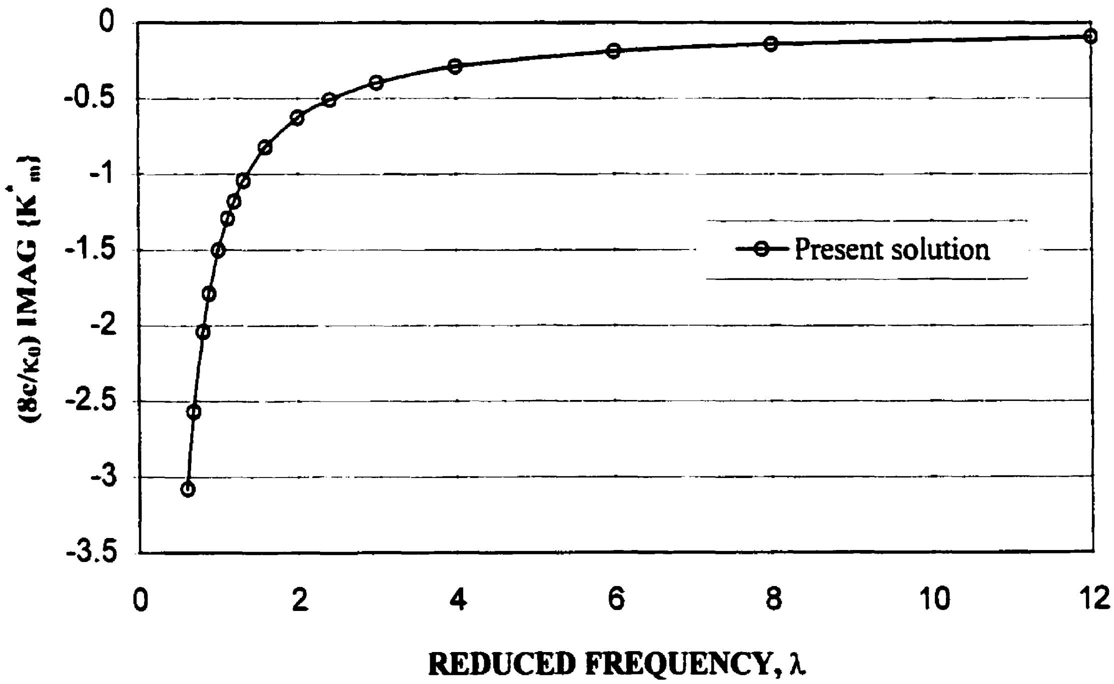

Fig 5.24 Real and imaginary parts of the reduced pitching moment coefficient for an airfoil with an *aileron* $(s_1 / c = 0.80)$ *executing parabolic flexural oscillations.*

Chapter 6

Conclusions

In this thesis, the steady and unsteady flow past fixed or oscillating airfoils has been analyzed. This work presents a new method based on velocity singularities for the analysis of the unsteady flows past oscillating airfoils.

The method of velocity singularities developed by Mateescu [11,13,14,16] for steady flows past airfoils. has been validated for the cases of rigid and flexible airfoils, in comparison with the previous solutions based on conformal transformations [14,21], or obtained by Nielsen and Thwaites [13,22,27]. A very good agreement has been obtained between the present solutions based on the velocity singularity method for steady flows and the previous results.

Closed form solutions were obtained for the pressure distribution and the aerodynamic forces acting on airfoils executing various harmonic oscillations. Closed form formulas were also derived for the pressure distribution and the aerodynamic forces acting on an airfoil with an aileron executing harmonic oscillations.

The method of velocity singularities for the unsteady flow past airfoils and ailerons executing harmonic oscillations, developed in this thesis, has proven to lead to accurate solutions, computationally efficient, in all studied problems. The solution of the unsteady flows obtained by the present method of velocity singularity is relatively simple, which avoid the mathematical difficulties encountered in the classical theories. The present method has been first validated for airfoils executing oscillatory translation and pitching rotation and for airfoils with ailerons executing pitching oscillations, in comparison with the previous results obtained by Theodorsen [15,26] and Postel and Leppert [24]. An excellent agreement has been obtained between the present velocity singularity solutions for unsteady flows and the previous results.

The method has then been extended to the unsteady flows past airfoils executing flexural harmonic oscillations. Closed form solutions were also derived for the pressure distributions and the aerodynamic forces acting on an airfoil with an aileron executing flexural oscillations. No comparisons were presented for the case of flexural oscillations since there are no previous results known.

In all problems treated in this thesis, the method of velocity singularities for steady and unsteady flows past fixed or oscillating airfoils has proven to be accurate, efficient and stable. The mathematical treatment also provides a convenient arrangement permitting a smooth treatment of all cases of oscillations.

As a suggestion for future work, the present method can be extended to the non-linear analysis of the unsteady flow past the oscillating airfoils. Also the method can be extended to the case when the amplitude of oscillations is decaying exponentially in time instead of being constant, as it is often the case in practice.

Bibliography

1- Abbott, H., and Von Doenhoff, A.E., Theory of wing sections., Dover, New York, 1959.

2- Basu, B.C., and Hancock, G.J., "The Unsteady Motion of a Two-Dimensional Airfoil in Incompressible Inviscid Flow," Journal of Fluid Mechanics, Vol. 87, 1978, pp. 159-78.

3- Carafoli E., Mateescu D., and Nastase A., Wing Theory in Supersonic Flow., Pergamon Press, 1969, pp. 1-591.

4- Dietz, "The Airforces on a Harmonically Oscillating Self Deforming Plate," Luftfahrtforschung, Vol. 16, No. 2, 1939, p.84.

5- Fung, Y.C., An Introduction to the Theory of Aeroelasticity, Dover, New York, 1993, pp. 381-462.

6- Glauert, H., The Elements of Aerofoil and Airscrew Theory., Cambridge University Press, Second edition.. 1926.

7- Gray, A., and Mathews, G.B., "A Treatise on Bessel Functions and Their Applications to physics," Dover, Second edition, pp. 20-25.

8- Kemp, N.H., and Homicz, G., "Approximate Unsteady Thin Airfoil Theory for Subsonic Flow," AIAA Journal, Vol. 14, 1976, pp. 1083-89.

9- Kussner, H.G., "Nonstationary Theory of Airfoils of Finite Thickness in Incompressible Flow," AGARD Manual on Aeroelasticity, Part II, Ch.8, 1960, Neuilly-sur-Seine, France.

10- Mateescu, D., " A Hyprid Panel method for Aerofoil Aerodynamics," Boundary Elements XII, Vol. 2, Applications in Fluid Mechanics and Field problems, edited by M. Tanaka, C. A.. Brebia, and T. Honma, Computational Mechanics Publications, Southampton, England, UK, and Springer-Verlag, Berlin, 1990, pp.3-14.

11- Mateescu, D., "Wing and Conical Body of Arbitrary Cross-Section in Supersonic Flow," Journal of Aircraft, Vol.24, No.4, 1987, pp.239-247.

12- Mateescu, D., Nadeau, Y., "A nonlinear analytical solution for airfoils in irrotational flow," Proceedings of the third international congress of Fluid Mechanics, Cairo, Egypt, Vol. IV, January 1990, pp. 1421-1432.

13- Mateescu, D., and Newman, B.G., "Analysis of Flexible-Membrane and Jet-Flapped Airfoils Using Velocity Singularities," Journal of Aircraft, Vol.28, No.11, 1991, pp.789-795.

14- Mateescu, D., "Subsonic Aerodynamics," Lecture Notes, McGill University, 1998.

15- Mateescu, D., "Unsteady Aerodynamics," Lecture Notes, McGill University, 1999.

16- Mateescu, D., " High-Speed Aerodynamics," Lecture Notes, McGill University, 1999.

17- Mateescu, D., "Private Communications," McGill University, Montreal. Canada, 1999.

18- McCroskey, W.J., "Unsteady Airfoils," Ann. Rev. Fluid Mech. 1982.14: 285-311.

19- McCroskey, W.J., "Inviscid Flow Field of an Unsteady Airfoil," AIAA Journal, Vol. 11, 1973, pp.1130-37.

20- McLachlan, N.W., "Bessel Functions For Engineers," Oxford at the Clarendon Press, 1934, pp. 61-70.

21- Milne-Thomson, L.M., Theoretical Aerodynamics., 4th edition, Dover, New York, 1966, pp. 136-145.

22- Nielsen, J.N., "Theory of Flexible Aerodynamic Surfaces," Journal of Applied Mechanics, Vol. 30, No. 9, 1963, pp. 435-442.

23- Papoulis, A., The Fourier Integral and Its Applications, McGraw-Hill, 1962, pp. 269-278.

24- Postel, E.E., and Leppert, E.L., Jr. 1948, "Theoretical Pressure Distribution for a thin Airfoil Oscillating in Incompressible flow," Journal of Aeronautical Sciences.15: 486-92.

25- Schwarz, "Calculation of the Pressure Distribution of a Wing Harmonically Oscillating in Two-Dimensional Flow," Luftfahrtforschung, Vol. 17, Nos. 11,12, 1940, p. 379.

26- Theodorsen, Theodore, "General Theory of Aerodynamic Instability and the Mechanism of Flutter," N.A.C.A. T.R. No. 496, 1935.

27- Thwaites, B., "The Aerodynamic Theory of sails: Two-Dimensional Sails," Proceedings of the Royal Society, series A, Vol. 261, 1961, pp. 402-422.

28- Von Kármán, T., and Sears, W.R., 1938, "Airfoil Theory for Nonuniform Motion," Journal of Aeronautical Sciences. 5: 379-90.

29- Watson, G.N., "Theory of Bessel Functions," Cambridge University Press, Second edition, 1966, pp. 160-183.

Appendix A: General integrals

A.1 The integral $F(z)$

Consider the integral $F(z)$ given by,

$$F(z)=\lim_{\sigma_n\to\infty}\left[\int_c^{\sigma_n} e^{-i\frac{\lambda}{c}(\sigma-c)}\cos^{-1}\sqrt{\frac{(c-z)\sigma}{c(\sigma-z)}}\,d\sigma\right], \tag{A-1}$$

By taking the derivative, one obtains,

$$\frac{d}{d\sigma}\left[\cos^{-1}\sqrt{\frac{(c-z)\sigma}{c(\sigma-z)}}\right]=\frac{\sqrt{(c-z)z}}{2(\sigma-z)\sqrt{(\sigma-c)\sigma}}, \tag{A-2}$$

Integrating by parts yields,

$$F(z)=\frac{c}{i\lambda}\lim_{\sigma_n\to\infty}\left[\int_c^{\sigma_n} e^{-i\frac{\lambda}{c}(\sigma-c)}\frac{\sqrt{(c-z)z}}{2(\sigma-z)\sqrt{(\sigma-c)\sigma}}\,d\sigma\right]. \tag{A-3}$$

A.2 The integral $J(x)$

Consider the integral $J(x)$ defined by,

$$J(x)=\lim_{\sigma_n\to\infty}\left[\int_c^{\sigma_n} e^{-i\frac{\lambda}{c}(\sigma-c)}\frac{\sigma}{x}\frac{\sqrt{(c-x)x}}{2(\sigma-x)\sqrt{(\sigma-c)\sigma}}\,d\sigma\right], \tag{A-4}$$

By integrating $J(x)$ from $x=0$ to x, one obtains,

$$\int_0^x J(x)\,dx=\lim_{\sigma_n\to\infty}\left[\int_c^{\sigma_n} e^{-i\frac{\lambda}{c}(\sigma-c)}\frac{\sigma}{\sqrt{(\sigma-c)\sigma}}\,d\sigma\right]\int_0^x\frac{\sqrt{(c-x)x}}{2x(\sigma-x)}\,dx, \tag{A-5}$$

The second integral is evaluated by,

$$\int_0^x\frac{\sqrt{(c-x)x}}{2x(\sigma-x)}\,dx=\int_0^x\frac{c-x}{2(\sigma-x)\sqrt{(c-x)x}}\,dx=\int_0^x\frac{(\sigma-x)-(\sigma-c)}{2(\sigma-x)\sqrt{(c-x)x}}\,dx, \tag{A-6}$$

One obtains thus two known integrals and the overall integral is given by,

$$\int_0^x \frac{\sqrt{(c-x)x}}{2x(\sigma-x)}dx = \frac{1}{2}\int_0^x \frac{dx}{\sqrt{(c-x)x}} - \frac{(\sigma-c)}{\sqrt{(\sigma-c)\sigma}}\int_0^x \frac{\sqrt{(\sigma-c)\sigma}}{2(\sigma-x)\sqrt{(c-x)x}}dx$$
$$= -\cos^{-1}\sqrt{\frac{x}{c}}\Big|_{x=0}^{x} - \frac{(\sigma-c)}{\sqrt{(\sigma-c)\sigma}}\cos^{-1}\sqrt{\frac{(c-x)\sigma}{c(\sigma-x)}}, \qquad \text{(A-7)}$$

By substituting the second integral into the integral of $J(x)$, one concludes,

$$\int_0^x J(x)dx = \lim_{\sigma_*\to\infty}\Big[\int_c^{\sigma_*} e^{-i\frac{\lambda}{c}(\sigma-c)}\left\{\frac{\sigma}{2\sqrt{(\sigma-c)\sigma}}\left[-2\cos^{-1}\sqrt{\frac{x}{c}}\right]_{x=0}^{x} - \cos^{-1}\sqrt{\frac{(c-x)\sigma}{c(\sigma-x)}}\right\}d\sigma\ \Big].$$

(A-8)

The value of the definite integral from $x=0$ to $x=c$ is given by,

$$\int_0^c J(x)\,dx = \frac{\pi}{2}\lim_{\sigma_*\to\infty}\Big[\int_c^{\sigma_*} e^{-i\frac{\lambda}{c}(\sigma-c)}\frac{\sigma}{\sqrt{(\sigma-c)\sigma}}d\sigma\ \Big] - \frac{\pi}{2}\lim_{\sigma_*\to\infty}\Big[\int_c^{\sigma_*} e^{-i\frac{\lambda}{c}(\sigma-c)}d\sigma\ \Big]. \qquad \text{(A-9)}$$

By substituting $\sigma = \frac{c}{2}(\zeta+1)$ into the finite integral appearing in the integral of $J(x)$, one obtains,

$$\int_c^\infty e^{-i\frac{\lambda}{c}(\sigma-c)}\frac{\sigma}{\sqrt{(\sigma-c)\sigma}}d\sigma = \frac{c}{2}\int_1^\infty e^{-i\frac{\lambda}{2}(\zeta-1)}\frac{\zeta+1}{\sqrt{\zeta^2-1}}d\zeta, \qquad \text{(A-10)}$$

Note that Hankel's integrals are defined by,

$$\int_1^\infty e^{-i\frac{\lambda}{2}\zeta}\frac{\zeta}{\sqrt{\zeta^2-1}}d\zeta = -\frac{\pi}{2}H_1^{(2)}(\lambda/2), \qquad \text{(A-11)}$$

$$\int_1^\infty e^{-i\frac{\lambda}{2}\zeta}\frac{1}{\sqrt{\zeta^2-1}}d\zeta = -i\frac{\pi}{2}H_0^{(2)}(\lambda/2). \qquad \text{(A-12)}$$

where $H_0^{(2)}(\lambda/2)$ and $H_1^{(2)}(\lambda/2)$ are Hankel's functions of second kind of zero and first order.

By substituting the known integrals of Hankel into the above integral, one obtains,

$$\int_c^{\infty} e^{-i\frac{\lambda}{c}(\sigma-c)} \frac{\sigma}{\sqrt{(\sigma-c)\sigma}}\, d\sigma = \frac{c}{2} e^{i\frac{\lambda}{2}} \left(-\frac{\pi}{2}\right) \left[H_1^{(2)}(\lambda/2) + i H_0^{(2)}(\lambda/2)\right]. \tag{A-13}$$

An important integral to note is that related to Fourier integrals given by (after integrating by parts),

$$\lim_{\sigma_\infty \to \infty} \left[\int_c^{\infty} e^{-i\frac{\lambda}{c}(\sigma-c)} d\sigma \right] = \frac{-c}{i\lambda}\left[E_\infty - 1\right] = \frac{c}{i\lambda}. \tag{A-14}$$

where as shown in (4-46),

$$E_\infty = \lim_{\sigma \to \infty} \left[e^{-i\frac{\lambda}{c}(\sigma-c)} \right] = 0. \tag{A-15}$$

which can be obtained from the Riemann-Lebesgue lemma on Fourier integrals [5,23], when the theory of distribution is used. Hence, the integral defined in (A-9) becomes,

$$\int_0^c J(x)\, dx = \left(\frac{\pi}{2}\right) \frac{c}{2} e^{i\frac{\lambda}{2}} \left(-\frac{\pi}{2}\right) \left[H_1^{(2)}(\lambda/2) + i\, H_0^{(2)}(\lambda/2)\right] - \left(\frac{\pi}{2}\right)\left(\frac{c}{i\lambda}\right). \tag{A-16}$$

A.3 Recurrence formulas for the integral I_k

Consider the recurrence integral defined by,

$$I_k = \int \frac{s^k}{\sqrt{(c-s)s}} ds, \tag{A-17}$$

Note that s^k can be written by,

$$s^k = -\frac{1}{2}\left[(c-2s)s^{k-1} - c s^{k-1}\right], \tag{A-18}$$

By substituting the value of s^k into the recurrence integral, one concludes,

$$I_k = -\left[\int \frac{s^{k-1}(c-2s)}{2\sqrt{s(c-s)}} ds - \int \frac{c s^{k-1}}{2\sqrt{s(c-s)}} ds \right], \tag{A-19}$$

Note that $\int \frac{s^{k-1}(c-2s)}{2\sqrt{s(c-s)}} ds = s^{k-1}\sqrt{s(c-s)} - (k-1)\int s^{k-2}\sqrt{s(c-s)}\, ds$

The second integral can be then given by,

$$\int s^{k-2}\sqrt{s(c-s)}\, ds = \int \frac{s^{k-2} s(c-s)}{\sqrt{(c-s)s}} ds = c\int \frac{s^{k-1}}{\sqrt{s(c-s)}} ds - \int \frac{s^k}{\sqrt{s(c-s)}} ds, \tag{A-20}$$

Substituting the above integral into the definition of the recurrence integral, one obtains,

$$I_k = -\left[s^{k-1}\sqrt{s(c-s)} - (k-1)(cI_{k-1} - I_k) - \frac{c}{2} I_{k-1} \right], \tag{A-21}$$

By arranging the terms, one concludes,

$$I_k = -\frac{s^{k-1}}{k}\sqrt{s(c-s)} + \left(\frac{2k-1}{2k}\right) c\, I_{k-1} . \tag{A-22}$$

The value of the integral at $k = 0$ (I_0) is given by,

$$I_0 = \int \frac{1}{\sqrt{s(c-s)}} ds = -2\cos^{-1}\sqrt{\frac{s}{c}}, \tag{A-23}$$

The value of the integral at $k = 1$ (I_1) is given by,

$$I_1 = \int \frac{s}{\sqrt{s(c-s)}} ds = -\sqrt{s(c-s)} - c\cos^{-1}\sqrt{\frac{s}{c}} . \tag{A-24}$$

The recurrence integral I_k with limits is given by,

1) $$I_k = \int_0^c \frac{s^k}{\sqrt{(c-s)s}} ds \tag{A-25}$$

$$I_k = \frac{2k-1}{2k} c\, I_{k-1} \qquad \text{where, } I_0 = \pi\ ,\ I_1 = c\frac{\pi}{2}. \tag{A-26}$$

a) The integral $\int_0^c s^{k-1}\sqrt{(c-s)s}\, ds$ is related to the recurrence integral as follows,

$$\int_0^c s^{k-1}\sqrt{(c-s)s}\, ds = \int_0^c \frac{s^{k-1}(c-s)s}{\sqrt{(c-s)s}} ds = c\, I_k - I_{k+1} = \frac{c}{2(k+1)} I_k . \tag{A-27}$$

b) The integral $\int_0^c s^k\sqrt{(c-s)s}\, ds$ is related to the recurrence integral as follows,

$$\int_0^c s^k\sqrt{(c-s)s}\, ds = \int_0^c \frac{s^k(c-s)s}{\sqrt{(c-s)s}} ds = c\, I_{k+1} - I_{k+2}, \tag{A-28}$$

where,

$$I_{k+1} = \frac{2k+1}{2(k+1)} c\, I_k \quad \text{and} \quad I_{k+2} = \frac{c^2}{4}\frac{(2k+1)(2k+3)}{(k+1)(k+2)} I_k , \tag{A-29}$$

The resultant formula is given by,

$$\int_0^c s^k \sqrt{(c-s)s}\, ds = \frac{c^2}{4}\frac{(2k+1)}{(k+1)(k+2)} I_k . \tag{A-30}$$

The recurrence integral I_k is evaluated from $x = s_1$ to $x = c$ and is given by,

2) $$I_k = \int_{s_1}^c \frac{s^k}{\sqrt{(c-s)s}}\, ds \tag{A-31}$$

$$I_k = \frac{s_1^{k-1}}{k}\sqrt{(c-s_1)s_1} + \frac{2k-1}{2k} c\, I_{k-1}, \tag{A-32}$$

$$I_0 = 2\cos^{-1}\sqrt{\frac{s_1}{c}} \qquad I_1 = \sqrt{(c-s_1)s_1} + c\cos^{-1}\sqrt{\frac{s_1}{c}}. \tag{A-33}$$

a) The integral $\int_{s_1}^c s^{k-1}\sqrt{(c-s)s}\, ds$ is related to the above integral as follows.

$$\int_{s_1}^c s^{k-1}\sqrt{(c-s)s}\, ds = c\, I_k - I_{k+1}, \tag{A-34}$$

where,

$$I_{k+1} = \frac{s_1^k}{k+1}\sqrt{(c-s_1)s_1} + \frac{2k+1}{2(k+1)} c\, I_k, \tag{A-35}$$

The resultant formula of the integral is given by,

$$\int_{s_1}^c s^{k-1}\sqrt{(c-s)s}\, ds = \frac{c}{2(k+1)} I_k - \frac{s_1^k}{k+1}\sqrt{(c-s_1)s_1}\,. \tag{A-36}$$

The following integrals are related to the recurrence integral and are evaluated in the same manner as above,

b) $$\int_{s_1}^c s^k\sqrt{(c-s)s}\, ds = \frac{c}{2(k+2)} I_{k+1} - \frac{s_1^{k+1}}{k+2}\sqrt{(c-s_1)s_1}\,, \tag{A-37}$$

c) $$\int_{s_1}^c s^{k+1}\sqrt{(c-s)s}\, ds = \frac{c}{2(k+3)} I_{k+2} - \frac{s_1^{k+2}}{k+3}\sqrt{(c-s_1)s_1}\,, \tag{A-38}$$

where,

$$I_{k+2} = \frac{s_1^{k+1}}{k+2}\sqrt{(c-s_1)s_1} + \frac{2k+3}{2(k+2)} c\, I_{k+1}. \tag{A-39}$$

A.4 Recurrence formulas for the integral Q_k

Consider the integral Q_k defined by,

$$Q_k = \int x^k \cosh^{-1}\sqrt{\frac{(c-x)s_1}{c(s_1-x)}}\,dx, \tag{A-40}$$

By taking the derivative of the $\cosh^{-1}\{\ \}$ function, one obtains,

$$H_1 = \cosh^{-1} R_1 \quad , \quad R_1 = \sqrt{\frac{(c-x)s_1}{c(s_1-x)}}, \tag{A-41}$$

$$\frac{d\,H_1}{d\,x} = \frac{\sqrt{(c-s_1)s_1}}{2(s_1-x)\sqrt{(c-x)x}}, \tag{A-42}$$

By integrating by parts, one concludes,

$$Q_k = \frac{x^{k+1}}{k+1}\cosh^{-1} R_1 - \int \frac{x^{k+1}\sqrt{(c-s_1)s_1}}{2(k+1)(s_1-x)\sqrt{(c-x)x}}\,dx, \tag{A-43}$$

By taking $x^{k+1} = s_1^{k+1} - (s_1-x)\sum_{n=0}^{k} x^n s_1^{k-n}$ the above recurrence formula will be.

$$Q_k = \left(\frac{x^{k+1}-s_1^{k+1}}{k+1}\right)\cosh^{-1}\sqrt{\frac{(c-x)s_1}{c(s_1-x)}} + \frac{\sqrt{(c-s_1)s_1}}{2(k+1)}\sum_{n=0}^{k} s_1^{k-n}\,\bar{I}_n. \tag{A-44}$$

where from section A.5,

$$\bar{I}_n = -\frac{x^{n-1}}{n}\sqrt{(c-x)x} + \left(\frac{2n-1}{2n}\right)c\,\bar{I}_{n-1}$$
$$\text{where, } \bar{I}_0 = -2\cos^{-1}\sqrt{\frac{x}{c}},\ \bar{I}_1 = -\sqrt{x(c-x)} - c\cos^{-1}\sqrt{\frac{x}{c}} \tag{A-45}$$

The following integrals are special cases of the recurrence integral Q_k,

1) At $k=0$, $Q_0 = \int \cosh^{-1}\sqrt{\frac{(c-x)s}{c(s-x)}}\,dx$

$$Q_0 = (x-s)\cosh^{-1}\sqrt{\frac{(c-x)s}{c(s-x)}} + \frac{\sqrt{(c-s)s}}{2}\,\bar{I}_0, \tag{A-46}$$

By taking the limits of the above integral from $x=0$ to $x=c$, one obtains,

$$Q_0 = \int_0^c \cosh^{-1}\sqrt{\frac{(c-x)s}{c(s-x)}}\,dx = (c-s)\left(j\frac{\pi}{2}\right) + \frac{\pi}{2}\sqrt{(c-s)s}, \tag{A-47}$$

The real part of the above integral is given by,

$$\text{Real}\,[Q_0]=\frac{\pi}{2}\sqrt{(c-s)s}\,. \tag{A-48}$$

2) At $k=1$, $Q_1=\int_0^c x\cosh^{-1}\sqrt{\frac{(c-x)s}{c(s-x)}}\,dx$

$$Q_1=\left[\left(\frac{x^2-s^2}{2}\right)\cosh^{-1}\sqrt{\frac{(c-x)s}{c(s-x)}}\right]_{x=0}^{c}+\frac{\sqrt{(c-s)s}}{4}\sum_{n=0}^{1}s^{k-n}\,\bar{I}_n\,, \tag{A-49}$$

$$\sum_{n=0}^{1}s^{k-n}\,\bar{I}_n=s\,\bar{I}_0+\bar{I}_1=\pi\left(s+\frac{c}{2}\right), \tag{A-50}$$

The resultant formula is expressed as,

$$Q_1=\left(\frac{c^2-s^2}{2}\right)\left(j\frac{\pi}{2}\right)+\frac{\pi}{4}\left(s+\frac{c}{2}\right)\sqrt{(c-s)s}\,, \tag{A-51}$$

The real part of the above integral is given by,

$$\text{Real}[Q_1]=\frac{\pi}{4}\left(s+\frac{c}{2}\right)\sqrt{(c-s)s}\,. \tag{A-52}$$

3) At $k=2$, $Q_2=\int_0^c x^2\cosh^{-1}\sqrt{\frac{(c-x)s}{c(s-x)}}\,dx$

By substituting into the recurrence integral Q_k, one concludes,

$$Q_2=\left[\left(\frac{x^3-s^3}{3}\right)\cosh^{-1}\sqrt{\frac{(c-x)s}{c(s-x)}}\right]_{x=0}^{c}+\frac{\sqrt{(c-s)s}}{6}\sum_{n=0}^{2}s^{k-n}\,\bar{I}_n\,, \tag{A-53}$$

$$\sum_{n=0}^{2}s^{k-n}\,\bar{I}_n=s^2\,\bar{I}_0+s\,\bar{I}_1+\bar{I}_2=\pi\left(s^2+\frac{c}{2}s+\frac{3}{8}c^2\right). \tag{A-54}$$

The resultant formula is given by,

$$Q_2=\left(\frac{c^3-s^3}{3}\right)\left(j\frac{\pi}{2}\right)+\frac{\pi}{6}\left(s^2+\frac{c}{2}s+\frac{3}{8}c^2\right)\sqrt{(c-s)s}\,, \tag{A-55}$$

The real part of the integral is evaluated as,

$$\text{Real}[Q_2]=\frac{\pi}{6}\left(s^2+\frac{c}{2}s+\frac{3}{8}c^2\right)\sqrt{(c-s)s}\,. \tag{A-56}$$

The following integrals are related to the recurrence integral Q_k and are given as,

4) $\text{Real}\left[\int_0^c (x-s)\cosh^{-1}\sqrt{\frac{(c-x)s}{c(s-x)}}\,dx\right] = Q_1 - sQ_0 = \left(\frac{\pi}{4}\right)\sqrt{(c-s)s}\left(\frac{c}{2}-s\right)$

5) $\text{Real}\left[\int_0^c x(x-s)\cosh^{-1}\sqrt{\frac{(c-x)s}{c(s-x)}}\,dx\right] = Q_2 - sQ_1 = (\pi)\sqrt{(c-s)s}\left(\frac{3}{48}c^2 - \frac{c}{24}s - \frac{s^2}{12}\right)$

A.5 Recurrence formulas for the integral F_k

Consider the recurrence integral F_k defined by,

$$F_k = \int s_1^k \cosh^{-1}\sqrt{\frac{(c-x)s_1}{c(s_1-x)}}\,ds_1 , \tag{A-57}$$

By integrating by parts, one concludes,

$$F_k = \frac{s_1^{k+1}}{k+1}\cosh^{-1} R_1 - \int \frac{s_1^{k+1}(-1)\sqrt{(c-x)x}}{2(k+1)(s_1-x)\sqrt{s_1(c-s_1)}}\,ds_1 , \tag{A-58}$$

where,

$$H_1 = \cosh^{-1} R_1 \quad . \quad R_1 = \sqrt{\frac{(c-x)s_1}{c(s_1-x)}} . \tag{A-59}$$

$$\frac{dH_1}{ds_1} = \frac{-\sqrt{(c-x)x}}{2(s_1-x)\sqrt{s_1(c-s_1)}} . \tag{A-60}$$

By taking $s_1^{k+1} = x^{k+1} + (s_1 - x)\sum_{n=0}^{k} s_1^n x^{k-n}$ one obtains.

$$F_k = \left(\frac{s_1^{k+1} - x^{k+1}}{k+1}\right)\cosh^{-1}\sqrt{\frac{s_1(c-x)}{c(s_1-x)}} + \frac{\sqrt{x(c-x)}}{2(k+1)}\sum_{n=0}^{k} x^{k-n} I_n , \tag{A-61}$$

From section A.5,

$$I_n = -\frac{s_1^{n-1}}{n}\sqrt{s_1(c-s_1)} + \left(\frac{2n-1}{2n}\right)c\, I_{n-1} . \tag{A-62}$$

By taking the limits from $x = 0$ to $x = c$, one obtains,

1) $F_k = \int_0^c s_1^k \cosh^{-1}\sqrt{\frac{(c-x)s_1}{c(s_1-x)}}\,ds_1$,

By substituting into the recurrence formula of F_k, one concludes,

$$F_k = \frac{x^{k+1}}{k+1}\left(j\frac{\pi}{2}\right) + \frac{\sqrt{(c-x)x}}{2(k+1)}\sum_{n=0}^{k} x^{k-n}\, I_n\,, \tag{A-63}$$

The real part of the integral is given by,

$$\text{Real}\,[F_k] = \frac{\sqrt{(c-x)x}}{2(k+1)}\sum_{n=0}^{k} x^{k-n}\, I_n\,. \tag{A-64}$$

Note that,

$$I_n = \frac{2n-1}{2n}\, c\, I_{n-1} \qquad \text{where, } I_0 = \pi \;,\; I_1 = c\frac{\pi}{2}.$$

The following is a special case of the above recurrence integral with limits and is concluded as,

$$F_{k-1} = \int_0^c s^{k-1}\cosh^{-1}\sqrt{\frac{(c-x)s}{c(s-x)}}\,ds\,. \tag{A-65}$$

$$\text{Real}\left[F_{k-1}\right] = \frac{1}{2k}\sqrt{\frac{c-x}{x}}\;\sum_{n=0}^{k-1} x^{k-n} I_n\,. \tag{A-66}$$

The following is an integral that is related to the recurrence formula and is given by,

2) $$\int_0^c (x-s)s^{k-1}\cosh^{-1}\sqrt{\frac{(c-x)s}{c(s-x)}}\,ds = x\,F_{k-1} - F_k$$
$$= \frac{1}{2(k+1)}\sqrt{(c-x)x}\left[\sum_{n=0}^{k-1}\frac{x^{k-n}}{k} I_n - I_k\right]^{\cdot} \tag{A-67}$$

The recurrence integral F_k is evaluated for the case of the limits from $x = s_1$ to $x = c$ and is given by,

3) $$F_k = \int_{s_1}^c s^k\cosh^{-1}\sqrt{\frac{(c-x)s}{c(s-x)}}\,ds$$

$$F_k = \left(\frac{x^{k+1} - s_1^{k+1}}{k+1}\right)\cosh^{-1}\sqrt{\frac{(c-x)s_1}{c(s_1-x)}} + \frac{\sqrt{(c-x)x}}{2(k+1)}\sum_{n=0}^{k} x^{k-n}\, I_n\,, \tag{A-68}$$

where,

$$I_n = \frac{s_1^{n-1}}{n}\sqrt{(c-s_1)s_1} + \frac{2n-1}{2n} c\, I_{n-1},$$

$$I_0 = 2\cos^{-1}\sqrt{\frac{s_1}{c}} \qquad I_1 = \sqrt{(c-s_1)s_1} + c\cos^{-1}\sqrt{\frac{s_1}{c}}. \tag{A-69}$$

A special case of the above recurrence formula is given below as,

$$F_{k-1} = \int_{s_1}^{c} s^{k-1}\cosh^{-1}\sqrt{\frac{(c-x)s}{c(s-x)}}\,ds, \tag{A-70}$$

$$F_{k-1} = \left(\frac{x^k - s_1^k}{k}\right)\cosh^{-1}\sqrt{\frac{(c-x)s_1}{c(s_1-x)}} + \frac{1}{2k}\sqrt{\frac{c-x}{x}}\sum_{n=0}^{k-1} x^{k-n} I_n. \tag{A-71}$$

A.6 Integrals related to I_k

The following are integrals related to the recurrence formula I_k,

$$1)\quad \int_0^c s^{k-1}\cos^{-1}\sqrt{\frac{s}{c}}\,ds \tag{A-72}$$

By performing the derivative, one obtains,

$$\frac{d}{ds}\left[\cos^{-1}\sqrt{\frac{s}{c}}\right] = \frac{-1}{2\sqrt{(c-s)s}}. \tag{A-73}$$

Integrating by parts,

$$\int_0^c s^{k-1}\cos^{-1}\sqrt{\frac{s}{c}}\,ds = \frac{1}{2k}\int_0^c \frac{s^k}{\sqrt{(c-s)s}}\,ds = \frac{1}{2k} I_k. \tag{A-74}$$

where,

$$I_k = \frac{2k-1}{2k} c\, I_{k-1} \qquad \text{where, } I_0 = \pi \;,\; I_1 = c\frac{\pi}{2}. \tag{A-75}$$

The following integral is a special case of the above recurrence formula,

$$2)\quad \int_{s_1}^{c} s^{k-1}\cos^{-1}\sqrt{\frac{s}{c}}\,ds = \frac{1}{k}s^k\cos^{-1}\sqrt{\frac{s}{c}}\Big|_{s=s_1}^{c} + \frac{1}{2k}\int_{s_1}^{c}\frac{s^k}{\sqrt{(c-s)s}}\,ds \tag{A-76}$$

The resultant expression is given by,

$$\int_{s_1}^{c} s^{k-1}\cos^{-1}\sqrt{\frac{s}{c}}\,ds = \frac{s_1^{k-1}}{k}\sqrt{(c-s_1)s_1} + \frac{2k-1}{2k} c\, I_{k-1}, \tag{A-77}$$

where,

$$I_k = \frac{s_1^{k-1}}{k}\sqrt{(c-s_1)s_1} + \frac{2k-1}{2k} c\, I_{k-1}, \tag{A-78}$$

$$I_0 = 2\cos^{-1}\sqrt{\frac{s_1}{c}} \qquad I_1 = \sqrt{(c-s_1)s_1} + c\cos^{-1}\sqrt{\frac{s_1}{c}}.$$

A.7 Recurrence formula for the integral I_r

Consider the recurrence integral I_r defined by,

$$I_r = \int \frac{x^r}{\sqrt{(c-x)x}}\, dx, \tag{A-79}$$

where (from section A.4),

$$I_r = -\frac{x^{r-1}}{r}\sqrt{(c-x)x} + \frac{2r-1}{2r} c\, I_{r-1}, \tag{A-80}$$

$$I_0 = -2\cos^{-1}\sqrt{\frac{x}{c}} \qquad I_1 = -\sqrt{(c-x)x} - c\cos^{-1}\sqrt{\frac{x}{c}}. \tag{A-81}$$

The following integrals are related to the recurrence integral I_r.

1) $$\int x^r \sqrt{\frac{c-x}{x}}\, dx = \int x^r \frac{c-x}{\sqrt{(c-x)x}} dx = c\, I_r - I_{r+1} \tag{A-82}$$

The resultant expression is given by,

$$\int x^r \sqrt{\frac{c-x}{x}}\, dx = \frac{x^r}{r+1}\sqrt{(c-x)x} + \frac{c}{2(r+1)} I_r. \tag{A-83}$$

2) $$\int_0^c x^r \sqrt{\frac{c-x}{x}}\, dx = \frac{c}{2(r+1)} I_r \tag{A-84}$$

where,

$$I_r = \int_0^c \frac{x^r}{\sqrt{(c-x)x}}\, dx = \frac{2r-1}{2r} c\, I_{r-1}, \tag{A-85}$$

$$I_0 = \pi \quad , \quad I_1 = c\frac{\pi}{2} \quad \text{and} \quad I_2 = \frac{3c^2}{8}\pi. \tag{A-86}$$

The following integrals are related to the recurrence integral I_r at various values of r,

3) $$\int_0^c \sqrt{\frac{c-x}{x}}\,dx = \frac{c}{2} I_0 = c\frac{\pi}{2}.$$ (A-87)

4) $$\int_0^c \sqrt{(c-x)x}\,dx = \int_0^c x\sqrt{\frac{c-x}{x}}\,dx = \frac{c}{4} I_1 = c^2\frac{\pi}{8}.$$ (A-88)

5) $$\int_0^c x\sqrt{(c-x)x}\,dx = \int_0^c x^2\sqrt{\frac{c-x}{x}}\,dx = \frac{c}{6} I_2 = \frac{3c^3}{48}\pi.$$ (A-89)

Appendix B: Theodorsen's formulas

B.1 Formulas related to Theodorsen's results

$$P_\omega = 1 - 2i\frac{V}{b\omega}(F+iG), \tag{B-1}$$

$$P_\varphi = \frac{1}{2} - i\frac{V}{b\omega}[1+2(F+iG)] - 2\left(\frac{V}{b\omega}\right)^2(F+iG), \tag{B-2}$$

$$P_\beta = -\frac{T_1}{\pi} + i\left(\frac{V}{b\omega}\right)\frac{T_4}{\pi} - i\frac{V}{b\omega}\frac{T_{11}}{\pi}(F+iG) - 2\left(\frac{V}{b\omega}\right)^2\frac{T_{10}}{\pi}(F+iG), \tag{B-3}$$

$$M_\omega = \frac{1}{2}, \quad M_\varphi = \frac{3}{8} - i\frac{V}{b\omega}, \tag{B-4}$$

$$M_\beta = -\frac{T_1}{\pi} - \left(c_1 + \frac{1}{2}\right)\frac{T_1}{\pi} + i\frac{V}{b\omega}\frac{T_4 - \frac{2}{3}\left(\sqrt{1-c_1^2}\right)^3}{\pi} - \left(\frac{V}{b\omega}\right)^2\frac{T_1+T_{10}}{\pi}, \tag{B-5}$$

$$T_\omega = -\frac{T_1}{\pi} - i\frac{V}{b\omega}\frac{T_{12}}{\pi}(F+iG), \tag{B-6}$$

$$T_\varphi = -\frac{1}{\pi}\left[T_7 + \left(c_1 + \frac{1}{2}\right)T_1\right] + i\frac{V}{b\omega}\frac{\frac{2}{3}\left(\sqrt{1-c_1^2}\right)^3 + 2T_1 + T_4}{2\pi} - i\frac{V}{b\omega}\frac{T_{12}}{\pi}(F+iG) - \left(\frac{V}{b\omega}\right)^2\frac{T_{12}}{\pi}(F+iG), \tag{B-7}$$

$$T_\beta = -\frac{T_3}{\pi^2} + i\frac{V}{b\omega}\frac{T_4 T_{11}}{2\pi^2} - i\frac{V}{b\omega}\frac{T_{11}T_{12}}{2\pi^2}(F+iG) - \left(\frac{V}{b\omega}\right)^2 \frac{T_5 - T_4 T_{10}}{\pi^2} - \left(\frac{V}{b\omega}\right)^2 \frac{T_{10}T_{12}}{\pi^2}(F+iG), \tag{B-8}$$

$$T_1 = -\frac{1}{3}\sqrt{1-c_1^2}\left(2+c_1^2\right) + c_1 \cos^{-1} c_1, \tag{B-9}$$

$$T_2 = c\left(1-c_1^2\right) - \sqrt{1-c_1^2}\left(1+c_1^2\right)\cos^{-1} c + c_1\left(\cos^{-1} c_1\right)^2, \tag{B-10}$$

$$T_3 = -\left(\frac{1}{8}+c_1^2\right)\left(\cos^{-1} c_1\right)^2 + \frac{1}{4}c_1\sqrt{1-c_1^2}\cos^{-1} c_1\left(7+2c_1^2\right) - \frac{1}{8}\left(1-c_1^2\right)\left(5c_1^2+4\right), \tag{B-11}$$

$$T_4 = -\cos^{-1} c_1 + c_1\sqrt{1-c_1^2}, \tag{B-12}$$

$$T_5 = -\left(1-c_1^2\right) - \left(\cos^{-1} c_1\right)^2 + 2c_1\sqrt{1-c_1^2}\cos^{-1} c_1. \tag{B-13}$$

$$T_6 = T_2, \tag{B-14}$$

$$T_7 = -\left(\frac{1}{8}+c_1^2\right)\cos^{-1} c_1 + \frac{1}{8}c_1\sqrt{1-c_1^2}\left(7+2c_1^2\right). \tag{B-15}$$

$$T_8 = -\frac{1}{8}\sqrt{1-c_1^2}\left(2c_1^2+1\right) + c_1\cos^{-1} c_1, \tag{B-16}$$

$$T_9 = \frac{1}{2}\left[\frac{1}{3}\left(\sqrt{1-c_1^2}\right)^3 + aT_4\right], \tag{B-17}$$

$$T_{10} = \sqrt{1-c_1^2} + \cos^{-1} c_1, \tag{B-18}$$

$$T_{11} = \cos^{-1} c_1\left(1-2c_1\right) + \sqrt{1-c_1^2}\left(2-c_1\right), \tag{B-19}$$

$$T_{12} = \sqrt{1-c_1^2}\left(2+c_1\right) - \cos^{-1} c_1\left(2c_1+1\right), \tag{B-20}$$

$$T_{13} = \frac{1}{2}\left[-T_7 - (c_1 - a)T_1\right], \tag{B-21}$$

$$T_{14} = \frac{1}{16} + \frac{1}{2}ac_1. \tag{B-22}$$

Note that,

$$V = U_\infty. \tag{B-23}$$

B.2 Theodorsen's function

The function $C(k)$ is called Theodorsen's function, The exact expression of it is given by,

$$C(k) = F + iG = \frac{H_1^{(2)}(k)}{H_1^{(2)}(k) + i\,H_0^{(2)}(k)}. \tag{B-24}$$

where $H_0^{(2)}(k)$ and $H_1^{(2)}(k)$ are Hankel functions [7,20,29] of second kind (zero and first order, respectively). The standard notations for the real and imaginary parts of $C(k)$ are F and G, which are tabulated in Table B.1.

Table B.1 Theodorsen's function $C(k) = F + iG$.

k	$1/k$	F	$-G$
∞	0.000	0.5000	0
10.00	0.100	0.5006	0.0124
6.00	0.16667	0.5017	0.0206
4.00	0.250	0.5037	0.0305
3.00	0.33333	0.5063	0.0400
2.00	0.500	0.5129	0.0577
1.50	0.66667	0.5210	0.0736
1.20	0.83333	0.5300	0.0877
1.00	1.000	0.5394	0.1003
0.80	1.250	0.5541	0.1165
0.66	1.51516	0.5699	0.1308
0.60	1.66667	0.5788	0.1378
0.56	1.78572	0.5857	0.1428
0.50	2.000	0.5979	0.1507
0.44	2.27273	0.6130	0.1592
0.40	2.500	0.6250	0.1650
0.34	2.94118	0.6469	0.1738
0.30	3.33333	0.6650	0.1793
0.24	4.16667	0.6989	0.1862
0.20	5.000	0.7276	0.1886
0.16	6.250	0.7628	0.1876
0.12	8.33333	0.8063	0.1801
0.10	10.000	0.8320	0.1723
0.08	12.500	0.8604	0.1604
0.06	16.66667	0.8920	0.1426
0.05	20.000	0.9090	0.1305
0.04	25.000	0.9267	0.1160
0.025	40.000	0.9545	0.0872
0.01	100.000	0.9824	0.0482
0	∞	1.000	0

Appendix C: Special complex functions

C.1 The complex function $H_1(z,s)$

Consider the following complex function,

$$H_1(z,s) = \cosh^{-1} R_1, \tag{C-1}$$

where,

$$R_1 = \sqrt{\frac{(c-z)s}{c(s-z)}}. \tag{C-2}$$

The derivative of the complex function is given by,

$$\frac{dH_1}{dz} = \frac{1}{\sqrt{R_1^2 - 1}} \frac{dR_1}{dz}, \tag{C-3}$$

where,

$$\frac{dR_1}{dz} = \frac{c-s}{2(s-z)\sqrt{(c-z)(s-z)}}\sqrt{\frac{s}{c}}, \tag{C-4}$$

$$\sqrt{R_1^2 - 1} = \sqrt{\frac{(c-s)z}{c(s-z)}}. \tag{C-5}$$

The derivative is given by,

$$\frac{dH_1}{dz} = \frac{\sqrt{(c-s)s}}{2(s-z)\sqrt{(c-z)z}}. \tag{C-6}$$

At $z = x > s$,

$$R_1 = jR_1^* \qquad \text{where, } R_1^* = \sqrt{\frac{(c-z)s}{c(z-s)}}. \tag{C-7}$$

The complex function can be expressed by,

$$H_1 = \cosh^{-1} R_1 = \ln\left(R_1 + \sqrt{R_1^2 - 1}\right), \tag{C-8}$$

At $R_1 = jR_1^*$,

$$H_1^* = \ln\left(jR_1^* + \sqrt{(jR_1^*)^2 - 1}\right) = \ln j + \ln\left(R_1^* + \sqrt{(R_1^*)^2 + 1}\right), \tag{C-9}$$

$$H_1^{*} = J\frac{\pi}{2} + \sinh^{-1} R_1^{*}. \tag{C-10}$$

where,

$$H_1^{*} = \sinh^{-1} R_1^{*} = \ln\left(R_1^{*} + \sqrt{\left(R_1^{*}\right)^2 + 1} \right). \tag{C-11}$$

The derivative of the complex function is given by,

$$\frac{dH_1^{*}}{dz} = \frac{d}{dz}\left(\sinh^{-1} R_1^{*}\right) = \frac{1}{\sqrt{\left(R_1^{*}\right)^2 + 1}} \frac{dR_1^{*}}{dz}, \tag{C-12}$$

where,

$$\frac{1}{\sqrt{\left(R_1^{*}\right)^2 + 1}} = \sqrt{\frac{c(z-s)}{(c-s)z}}, \tag{C-13}$$

$$\frac{dR_1^{*}}{dz} = \frac{s-c}{2(z-s)\sqrt{(c-z)(z-s)}}\sqrt{\frac{s}{c}}. \tag{C-14}$$

The derivative is given by,

$$\frac{dH_1^{*}}{dz} = \frac{\sqrt{(c-s)s}}{2(s-z)\sqrt{(c-z)z}}. \tag{C-15}$$

From the above derivations, one concludes,

$$\frac{dH_1}{dz} = \frac{dH_1^{*}}{dz}. \tag{C-16}$$

At $z = x > c$,

$$R_1 = \overline{R}_1 = \sqrt{\frac{s}{c}}\frac{(-j)\sqrt{z-c}}{(-j)\sqrt{z-s}} = \sqrt{\frac{s(z-c)}{c(z-s)}}. \tag{C-17}$$

Note that,

$$\overline{R}_1^2 < 1, \tag{C-18}$$

$$H_1 = \ln\left(R_1 + \sqrt{R_1^2 - 1}\right) = \ln\left(\overline{R}_1 + j\sqrt{1 - \overline{R}_1^2}\right) = \pm j\cos^{-1}\overline{R}_1 = \pm j\overline{H}_1. \tag{C-19}$$

Note that,

$$\overline{H}_1 = \cos^{-1}\overline{R}_1. \tag{C-20}$$

$$\frac{d\overline{H}_1}{dz} = \frac{-1}{\sqrt{1-\overline{R}_1^2}}\frac{d\overline{R}_1}{dz} = \frac{\sqrt{(c-s)s}}{2(s-z)\sqrt{(z-c)z}}. \tag{C-21}$$

By comparing the derivatives, one concludes,

$$\frac{dH_1}{dz} = +j\frac{d\overline{H}_1}{dz}, \tag{C-22}$$

$$H_1 = +j\overline{H}_1. \tag{C-23}$$

For $z = x < s < c$,

$$R_1 = \widetilde{R}_1 = \sqrt{\frac{(c-z)s}{c(s-z)}},\ \ \overline{R}_1 > 1 \tag{C-24}$$

$$\frac{dH_1}{dz} = \frac{-j\sqrt{s(c-s)}}{2(s-z)\sqrt{(c-z)(-z)}}, \tag{C-25}$$

$$1-\widetilde{R}_1^2 = \frac{(-z)(c-s)}{c(s-z)} > 0, \tag{C-26}$$

The complex function in this domain is expressed by.

$$H_1 = \cosh^{-1} R_1 = \ln\left(\widetilde{R}_1 + j\sqrt{1-\widetilde{R}_1^2}\right) = +j\cos^{-1}\widetilde{R}_1 = +j\widetilde{H}_1. \tag{C-27}$$

Note that,

$$\frac{d\widetilde{H}_1}{dz} = \frac{d}{dz}\left(\cos^{-1}\widetilde{R}_1\right) = \frac{-1}{\sqrt{1-\widetilde{R}_1^2}}\frac{d\widetilde{R}_1}{dz} = \frac{-\sqrt{(c-s)s}}{2(s-z)\sqrt{(-z)(c-z)}}. \tag{C-28}$$

By comparing the derivatives, one concludes,

$$\frac{dH_1}{dz} = j\frac{d\widetilde{H}_1}{dz}, \tag{C-29}$$

$$H_1 = j\widetilde{H}_1. \tag{C-30}$$

Note that for $s < z = x < c$,

$$\oint_{z \to s} \frac{dH_1}{dz}dz = \frac{1}{2}\oint\frac{dz}{s-z} = -\frac{1}{2}\ln(z-s)\Big|_{\theta=\pi}^{\theta=0} = j\frac{\pi}{2}. \tag{C-31}$$

$$\mathrm{Im}(H_1) = j\frac{\pi}{2}. \tag{C-32}$$

The following are special cases of the complex function $H_1(z,s)$,

$$H_1(z,c) = 0, \tag{C-33}$$

$$H_1(z,0)=\begin{cases} j\dfrac{\pi}{2}+\lim\limits_{s\to 0}\left(\sinh^{-1}\sqrt{\dfrac{(c-z)s}{c(z-s)}}\right)=j\dfrac{\pi}{2} & 0<z<c \\ j\lim\limits_{s\to 0}\left(\cos^{-1}\sqrt{\dfrac{(c-z)s}{c(z-s)}}\right)=j\dfrac{\pi}{2} & c<z<\infty \\ j\dfrac{\pi}{2} & -\infty<z<0 \end{cases}, \tag{C-34}$$

One concludes,

$$H_1(z,0)=j\frac{\pi}{2},\ \text{for any } z, \tag{C-35}$$

$$H_1(\infty,c)=0, \tag{C-36}$$

$$H_1(\infty,0)=j\frac{\pi}{2}. \tag{C-37}$$

C.2 The complex function $A_1(z,\sigma)$

Consider the complex function $A_1(z,\sigma)$ given by,

$$A_1(z,\sigma)=\cos^{-1} R_1, \tag{C-38}$$

where,

$$R_1=\sqrt{\frac{(c-z)\sigma}{c(\sigma-z)}}. \tag{C-39}$$

The derivative of the above complex function is given by,

$$\frac{dA_1}{dz}=\frac{-1}{\sqrt{1-R_1^2}}\frac{dR_1}{dz}. \tag{C-40}$$

where,

$$\frac{dR_1}{dz}=\frac{c-\sigma}{2(\sigma-z)\sqrt{(c-z)(\sigma-z)}}, \tag{C-41}$$

$$\sqrt{1-R_1^2}=\sqrt{\frac{(\sigma-c)z}{c(\sigma-z)}}, \tag{C-42}$$

The derivative is given by,

$$\frac{dA_1}{dz}=\frac{\sqrt{(\sigma-c)\sigma}}{2(\sigma-z)\sqrt{(c-z)z}}. \tag{C-43}$$

For $\sigma > z = x > c$,

$$\frac{dA_1}{dz} = j\frac{\sqrt{(\sigma-c)\sigma}}{2(\sigma-z)\sqrt{(z-c)z}} = j\frac{dA_1^*}{dz}, \tag{C-44}$$

$$R_1 = -j\sqrt{\frac{(z-c)\sigma}{c(\sigma-z)}} = -j\,R_1^*, \tag{C-45}$$

The complex function in this range is expressed as,

$$A_1 = \cos^{-1} R_1 = \cos^{-1}\left(-jR_1^*\right) = j\ln\left(\left(-jR_1^*\right) + j\sqrt{1-\left(-jR_1^*\right)^2}\right), \tag{C-46}$$

$$A_1 = j\ln(-j)\left(R_1^* + \sqrt{1+\left(R_1^*\right)^2}\right) = \frac{\pi}{2} + j\sinh^{-1} R_1^*. \tag{C-47}$$

Note that,

$$A_1^* = \sinh^{-1} R_1^*, \tag{C-48}$$

The derivative of the above complex function is given by,

$$\frac{dA_1^*}{dz} = \frac{1}{\sqrt{1+\left(R_1^*\right)^2}}\frac{dR_1^*}{dz}, \tag{C-49}$$

where,

$$\frac{dR_1^*}{dz} = \frac{\sigma-c}{2(\sigma-z)\sqrt{(\sigma-z)(z-c)}}\sqrt{\frac{\sigma}{c}}, \tag{C-50}$$

$$\sqrt{1+\left(R_1^*\right)^2} = \sqrt{\frac{(\sigma-c)z}{c(\sigma-z)}}, \tag{C-51}$$

The derivative is given by,

$$\frac{dA_1^*}{dz} = \frac{\sqrt{(\sigma-c)\sigma}}{2(\sigma-z)\sqrt{(z-c)z}}. \tag{C-52}$$

By comparing the derivatives in this range, one concludes,

$$\frac{dA_1}{dz} = j\frac{dA_1^*}{dz}. \tag{C-53}$$

$$\oint_{|z-\sigma|<\varepsilon} \frac{dA_1}{dz}dz = j\oint\frac{dA_1^*}{dz}dz = -j\frac{1}{2}\oint\frac{dz}{z-\sigma}, \tag{C-54}$$

$$\oint\frac{dA_1}{dz}dz = -j\frac{1}{2}\left[\ln|z-\sigma| + i\theta\right]_{\theta=0}^{\theta=\pi} = \frac{\pi}{2}. \tag{C-55}$$

For $z = x > \sigma > c$, one obtains,

$$R_1 = \sqrt{\frac{(z-c)\sigma}{c(z-\sigma)}} = \overline{R}_1, \tag{C-56}$$

The complex function is expressed by,

$$A_1 = \cos^{-1} R_1 = j\ln\left(\overline{R}_1 + \sqrt{\overline{R}_1^2 - 1}\right) = j\cosh^{-1}\overline{R}_1, \tag{C-57}$$

$$A_1 = \cos^{-1} R_1 = j\cosh^{-1}\overline{R}_1 = j\overline{A}_1. \tag{C-58}$$

The above conclusion is supported by comparing the derivatives,

$$\frac{d\overline{A}_1}{dz} = \frac{\sqrt{(\sigma-c)\sigma}}{2(\sigma-z)\sqrt{(z-c)z}}, \tag{C-59}$$

For $z = x > \sigma > c$, one obtains,

$$\frac{dA_1}{dz} = \frac{\sqrt{(\sigma-c)\sigma}}{2(\sigma-z)(-j)\sqrt{(z-c)z}} = j\frac{d\overline{A}_1}{dz}. \tag{C-60}$$

For $z = x < 0 < c < \sigma$, one obtains,

$$R_1 = \sqrt{\frac{(c-z)\sigma}{c(\sigma-z)}} = \widetilde{R}_1, \tag{C-61}$$

$$\frac{dA_1}{dz} = -j\frac{\sqrt{(\sigma-c)\sigma}}{2(\sigma-z)\sqrt{(c-z)(-z)}}, \tag{C-62}$$

The complex function is expressed by.

$$A_1 = \cos^{-1}\widetilde{R}_1 = \pm j\ln\left(\widetilde{R}_1 + \sqrt{\widetilde{R}_1^2 - 1}\right) = \pm j\cosh^{-1}\widetilde{R}_1 = \pm j\widetilde{A}_1. \tag{C-63}$$

The derivative of the complex function in this range is given by,

$$\frac{d\widetilde{A}_1}{dz} = \frac{1}{\sqrt{\widetilde{R}_1^2 - 1}}\frac{d\widetilde{R}_1}{dz} = -\frac{\sqrt{(\sigma-c)\sigma}}{2(\sigma-z)\sqrt{(c-z)(-z)}}. \tag{C-64}$$

By comparing the derivatives, one concludes,

$$\frac{dA_1}{dz} = j\frac{d\widetilde{A}_1}{dz}, \tag{C-65}$$

$$A_1 = j\widetilde{A}_1. \tag{C-66}$$

The following are special cases of the complex function $A_1(z,\sigma)$,

$$A_1(z,\sigma) = \cos^{-1}\sqrt{\frac{(c-z)\sigma}{c(\sigma-z)}}, \tag{C-67}$$

$$A_1(z,c) = 0, \tag{C-68}$$

$$A_1(z,\infty) = \left\{ \begin{array}{ll} \cos^{-1}\sqrt{\dfrac{c-z}{c}} & 0 < z < c \\ \dfrac{\pi}{2} + j\lim\limits_{\sigma\to\infty}\left(\sinh^{-1}\sqrt{\dfrac{(z-c)\sigma}{c(\sigma-z)}}\right) & c < z < \infty \\ j\lim\limits_{s\to-\infty}\left(\cosh^{-1}\sqrt{\dfrac{(c-z)\sigma}{c(\sigma-z)}}\right) & -\infty < z < 0 \end{array} \right\}, \tag{C-69}$$

The final expression of the complex function for this special case is given by,

$$A_1(z,\infty) = \left\{ \begin{array}{ll} \cos^{-1}\sqrt{\dfrac{c-z}{c}} & 0 < z < c \\ \dfrac{\pi}{2} + j\sinh^{-1}\sqrt{\dfrac{z-c}{c}} & c < z < \infty \\ j\cosh^{-1}\sqrt{\dfrac{c-z}{c}} & -\infty < z < 0 \end{array} \right\}. \tag{C-70}$$

C.3 Summary of the behavior of the special complex functions

Below is a summary of the behavior of the special complex functions, represented in Tables C.1 and C.2.

Table C.1 General behavior of a special complex singularity $H_1(z,s)$.

Part	$-\infty < z = x < 0$	$0 \le z = x < s$	$s \le z = x < c$	$c \le z = x < \infty$
$\mathrm{Real}[H_1]$	0	$H_1 = \cosh^{-1} R_1$	$H_1^{\bullet} = \sinh^{-1} R_1^{\bullet}$	0
$\mathrm{Imag}[H_1]$	$j\widetilde{H}_1 = j\cos^{-1}\widetilde{R}_1$	0	$j\frac{\pi}{2}$	$j\overline{H}_1 = j\cos^{-1}\overline{R}_1$
R_1	$\widetilde{R}_1 = \sqrt{\frac{(c-z)s}{c(s-z)}} = R_1$ $\widetilde{R}_1\big\|_{z\to-\infty} = \sqrt{\frac{s}{c}}$	$R_1 = \sqrt{\frac{(c-z)s}{c(s-z)}}$	$R_1^{\bullet} = \sqrt{\frac{(c-z)s}{c(z-s)}}$	$\overline{R}_1 = \sqrt{\frac{(z-c)s}{c(z-s)}}$ $\overline{R}_1\big\|_{z\to\infty} = \sqrt{\frac{s}{c}}$

Table C.2 General behavior of a special complex singularity $A_1(z,\sigma)$.

Part	$-\infty < z = x \le 0$	$0 < z = x < c$	$c \le z = x < \sigma$	$\sigma \le z = x < \infty$
$\mathrm{Real}[A_1]$	0	$A_1 = \cos^{-1} R_1$	$\frac{\pi}{2}$	0
$\mathrm{Imag}[A_1]$	$j\widetilde{A}_1 = j\cosh^{-1}\widetilde{R}_1$	0	$jA_1^{\bullet} = j\sinh^{-1} R_1^{\bullet}$	$j\overline{A}_1 = j\cosh^{-1}\overline{R}_1$
R_1	$\widetilde{R}_1 = \sqrt{\frac{(c-z)\sigma}{c(\sigma-z)}} = R_1$ $\widetilde{R}_1\big\|_{z\to-\infty} = \sqrt{\frac{\sigma}{c}}$	$R_1 = \sqrt{\frac{(c-z)\sigma}{c(\sigma-z)}}$	$R_1^{\bullet} = \sqrt{\frac{(z-c)\sigma}{c(\sigma-z)}}$	$\overline{R}_1 = \sqrt{\frac{(z-c)\sigma}{c(z-\sigma)}}$ $\overline{R}_1\big\|_{z\to\infty} = \sqrt{\frac{\sigma}{c}}$

The two complex singularities at special positions along the airfoil behave as,

$$H_1(z,c) = 0, \tag{C-71}$$

$$H_1(z,0) = j\frac{\pi}{2}, \tag{C-72}$$

$$A_1(z,c) = 0, \tag{C-73}$$

$$A_1(z,\infty) = \begin{bmatrix} \cos^{-1}\sqrt{\dfrac{c-z}{c}} & 0 < z < c \\ \dfrac{\pi}{2} + j\sinh^{-1}\sqrt{\dfrac{z-c}{c}} & c < z < \infty \\ j\cosh^{-1}\sqrt{\dfrac{c-z}{c}} & -\infty < z < 0 \end{bmatrix}. \tag{C-75}$$

Appendix D

Derivation of the unsteady pressure coefficient

D.1 Unsteady pressure coefficient for the airfoil

The equation of the reduced pressure coefficient $\delta \hat{C}_p(x)$ is expressed as,

$$\delta \hat{C}_p(x) = -\frac{2}{U_\infty}\left[i\frac{\lambda}{c}\frac{1}{2}\delta\hat{\Gamma}(x) + \delta\hat{u} \right]. \tag{D-1}$$

where λ is the reduced frequency.

The expression of the reduced velocity on the airfoil $\delta\hat{u}$ is given by, (See chapter 4),

$$\delta\hat{u} = \mathrm{Re}\left\lfloor \delta\hat{W}(z) \right\rfloor_{z=x}, \tag{D-2}$$

By taking the real part of the complex velocity $\delta\hat{W}(z)$, the expression of $\delta\hat{u}$ is given by,

$$\begin{aligned} \delta\hat{u}(x) = &-b_0\sqrt{\frac{c-x}{c}} - \frac{2}{\pi}\delta\hat{V}\left[\cosh^{-1}\sqrt{\frac{(c-x)s}{c(s-x)}} + \sqrt{\frac{c-x}{x}}\cos^{-1}\sqrt{\frac{s}{c}} \right] \\ &+ \frac{1}{2}\frac{\lambda^2}{c^2}\delta\hat{\Gamma}(c)\frac{2}{\pi}\left(-\frac{c}{i\lambda} \right) J(x) \end{aligned} \tag{D-3}$$

The expression of $\delta\hat{\Gamma}(x)$ is expressed as,

$$\begin{aligned} \frac{1}{2}\delta\hat{\Gamma}(x) = &-b_0\int_0^x\sqrt{\frac{c-x}{x}}\,dx - \frac{2}{\pi}\delta\hat{V}\int_0^x\left[\cosh^{-1}\sqrt{\frac{(c-x)s}{c(s-x)}} + \sqrt{\frac{c-x}{x}}\cos^{-1}\sqrt{\frac{s}{c}} \right]dx \\ &+ \frac{1}{2}\frac{\lambda^2}{c^2}\delta\hat{\Gamma}(c)\frac{2}{\pi}\left(-\frac{c}{i\lambda} \right)\int_0^x J(x)\,dx \end{aligned} \tag{D-4}$$

By evaluating the integrals appearing in equation (D-4), see Appendix A, one obtains,

$$\begin{aligned} \frac{1}{2}\delta\hat{\Gamma}(x) = &\left[\sqrt{(c-x)x} + c\left(\frac{\pi}{2} - \cos^{-1}\sqrt{\frac{x}{c}} \right) \right]\left[-b_0 - \frac{2}{\pi}\delta\hat{V}\cos^{-1}\sqrt{\frac{s}{c}} \right] - \\ &-\frac{2}{\pi}\delta\hat{V}\left[(x-s)\cosh^{-1}\sqrt{\frac{(c-x)s}{c(s-x)}} + \sqrt{(c-s)s}\left(\frac{\pi}{2} - \cos^{-1}\sqrt{\frac{x}{c}} \right) \right] + \\ &+\frac{1}{2}\frac{\lambda^2}{c^2}\delta\hat{\Gamma}(c)\frac{2}{\pi}\left(\frac{-c}{i\lambda} \right)\int_0^x J(x)\,dx \end{aligned} \tag{D-5}$$

The expression of $\delta\hat{\Gamma}(c)$ is given by

$$\delta\hat{\Gamma}(c)=G\left\{-b_0 c-\frac{2}{\pi}\partial\hat{V}\left[\sqrt{(c-s)s}+c\cos^{-1}\sqrt{\frac{s}{c}}\right]\right\}, \tag{D-6}$$

where,

$$G=-\frac{4i}{\lambda}\frac{e^{-i\frac{\lambda}{2}}}{H_1^{(2)}(\lambda/2)+i H_0^{(2)}(\lambda/2)}. \tag{D-7}$$

The integral $J(x)$ is defined by,

$$J(x)=\lim_{\sigma_n\to\infty}\left[\int_c^{\sigma_n} e^{-i\frac{\lambda}{c}(\sigma-c)}\frac{\sigma}{x}\frac{\sqrt{(c-x)x}}{2(\sigma-x)\sqrt{(\sigma-c)\sigma}}d\sigma\right], \tag{D-8}$$

The above integral can be expressed as,

$$J(x)=\lim_{\sigma_n\to\infty}\left[\int_c^{\sigma_n} e^{-i\frac{\lambda}{c}(\sigma-c)}\left[\frac{\sqrt{(c-x)x}}{2(\sigma-x)\sqrt{(\sigma-c)\sigma}}+\sqrt{\frac{c-x}{x}}\frac{1}{2\sqrt{(\sigma-c)\sigma}}\right]d\sigma\right], \tag{D-9}$$

By performing the second integral, one obtains,

$$J(x)=\lim_{\sigma_n\to\infty}\left[\int_c^{\sigma_n} e^{-i\frac{\lambda}{c}(\sigma-c)}\left[\frac{\sqrt{(c-x)x}}{2(\sigma-x)\sqrt{(\sigma-c)\sigma}}\right]d\sigma\right]+\frac{1}{2}\sqrt{\frac{c-x}{x}}\left(\frac{-i\pi}{2}\right)e^{i\frac{\lambda}{2}}H_0^{(2)}(\lambda/2). \tag{D-10}$$

The integral of the above equation is given by,

$$\int_0^x J(x)dx=\lim_{\sigma_n\to\infty}\left[\int_c^{\sigma_n} e^{-i\frac{\lambda}{c}(\sigma-c)}\left\{\frac{\sigma}{2\sqrt{(\sigma-c)\sigma}}\left[-2\cos^{-1}\sqrt{\frac{x}{c}}\right]_{x=0}^{x}-\cos^{-1}\sqrt{\frac{(c-x)\sigma}{c(\sigma-x)}}\right\}d\sigma\right] \tag{D-11}$$

By performing the integrals in the above equation, one obtains,

$$\begin{aligned}\int_0^x J(x)dx&=2\left(\frac{\pi}{2}-\cos^{-1}\sqrt{\frac{x}{c}}\right)\frac{c}{4}e^{i\frac{\lambda}{2}}\left(-\frac{\pi}{2}\right)\left[H_1^{(2)}(\lambda/2)+i H_0^{(2)}(\lambda/2)\right]+\\&+\left(-\frac{c}{i\lambda}\right)\lim_{\sigma_n\to\infty}\left[\int_c^{\sigma_n} e^{-i\frac{\lambda}{c}(\sigma-c)}\frac{\sqrt{(c-x)x}}{2(\sigma-x)\sqrt{(\sigma-c)\sigma}}d\sigma\right]\end{aligned}, \tag{D-12}$$

By inserting equations (D-3) and (D-5) into the expression of the pressure coefficient $\delta\hat{C}_p(x)$ (equation (D-1)), one obtains,

$$-\frac{U_\infty}{2}\delta\hat{C}_p(x)=\left(\frac{i\lambda}{c}\right)\left[-b_0-\frac{2}{\pi}\delta\hat{V}\cos^{-1}\sqrt{\frac{s}{c}}\right]\left[\sqrt{(c-x)x}+c\left(\frac{\pi}{2}-\cos^{-1}\sqrt{\frac{x}{c}}\right)\right]+$$
$$+\left(\frac{i\lambda}{c}\right)\left(\frac{-2}{\pi}\delta\hat{V}\right)\left[(x-s)\cosh^{-1}\sqrt{\frac{(c-x)s}{c(s-x)}}+\sqrt{(c-s)s}\left(\frac{\pi}{2}-\cos^{-1}\sqrt{\frac{x}{c}}\right)\right]-$$
$$-b_0\sqrt{\frac{c-x}{x}}-\frac{2}{\pi}\delta\hat{V}\left[\cosh^{-1}\sqrt{\frac{(c-x)s}{c(s-x)}}+\sqrt{\frac{c-x}{x}}\cos^{-1}\sqrt{\frac{s}{c}}\right]+$$
$$+\frac{1}{2}\frac{\lambda^2}{c^2}\delta\hat{\Gamma}(c)\frac{2}{\pi}\left(-\frac{c}{i\lambda}\right)\left[\frac{i\lambda}{c}\int_0^x J(x)dx+J(x)\right]$$

(D-13)

Let us consider $\psi(x)$ as,

$$\psi(x)=\frac{i\lambda}{c}\int_0^x J(x)dx+J(x), \tag{D-14}$$

By inserting the terms that appear in equation (D-14), one obtains,

$$\psi(x)=\left[\frac{i\lambda}{c}\left(-\frac{c}{i\lambda}\right)+1\right]\lim_{\sigma_*\to\infty}\left[\int_c^{\sigma_*}e^{-i\frac{\lambda}{c}(\sigma-c)}\frac{\sqrt{(c-x)x}}{2(\sigma-x)\sqrt{(\sigma-c)\sigma}}d\sigma\right]+$$
$$+\left(\frac{i\lambda}{c}\right)\left(\frac{c}{2}\right)\left(\frac{\pi}{2}-\cos^{-1}\sqrt{\frac{x}{c}}\right)e^{i\frac{\lambda}{2}}\left(-\frac{\pi}{2}\right)\left[H_1^{(2)}(\lambda/2)+iH_0^{(2)}(\lambda/2)\right]+,$$
$$+\frac{1}{2}\sqrt{\frac{c-x}{x}}\left(-i\frac{\pi}{2}\right)e^{i\frac{\lambda}{2}}H_0^{(2)}(\lambda/2)$$

(D-15)

After arrangement, one obtains,

$$\psi(x)=\frac{-\pi}{G}\left[\frac{\pi}{2}-\cos^{-1}\sqrt{\frac{x}{c}}\right]-i\frac{\pi}{4}\sqrt{\frac{c-x}{x}}e^{i\frac{\lambda}{2}}H_0^{(2)}(\lambda/2). \tag{D-16}$$

Note that,

$$\delta\hat{\Gamma}(c)\psi(x)=\left\{-b_0 c-\frac{2}{\pi}\delta\hat{V}\left[\sqrt{(c-s)s}+c\cos^{-1}\sqrt{\frac{s}{c}}\right]\right\}\left\{(-\pi)\left(\frac{\pi}{2}-\cos^{-1}\sqrt{\frac{x}{c}}\right)+\right.$$

$$\left.+\frac{i\pi}{\lambda}\sqrt{\frac{c-x}{x}}(1-C(\lambda/2))\right\}$$

(D-17)

By inserting equation (D-17) into the expression of the pressure coefficient, one obtains,

$$-\frac{U_\infty}{2}\delta\hat{C}_p(x)=\left(\frac{i\lambda}{c}\right)\left[-b_0-\frac{2}{\pi}\delta\hat{V}\cos^{-1}\sqrt{\frac{s}{c}}\right]\sqrt{(c-x)x}$$

$$+\left(\frac{i\lambda}{c}\right)\left(-\frac{2}{\pi}\delta\hat{V}\right)\left[(x-s)\cosh^{-1}\sqrt{\frac{(c-x)s}{c(s-x)}}\right]-b_0\sqrt{\frac{c-x}{x}}$$

$$-\frac{2}{\pi}\delta\hat{V}\left[\cosh^{-1}\sqrt{\frac{(c-x)s}{c(s-x)}}+\sqrt{\frac{c-x}{x}}\cos^{-1}\sqrt{\frac{s}{c}}\right]$$

$$+\left(-\frac{1}{c}\right)\sqrt{\frac{c-x}{x}}(1-C(\lambda/2))\left[-b_0 c-\frac{2}{\pi}\delta\hat{V}\left(c\cos^{-1}\sqrt{\frac{s}{c}}+\sqrt{(c-s)s}\right)\right]$$

(D-18)

The above equation can be represented after mathematical arrangements as,

$$-\frac{U_\infty}{2}\delta\hat{C}_p(x)=(i\lambda)\sqrt{(c-x)x}\left(\frac{1}{c}-\frac{i}{\lambda x}C(\lambda/2)\right)\left[-b_0-\frac{2}{\pi}\delta\hat{V}\cos^{-1}\sqrt{\frac{s}{c}}\right]$$

$$-\frac{2}{\pi}\delta\hat{V}\cosh^{-1}\sqrt{\frac{(c-x)s}{c(s-x)}}\left[\frac{i\lambda}{c}(x-s)+1\right] \qquad \text{(D-19)}$$

$$+\left(\frac{1}{c}\right)\sqrt{\frac{c-x}{x}}(1-C(\lambda/2))\frac{2}{\pi}\delta\hat{V}\sqrt{(c-s)s}$$

where $C(\lambda/2)$ is Theodorsen's function. The values of Theodorsen function are given in Appendix B.

D.2 Unsteady pressure coefficient for the airfoil with an oscillating aileron

The equation of the reduced pressure coefficient $\delta\hat{C}_p(x)$ is expressed as,

$$\delta\hat{C}_p(x) = -\frac{2}{U_\infty}\left[i\frac{\lambda}{c}\frac{1}{2}\delta\hat{\Gamma}(x) + \delta\hat{u}\right]. \tag{D-20}$$

The expression of the reduced velocity on the airfoil $\delta\hat{u}$ is given by,

$$\delta\hat{u} = \mathrm{REAL}_j\left[\delta\hat{W}(z)\right]_{z=x}, \tag{D-21}$$

The expression of $\delta\hat{u}$ is given by,

$$\begin{aligned}\delta\hat{u}(x) = &-\frac{2}{\pi}\hat{V}(s_1)\left[\sqrt{\frac{c-x}{x}}\cos^{-1}\sqrt{\frac{s_1}{c}} + \cosh^{-1}\sqrt{\frac{(c-x)s_1}{c(s_1-x)}}\right] \\ &-\frac{2}{\pi}\delta\hat{V}\left[\cosh^{-1}\sqrt{\frac{(c-x)s}{c(s-x)}} + \sqrt{\frac{c-x}{x}}\cos^{-1}\sqrt{\frac{s}{c}}\right] + \frac{1}{2}\frac{\lambda^2}{c^2}\delta\hat{\Gamma}(c)\frac{2}{\pi}\left(-\frac{c}{i\lambda}\right)J(x)\end{aligned} \tag{D-22}$$

The expression of the reduced circulation for the prototype problem at any position x is given by,

$$\begin{aligned}\frac{1}{2}\delta\hat{\Gamma}(x) = &-\frac{2}{\pi}\hat{V}(s_1)\left[\cos^{-1}\sqrt{\frac{s_1}{c}}\cdot\int_0^x\sqrt{\frac{c-x}{x}}dx + \int_0^x\cosh^{-1}\sqrt{\frac{(c-x)s_1}{c(s_1-x)}}dx\right] \\ &-\frac{2}{\pi}\delta\hat{V}\int_0^x\left[\cosh^{-1}\sqrt{\frac{(c-x)s}{c(s-x)}} + \sqrt{\frac{c-x}{x}}\cos^{-1}\sqrt{\frac{s}{c}}\right]dx + \frac{1}{2}\frac{\lambda^2}{c^2}\delta\hat{\Gamma}(c)\frac{2}{\pi}\left(-\frac{c}{i\lambda}\right)\int_0^x J(x)dx\end{aligned}$$

(D-23)

The resultant of the above equation is given by,

$$\begin{aligned}\frac{1}{2}\delta\hat{\Gamma}(x) = &\frac{-2}{\pi}\left[\hat{V}(s_1)\cos^{-1}\sqrt{\frac{s_1}{c}} + \delta\hat{V}\cos^{-1}\sqrt{\frac{s}{c}}\right]\left[\sqrt{(c-x)x} + c\left(\frac{\pi}{2} - \cos^{-1}\sqrt{\frac{x}{c}}\right)\right] - \\ &\frac{-2}{\pi}\hat{V}(s_1)\left[(x-s_1)\cosh^{-1}\sqrt{\frac{(c-x)s_1}{c(s_1-x)}} + \left(\frac{\pi}{2} - \cos^{-1}\sqrt{\frac{x}{c}}\right)\sqrt{(c-s_1)s_1}\right] - \\ &-\frac{2}{\pi}\delta\hat{V}\left[(x-s)\cosh^{-1}\sqrt{\frac{(c-x)s}{c(s-x)}} + \left(\frac{\pi}{2} - \cos^{-1}\sqrt{\frac{x}{c}}\right)\sqrt{(c-s)s}\right] + \\ &+\frac{1}{2}\frac{\lambda^2}{c^2}\delta\hat{\Gamma}(c)\frac{2}{\pi}\left(-\frac{c}{i\lambda}\right)\int_0^x J(x)dx\end{aligned}$$

(D-24)

The above integrals are evaluated in Appendix A.

The resultant equation of the reduced circulation for the airfoil with an oscillating aileron is given by,

$$\delta\hat{\Gamma}(c)=G\left\{-\frac{2}{\pi}\hat{V}(s_1)\left[\sqrt{(c-s_1)s_1}+c\cos^{-1}\sqrt{\frac{s_1}{c}}\right]-\frac{2}{\pi}\partial\hat{V}\left[\sqrt{(c-s)s}+c\cos^{-1}\sqrt{\frac{s}{c}}\right]\right\}$$

(D-25)

where,

$$G=-\frac{4i}{\lambda}\frac{e^{-i\frac{\lambda}{2}}}{H_1^{(2)}(\lambda/2)+iH_0^{(2)}(\lambda/2)}. \tag{D-26}$$

where $H_1^{(2)}(\lambda/2)$ and $H_0^{(2)}(\lambda/2)$ are the Hankel's integrals of second kind of orders of one and zero, respectively. By inserting the above equations into the expression of the pressure coefficient and performing a similar analysis to section D.1, one obtains.

$$\begin{aligned}
-\frac{U_\infty}{2}\delta\hat{C}_p(x)=&\left(\frac{i\lambda}{c}\right)\left[-\frac{2}{\pi}\hat{V}(s_1)\cos^{-1}\sqrt{\frac{s_1}{c}}-\frac{2}{\pi}\delta\hat{V}\cos^{-1}\sqrt{\frac{s}{c}}\right]\sqrt{(c-x)x}\\
&+\left(-\frac{1}{c}\right)\sqrt{\frac{c-x}{x}}(1-C(\lambda/2))\{\ -\frac{2}{\pi}\hat{V}(s_1)\left[\sqrt{(c-s_1)s_1}+c\cos^{-1}\sqrt{\frac{s_1}{c}}\right]-\\
&\qquad\qquad -\frac{2}{\pi}\delta\hat{V}\left[\sqrt{(c-s)s}+c\cos^{-1}\sqrt{\frac{s}{c}}\right]\ \}\\
&-\frac{2}{\pi}\left(\frac{i\lambda}{c}\right)\hat{V}(s_1)\left[(x-s_1)\cosh^{-1}\sqrt{\frac{(c-x)s_1}{c(s_1-x)}}\right]-\frac{2}{\pi}\left(\frac{i\lambda}{c}\right)\delta\hat{V}\left[(x-s)\cosh^{-1}\sqrt{\frac{(c-x)s}{c(s-x)}}\right]-,\\
&-\frac{2}{\pi}\hat{V}(s_1)\left[\sqrt{\frac{c-x}{x}}\cos^{-1}\sqrt{\frac{s_1}{c}}+\cosh^{-1}\sqrt{\frac{(c-x)s_1}{c(s_1-x)}}\right]-\\
&-\frac{2}{\pi}\delta\hat{V}\left[\cosh^{-1}\sqrt{\frac{(c-x)s}{c(s-x)}}+\sqrt{\frac{c-x}{x}}\cos^{-1}\sqrt{\frac{s}{c}}\right]
\end{aligned}$$

(D-27)